

Titre: Biomechanical Modeling and Characterization of the Postural
Title: Parameters in Adolescent Idiopathic Scoliosis

Auteur: Saba Pasha
Author:

Date: 2012

Type: Mémoire ou thèse / Dissertation or Thesis

Référence: Pasha, S. (2012). Biomechanical Modeling and Characterization of the Postural
Parameters in Adolescent Idiopathic Scoliosis [Thèse de doctorat, École
Polytechnique de Montréal]. PolyPublie. <https://publications.polymtl.ca/915/>

Document en libre accès dans PolyPublie

Open Access document in PolyPublie

URL de PolyPublie: <https://publications.polymtl.ca/915/>
PolyPublie URL:

Directeurs de recherche: Carl-Éric Aubin, & Jean-Marc Mac-Thiong
Advisors:

Programme: Génie biomédical
Program:

UNIVERSITÉ DE MONTRÉAL

BIOMECHANICAL MODELING AND CHARACTERIZATION OF THE
POSTURAL PARAMETERS IN ADOLESCENT IDIOPATHIC SCOLIOSIS

SABA PASHA

INSTITUT DE GÉNIE BIOMÉDICAL
ÉCOLE POLYTECHNIQUE DE MONTRÉAL

THÈSE PRÉSENTÉE EN VUE DE L'OBTENTION
DU DIPLÔME DE PHILOSOPHIAE DOCTOR
(GÉNIE BIOMÉDICAL)

AOÛT 2012

UNIVERSITÉ DE MONTRÉAL

ÉCOLE POLYTECHNIQUE DE MONTRÉAL

Cette thèse intitulée:

BIOMECHANICAL MODELING AND CHARACTERIZATION OF THE
POSTURAL PARAMETERS IN ADOLESCENT IDIOPATHIC SCOLIOSIS

présentée par : PASHA Saba

en vue de l'obtention du diplôme de : Philosophiae Doctor

a été dûment acceptée par le jury d'examen constitué de :

M. RAISON Maxime, Ph.D., président

M. AUBIN Carl-Éric, Ph.D., membre et directeur de recherche

M. MAC-THIONG Jean-Marc, Ph.D., membre et codirecteur de recherche

M. MATHIEU Pierre A., D.Sc.A., membre

M. AISSAOUI Rachid, Ph.D., membre

DEDICATION

*To my parents,
for their love and support.*

ACKNOWLEDGMENT

I would like to first thank my research advisor, Professor Carl-Éric Aubin, who without his guidance and insights the presented thesis was not realized. I truly appreciate his effort to comprehend my idea and to lead me in the right direction. I would also like to thank my co-advisor, Dr Jean-Marc Mac-Thiong, for his clinical insights and genuine support of my work. I would like to thank Drs Hubert Labelle and Stefan Parent for all their constructive suggestions on my work during the last four years. I also would like to thank Dr Archana Sangole for her initiative role in my project. I would like to thank my colleagues at Sainte-Justine University Hospital and École Polytechnique particularly Drs Julien Clin and Eric Wagnac for all their technical help and consult. I would like to take the chance to acknowledge Dr Paul Allard's collaboration in extensive sharing of lab facilities in Sainte Justine Hospital and Dr Marline Beaulieu who helped me with the data acquisition. I would like to thank Ms Julie Joncas, Ms Marjolaine Roy-Beaudry, Mr Christian Bellefleur, and Mr Philippe Labelle who helped me to get the essential data for my project. I also appreciate the participation of all the patients and volunteers in Sainte-Justine Hospital in different parts of my research. A special thanks to all my friends in Montreal who made this period a very enjoyable time. Finally, I would like to thank our financial partners, Fonds de Recherche en Nature et Technologies (FQRNT), the Natural Sciences and Engineering Research Council of Canada (NSERC), and the industrial chair with Medtronic.

RÉSUMÉ

La scoliose est une déformation 3D de la colonne vertébrale qui influence la morphologie et l'alignement de la colonne vertébrale, du bassin et de la cage thoracique. Bien que plusieurs paramètres soient introduits pour identifier et évaluer les courbes chez les sujets scoliotiques, la relation biomécanique entre la colonne vertébrale et le bassin ainsi que ses impacts sur la posture et l'équilibre général des sujets scoliotiques n'est pas encore élucidée.

Le but de ce projet doctoral était d'examiner l'interaction spino-pelvienne en mesurant les paramètres biomécaniques chez les sujets atteints de scolioses idiopathiques adolescentes (SIA). La cinématique pelvienne, l'orientation spino-pelvienne relative et le chargement biomécanique lombo-sacré ont été examinés chez des sujets avec des courbures différentes. L'hypothèse que nous souhaitons vérifier est que l'interaction spino-pelvienne (au niveau des paramètres statiques, cinématiques et des chargements biomécaniques à l'interface entre le rachis et le bassin) est non seulement différente entre les SIA et les contrôles, mais varie aussi entre les sujets présentant différents types de scolioses. De plus, l'effet d'une instrumentation chirurgicale du rachis sur l'équilibre ainsi que sur l'interaction biomécanique spino-pelvienne a été étudié post opérativement.

Donc, après avoir examiné la littérature pertinente, trois chapitres ont été consacrés pour examiner l'hypothèse générale de ce projet. Chaque chapitre aborde un aspect de l'interaction spino-pelvienne chez les sous-groupes scoliotiques et compare les résultats avec un groupe de contrôles de la même catégorie d'âge sexe.

Bien que l'orientation pelvienne entre les sujets SIA et le groupe contrôle était différente, il n'est pas vérifié dans quelle mesure l'orientation pelvienne et l'alignement spino-pelvien affectent la cinématique du bassin chez les sujets présentant différents types de courbures. Par la suite, l'interférence entre l'orientation du bassin et le mouvement spino-pelvien a été étudiée. Un protocole expérimental a été conçu pour examiner le mouvement pelvien en 3D lors du mouvement du tronc *in vivo*. 17 sujets avec scoliose thoracique droite (TD), 8 sujets avec une scoliose thoracique droite et une courbure compensatoire lombaire gauche (TDLG), et 12 contrôles sans aucune histoire de maladie rachidienne ont été recrutés. Les sujets ayant reçu un traitement par corset ou chirurgical ont été exclus. Plusieurs marqueurs ont été attachés sur la peau à des points anatomiques spécifiques: acromions (pour définir la gamme totale de

mouvement du tronc) et ASIS et PSIS gauches et droits pour analyser la cinématique pelvienne. Les mouvements de tronc, c.-à-d. la flexion/extension, la rotation axiale et la flexion latérale ont été exécutés et ont été répétés trois fois pour chaque participant. Les coordonnées 3D des points anatomiques ont été enregistrées avec un système opto-électronique. Les amplitudes des mouvements pelviens (le ROM) dans les trois plans anatomiques ont été calculées et ont été comparées entre les trois groupes. D'après les résultats, l'orientation pelvienne était différente de manière significative pour les trois types de mouvement entre les groupes étudiés ($p<0,001$). La contribution du mouvement pelvien au ROM était différente dans les groupes étudiés. La pente sagittale pelvienne et la rotation axiale pelvienne étaient également significativement différentes entre les deux groupes de sujets scoliotiques ($p<0,05$). Les résultats ont montré que l'orientation initiale du bassin dans les trois plans anatomiques joue un rôle important dans la détermination de la contribution pelvienne au ROM maximum chez les sous-groupes scoliotiques.

Bien que le but principal du diagnostic et de l'évaluation de la scoliose consiste à déterminer la position et la sévérité des courbures spinales, les différentes études précédemment publiées ont montré la présence d'une déformation pelvienne significative chez les sujets avec une scoliose notamment dans le cas des courbures sévères. Toutefois, la relation entre la déformation pelvienne et les courbures vertébrales chez les sujets avec différents types de scoliose n'a pas encore été caractérisée. Afin d'établir cette relation, les images radiographiques latérales et postéro-antérieures de 80 sujets avec une courbure thoracique droite (TD), 80 sujets avec une courbure thoraco-lombaire/lombaire gauche (TL/L) et 35 contrôles ont été obtenues. La reconstruction 3D de la colonne vertébrale et du bassin a été produite en utilisant les images radiographies biplanaires de chaque sujet. L'orientation 3D du bassin a été mesurée en utilisant les coordonnées 3D des épines iliaques antéro-supérieures et postéro-supérieures (gauches et droites) (ASIS et PSIS). Un trapézoïde a été tracé en connectant ces quatre points. L'angle entre les projections de la ligne qui joint le milieu de l'ASIS et PSIS sur chaque côté sur les plans sagittal, frontal et transverse et les axes horizontal et vertical ont été utilisés pour définir l'orientation pelvienne dans les plans sagittal et frontal et la rotation axiale pelvienne. L'orientation pelvienne moyenne (en valeur absolue) a été respectivement mesurée dans les plans frontal et transverse à 2° [plage $0^\circ, 7^\circ$] et 4° [plage $0^\circ, 10^\circ$] dans le groupe de TD et à 4° [plage $0^\circ, 8^\circ$] et 5° [plage $0^\circ, 11^\circ$] dans le groupe de TL/L. Alors que l'orientation frontale pelvienne correspondait à la position de la courbe vertébrale dans le plan frontal, c.-à-d. les courbures

thoracique et lombaire, plus de 70% des sujets scoliotiques dans chaque groupe ont leur courbure thoracique principale et leur bassin tourné dans la même direction dans le plan transverse ($p<0,05$). 91 % des contrôles ont moins de $1,8^\circ$ d'obliquité pelvienne [0° , 3°] sur la vue postéro-antérieure avec une rotation axiale pelvienne non significative de $1,2^\circ$ [0° , 3°] dans le plan transverse. Une corrélation significative a été trouvée entre l'orientation pelvienne et les déformations vertébrales thoraciques et lombaires dans les plans frontal et transverse pour les deux sous-groupes de SIA.

Il était également d'intérêt de montrer si l'orientation spino-pelvienne pour les sous-groupes de SIA interfère avec le chargement biomécanique du sacrum. Par conséquent, l'impact biomécanique de l'alignement relatif spino-pelvien sur le sacrum a été étudié. Un modèle par éléments finis (MÉF) a été développé pour calculer le chargement biomécanique du sacrum pour 11 scolioses TD, 23 scolioses TL/L gauche et 12 sujets contrôles. Les radiographies des sujets ont été utilisées pour développer les reconstructions 3D de la colonne, du bassin et de la cage thoracique. Les propriétés mécaniques des vertèbres, disques intervertébraux et ligaments et la position du centre de masse (CDM) au niveau de chaque vertèbre dans le modèle proviennent de données pertinentes publiées. La force de gravité a été appliquée à niveau de chaque vertèbre. Une méthode d'optimisation a été utilisée pour assurer la similarité maximale entre la reconstruction 3D à partir des radiographies et le MÉF après les simulations. Le chargement mécanique sur S1 a été calculé pour tous les sujets. Les forces de compression sur S1 ont été normalisées par rapport au poids du patient et ont été graduées entre les magnitudes maximale et minimale de la compression sur S1. La position du barycentre de la distribution des contraintes sur le sacrum (CDP_{S1}) a été déterminée pour chaque sujet. D'après les résultats, la distribution des contraintes compressives était différente de manière significative entre les contrôles et les sujets TL/L ($p<0,05$). Bien que la distribution des contraintes était symétrique pour les sujets TD et les contrôles, chez les sujets TL/L une contrainte plus élevée a été observée du côté gauche du sacrum comparé au côté droit. Les résultats montrent donc que le chargement biomécanique du sacrum a varié pour les sous-groupes de scoliose et les contrôles. Le chargement biomécanique du sacrum n'a pas été seulement affecté par la position de la courbure scoliotique majeure mais il a aussi été modifié par l'alignement relatif spino-pelvien pour les sous-groupes scoliotiques.

Bien que l'étude précédente a souligné l'effet de la déformation vertébrale sur le chargement biomécanique du sacrum pour les sous-groupes de SIA, l'effet de la position du

CDM sur les résultats de la simulation de MÉF n'a pas encore été déterminé. Afin de déterminer la position du CDM chez un sujet scoliotique, une méthode mathématique a été développée. L'oscillation du centre de pression (le CDP) de 17 sujets TD et 4 sujets TDLG a été enregistrée au moyen de deux plaques de force pendant 30s en position début. La technique d'intégration double a été utilisée pour calculer la projection du COM sur le plan transverse au moyen de l'emplacement 2D de l'oscillation du CDP. Dans cette méthode, les intervalles entre lesquels la composante horizontale de la force de réaction du sol était égale à zéro étaient doublement intégrées pour estimer la position de la masse oscillante c.-à-d. le COM du sujet. Une analyse linéaire de régression a associé la position du CDP et la position 2D du CDM dans le plan transverse pour la cohorte de sujets scoliotiques. Cette équation a été utilisée pour transférer la position du CDP à la position de CDM dans les CDP-radiographies synchronisés qui ont été enregistrés pour neuf autres sujets scoliotiques. Une méthode d'optimisation a été appliquée pour calculer la position du CDM de chaque tranche de tronc dans les plans frontal et sagittal afin que la distance entre le CDM résultant de la méthode d'optimisation et le CDM de l'équation de régression soit minimisée. Les résultats de l'optimisation ont montré que la position nette du CDM après l'optimisation était plus proche du centre de la tête fémorale qu'avant l'optimisation (26% dans la position antéro-postérieure et 15% dans la direction médio-latérale). La position optimisée du CDM a été appliquée dans le MÉF et le chargement mécanique du sacrum a été recalculé pour les neuf sujets scoliotiques. Bien que la magnitude de la contrainte normalisée sur le sacrum ait été réduite après optimisation de la position du CDM, aucune différence significative n'a été observée au niveau de la tendance générale de la distribution de contraintes sur le sacrum. L'algorithme proposé a rendu possible l'évaluation de la position personnalisée du CDM au niveau de chaque vertèbre pour les sujets scoliotiques. La méthode proposée était applicable pour la simulation biomécanique du rachis scoliotique et a permis d'améliorer l'évaluation du chargement biomécanique de la colonne vertébrale dans les modèles ÉF des patients.

Enfin, une étude de cas a été effectuée pour analyser l'effet de la correction chirurgicale de la scoliose sur le chargement biomécanique du sacrum chez les sujets avec différents types de déformations scoliotiques. Cinq sujets TD et quatre sujets thoracique droit/lombaire gauche (TD/LG) qui avaient subi leur première chirurgie avec un suivi moyen de 16 mois [12-18 mois] ont été choisis. Les radiographies biplanaires de 12 sujets asymptomatiques ont été ajoutées

comme le groupe contrôle. Plusieurs paramètres morphologiques et biomécaniques du rachis et du bassin (les angles de Cobb thoraciques et lombaires, cyphose, lordose, CDM, incidence pelvienne, la pente pelvienne, la pente sacrée et la position de CDP_{SI}) ont été mesurés avant et après l'opération pour tous les sujets scoliotiques. La corrélation entre les paramètres spinaux et pelviens a été calculée pour les contrôles et les sujets avec SIA pré- et post- opération. Comme les résultats l'ont indiqué pour la position du CDM et CDP_{SI} , en plus des autres paramètres du rachis, c.-à-d. les angles de Cobb thoraciques et lombaires, étaient significativement différents entre les groupes SIA et les contrôles avant opération ($p<0,05$). Après l'opération, les angles de Cobb thoracique et lombaire étaient différents de manière significative entre les groupes scoliotique et les contrôles ($p<0,05$). La position du CDP_{SI} était différente de manière significative entre les sujets préopératoires et contrôles ($p<0,05$) alors qu'aucune différence n'a été observée entre les sujets contrôles et les sujets SIA après l'opération. Ces résultats montrent que la correction chirurgicale de la scoliose a tendance à normaliser les contraintes au niveau du sacrum. De plus, l'effet de la chirurgie d'instrumentation sur l'équilibre du chargement biomécanique du sacrum a été montré dans le groupe de sujets scoliotiques après la chirurgie.

En résumé, la thèse actuelle a examiné différents aspects de l'interaction spino-pelvienne pour les sous-groupes scoliotiques en 3D. Les résultats ont souligné les interactions biomécaniques entre le rachis et le bassin pour les sous-groupes SIA avant et après l'instrumentation chirurgicale. Considérer l'interaction relative spino-pelvienne comme une caractéristique de chaque sous-groupe de sujets scoliotiques pourrait s'avérer avantageux pour le traitement et la correction de la SIA.

ABSTRACT

Scoliosis is a 3D spinal deformity which impacts the morphology and alignment of the spine, the pelvis, and the ribcage. Although several spinal parameters are introduced to identify and evaluate scoliotic curves, there is not much known about the biomechanical relationship between the spine and the pelvis and its impact on the overall posture and equilibrium of the scoliotic patients.

The focus of this Ph.D. project was to investigate the spino-pelvic biomechanical interaction in adolescent idiopathic scoliosis (AIS) more closely. Spine and pelvic kinematic, relative spino-pelvic orientation in static, and lumbosacral biomechanical loading were investigated in subjects with different curve patterns. We hypothesized that spino-pelvic interaction is not only different between AIS and controls, but also varies between subjects with different scoliotic types in static, kinematic, and biomechanical loading. Furthermore the hypothetical effect of the spinal operation on equilibrating the spino-pelvic biomechanical interaction was tested postoperatively.

Hence, after reviewing the pertinent literatures, 3 chapters were devoted to investigate the general hypothesis of this project. Each chapter tries to investigate one aspect of the spine and pelvis interaction in scoliotic subgroups and compares the results with an age-gender match group of controls.

Although the pelvic alignment in the AIS group was different from the age-gender matched control group, it is not closely verified to what extent the pelvic orientation and the spino-pelvic alignment affect the pelvis kinematic in subjects with different curve types and subsequently its impact on the spino-pelvic movement is not determined. An experimental setup was designed to investigate the pelvic 3D motion during simple trunk movement *in vivo*. 17 right thoracic (RT), 8 right thoracic with compensatory left lumbar curve (RTLL) scoliosis, and 12 controls with no history of spinal disease were recruited. Subjects who had received any sort of treatment by spinal operation or bracing were excluded from the scoliotic group. Several skin markers were attached to specific anatomical landmarks: acromions (to define the total range of motion of the trunk) and left and right ASIS and PSIS to analyze pelvic kinematic. Simple trunk movements *i.e.* flexion/extension, axial rotation, and lateral bending were performed and repeated three times by each participant. Skin markers' 3D coordinates were registered

throughout the experience by an optoelectronic system. Pelvic range of motions (ROM) in the three anatomical planes were computed and compared between the three groups. Pelvic orientation was significantly different during three types of movement between the studied groups ($p<0.001$). Different pelvic range of motion in the anatomical planes was measured in the studied groups. Pelvic sagittal tilt and pelvic axial rotation were significantly different between the two scoliotic groups ($p<0.05$). The result suggests that pelvic initial alignment in the three anatomical planes plays an important role in determining the pelvic contribution to the maximum ROM in the scoliotic subgroups.

Although the main focus in diagnosing and evaluating the scoliosis is on the location and severity of the spinal deformities, different published literatures have shown the presence of a significant pelvic obliquity or rotation in scoliosis particularly in subjects with severe curves. However, the relationship between the pelvic orientation and spinal curves in subjects with different types of scoliosis was not characterized yet in 3D. In order to investigate this relationship, the lateral and postero-anterior radiographs of 80 main right thoracic (MT), 80 left thoraco-lumbar/ lumbar (TL/L), and 35 controls were obtained. 3D reconstruction of the spine and pelvis was generated from bi-planar radiographs of each patient. Pelvic 3D alignments were measured by means of the 3D coordinates of the left and right anterior and posterior iliac spine landmarks (ASIS and PSIS). A trapezoid was schemed by connecting these four points. The angle between the projections of the line connecting the midpoint of the ASIS and PSIS on each side on frontal and transverse planes and true horizontal and vertical axes were used to define the pelvic frontal tilt, and pelvic axial rotation respectively. The average pelvic orientation (absolute value) was measured respectively in frontal and transverse planes at $2.6^\circ \pm 2$ [range: -6° , 5°] and at $3.8^\circ \pm 2$ [-7° , 8°] in the MT group, and at $3.2^\circ \pm 1$ [-8° , 4°] and at $4.4^\circ \pm 2$ [-10° , 10°] in the TL/L group. While pelvic frontal tilt correlated to the position of the spinal curve in the frontal plane (the thoracic and lumbar segments) more than 70% of the scoliotic subjects in each group had their main thoracic and pelvis rotated in the same direction in the transverse plane ($p<0.05$). 91% of the controls had less than 1.8° pelvic obliquity [0° , 3°] and a non-significant 1.2° pelvic axial rotation [0° , 3°] in the transverse plane. The results highlighted a significant correlation between pelvic orientation and both thoracic and lumbar spinal deformities in frontal and transverse planes in the two AIS subgroups.

It was also of interest to show the impact of the altered spino-pelvic orientation on the biomechanical loading of the sacrum in AIS subgroups. The biomechanical impact of the relative spino-pelvic alignment on the sacrum was studied. A finite element model (FEM) was developed to compute the sacral loading in 11 right MT, 23 left TL/L (thoracolumbar/lumbar), and 12 control subjects. The material properties of the vertebrae, intervertebral disks, and ligaments in the model and the position of the center of mass (COM) at the level of each vertebra were derived from the pertinent literatures. The gravitational force was applied at the COM of each vertebral level. An optimization technique was used to assure the maximum similarity between the 3D reconstruction of the digitized radiographs and the FEM after running the simulations. Mechanical loading on the S1 endplate was computed for all the subjects. Compressive stress on the S1 endplate was normalized to the patient weight and was scaled between the maximum and minimum stress magnitude on the S1. The position of the barycentre of the compressive stress distribution on the superior sacrum endplate (COP_{SI}) was determined in each subject. Compressive stress distribution on the sacrum was significantly different between controls and TL/L subjects $p<0.05$. Although sacral compressive stress distribution was symmetric in MT and controls, in TL/L higher stress was observed at the left side of the sacrum as compared to the right side. Biomechanical loading of the sacrum varied between the AIS subgroups and controls. The biomechanical loading of the sacrum was not only affected by the location of the major curve but it was also modified by the relative spino-pelvic alignment in the scoliotic subgroups.

Even though the previous study highlighted the effect of the spinal deformity on the biomechanical loading of the sacrum in AIS subgroups, the effect of the position of the COM on the results of the FEM simulation was not determined yet. In order to determine the personalized position of the COM in a scoliotic subject a mathematical method was developed to estimate the 3D location of the COM at the level of each vertebra in the scoliotic spine. The developed method consisted of two sections: in the first experiment center of pressure (COP) oscillation of 17 RT and 4 RTLL was registered by means of two force plates during 30s of quite stance. Double integration technique was used to calculate the projection of the center of mass on the transverse plane by means of the 2D location of the COP oscillation. In this method the horizontal component of the ground reaction force was double integrated to estimate the location of the oscillating mass *i.e.* COM of the subject in the transverse plane. A linear regression analysis correlated the position of the COP and the 2D position of the COM in the transverse

plane in the cohort of subjects. This regression equation was used in the second experiment to transfer the position of the COP to the COM in a series of synchronized COP and X-ray data attained in 9 other AIS patients. An optimization method was applied to optimize the location of the COM of each trunk slice in the frontal and sagittal planes (from literature) in such way that the distance between the resultant COM from the optimization method and the COM from the regression equation was minimized. As the result of the optimization showed, the net position of the COM after optimization was closer to the midpoint of the femoral heads axis as compared to the same distance before operation. 26% decrease in the anterior-posterior position and 15% decrease in the medial-lateral position in the distance between the COM and center of the femoral heads axis after the optimization process were calculated. The optimized position of the COM was applied in the FE model and the mechanical loading of the sacrum was calculated for the latter 9 subjects. Although the magnitude of the normalized stress on the sacrum was reduced after the optimization of the COM position in the FEM, no significant difference was observed in the general trend of the stress distribution on the sacrum. The proposed algorithm made it possible to assess the personalized position of the COM at the level of each vertebra in scoliotic subjects during routine clinical visits. The proposed method was applicable in the biomechanical simulation of the scoliotic spine and permitted to better analyze the biomechanical loading of the spine in patient-specific FE models.

Finally a case study was performed to analyze the effect of the spinal surgery on the biomechanical loading of the sacrum in subjects with different types of scoliosis. 5 right MT and 4 right thoracic/ left lumbar, who had undergone their first posterior spinal fusion with an average follow-up of 16 months [12-18 months] were selected. The bi-planar radiographs of 12 asymptomatic subjects were added as the control group. Several spine and pelvic morphological and biomechanical parameters (thoracic and lumbar Cobb angles, kyphosis, lordosis, pelvic incidence, pelvic tilt, sacral slope, and the position of the COM and the COP_{SI}) were measured before and after operation in all subjects. The correlation between spine and pelvic parameters were calculated in controls and pre- and post- operative AIS. The position of the COP_{SI} was significantly different between pre-operative and control subjects ($p<0.05$) while no such difference was observed between the post-operative subjects and controls. The application of both spino-pelvic biomechanical and morphological parameters permitted to evaluate the biomechanical outcome of the surgical instrumentation of the spine. The effect of the spinal

surgery on equilibrating the biomechanical loading of the sacrum and making it more similar to the values observed in controls was shown in the post-operative group.

In summary, the current thesis investigated different aspects of the spino-pelvic interaction in selected scoliotic subgroups in 3D. The results highlighted the interactive relationship between the spine and pelvis in AIS subgroups before and after operation. Considering the spino-pelvic relative interaction as a characteristic of each scoliotic subgroup is beneficial in the treatment and assessment of the AIS.

TABLE OF CONTENTS

DEDICATION	III
ACKNOWLEDGMENT	IV
RÉSUMÉ	V
ABSTRACT	X
TABLE OF CONTENTS	XV
LIST OF TABLES	XIX
LIST OF FIGURES	XXI
LIST OF SYMBOLS AND ABBREVIATIONS	XXV
INTRODUCTION	1
CHAPTER 1 LITERATURE REVIEW	4
1.1 Descriptive anatomy and functions of the normal trunk	4
1.1.1 Spine	4
1.1.2 Pelvis	6
1.1.3 Anatomy of the sacrum	8
1.1.4 Anatomy of the sacroiliac joint (SIJ)	9
1.1.5 Sacroiliac joint function	9
1.1.6 Sacroiliac joint ligaments	10
1.1.7 Pelvic muscles	11
1.2 Scoliotic spine and pelvis	13
1.2.1 Scoliotic spine deformities	13
1.2.2 Pelvic parameters in scoliosis	14
1.3 Spino-pelvic relative alignment	17
1.3.1 Spino-pelvic alignment in controls	17

1.3.2 Spino-pelvic alignment in scoliosis.....	19
1.4 Kinematic of the spine and pelvic in scoliosis	22
1.5 Center of pressure and center of mass	24
1.5.1 Center of pressure: Facts and measurement.....	24
1.5.1.1 Direct measurement of the COM.....	24
1.5.1.2 Indirect measurement of the COM: Measurement of the COM via the position of the COP.....	25
1.5.2 Center of pressure related stability measurement in control and scoliosis	28
1.6 Spinal equilibrium in scoliosis	30
1.7 Scoliotic spine modeling	31
1.8 Scoliotic spine biomechanics before and after spinal fusion and instrumentation	35
CHAPTER2 OBJECTIVES AND HYPOTHESES	37
CHAPTER3 PELVIC 3D KINEMATIC AND ORIENTATION IN ADOLESCENT IDIOPATHIC SCOLIOSIS	40
3.1 Presentation of the first article.....	40
3.2 First article: Characterizing pelvis dynamics in adolescent with idiopathic scoliosis.....	41
3.2.1 Abstract	42
3.2.2 Introduction	43
3.2.3 Materials and Methods	45
3.2.3.1 Subjects.....	45
3.2.3.2 Statistical analysis.....	46
3.2.4 Results.....	47
3.2.5 Discussion	49
3.2.6 Conclusion.....	51
3.2.7 References	52

3.2.8 Figures and Tables	54
3.3 Analysis of the spino-pelvic relative orientation in scoliotic subgroups in the standing posture	58
3.3.1 Materials and Methods	58
3.3.1.1 Subjects.....	59
3.3.1.2 Pelvic orientation in the global coordinate system.....	61
3.3.1.3 Pelvic orientation with respect to the thoracic and lumbar spinal deformities.....	62
3.3.2 Results.....	62
3.3.2.1 Pelvic orientation in the global coordinate system.....	62
3.2.2.2 Pelvic orientation with respect to the thoracic and lumbar spinal deformities.....	64
3.3.2.3 Impact of the reconstruction error on the pelvic orientation: a sensitivity analysis	65
CHAPTER4 FINITE ELEMENT ANALYSIS OF THE BIOMECHANICAL LOADING OF THE SACRUM IN ADOLESCENT IDIOPATHIC SCOLIOSIS	67
4.1 Presentation of the second article.....	67
4.2 Second article: Biomechanical loading of the sacrum in adolescent idiopathic scoliosis	68
4.2.1 Abstract	69
4.2.2 Introduction	70
4.2.3 Materials and methods	71
4.2.3.1 Subjects.....	71
4.2.3.2 Measurement of the patient's morphological parameters.....	71
4.2.3.3 Finite element modeling and simulation.....	74
4.2.4 Results	75

4.2.4.1 Subjects.....	75
4.2.4.2 Statistical analysis.....	75
4.2.4.3 Spine and pelvic parameters in the global coordinate system.....	75
4.2.4.4 Sacral loading in the local coordinate system of the sacrum	76
4.2.5 Discussion	77
4.2.6 Conclusion.....	80
4.2.7 References	80
4.2.8 Figures and Tables	85
4.3 The effect of the position of the center of mass (COM) on the biomechanical loading of the sacrum: Sensitivity analysis and validation of the position of COM in the FE model	91
4.3.1 First experiment: study the relationship between the position of the COP and the COM in AIS.....	92
4.3.2 Second experiment: Optimization of the COM position at the level of each vertebra	94
4.3.3 Sensitivity analysis: the impact of the COM position on the biomechanical loading of the sacrum.....	97
4.4 Results	97
4.4.1 Results of the first experiment (regression analysis)	97
4.4.2 Results of the second experiment (optimization process)	99
4.4.3 Sensitivity analysis: the impact of the COM position on the biomechanical loading of the sacrum.....	101
CHAPTER5 STUDY OF THE IMPACT OF SPINAL INSTRUMENTATION ON THE SACRUM BIOMECHANICAL LOADING IN ADOLESCENT IDIOPATHIC SCOLIOSIS.	102
5.1 Materials and methods	102
5.1.1 Cohort description.....	102

5.1.2 Computation of the geometrical and biomechanical parameters of the spine and pelvis	103
5.1.3 Statistical analysis	103
5.2 Results	104
5.2.1 Case presentation.....	104
5.2.2. Comparison between the spinal and pelvic geometrical parameters pre- and post-operatively.....	105
5.2.3 Comparison between the spinal and pelvic biomechanical parameters pre- and post-operatively.....	105
CHAPTER6 GENERAL DISCUSSION.....	107
CHAPTER7 CONCLUSIONS AND RECOMMENDATIONS	115
REFERENCES	117

LIST OF TABLES

Table 1.1 :Muscles connecting the pelvis to the lower extremities	11
Table 1.2: Muscles connecting the pelvis to trunk	12
Table 3.1: Pelvic dynamics established sequentially by resolving pelvic 3D alignment into its three planar components: sagittal tilt (P_S), frontal tilt (P_F) and transverse plane rotation (P_T). The parentheses indicate compound movement of the pelvis.....	57
Table 3.2: Spinal and pelvic parameters of the studied sample.....	59
Table 3.3: Case presentation: Spine and pelvic parameters of the selected patients in scoliotic subgroups (MT and TL/L subjects) with different pelvic orientation.....	61
Table 3.4: The initial, average and standard deviation of the generated pelvic orientation.....	65
Table 4.1: Average and standard deviation of the geometrical parameters in the three studied groups: controls, subjects with main right thoracic (MT) deformity and subjects with left thoraco- lumbar/lumbar (TL/L) deformity.....	90
Table 4.2: The average and standard deviation of the position of the COM and COP_{SI} in the transverse plane.....	90
Table 4.3: The position of the spinal apices and spinal curvatures (angles) in frontal and sagittal planes for patient 1	100
Table 4.4 : The distance between the center of each vertebra and the position of the center of mass at the level of each vertebrae in sagittal and frontal planes (+ direction is anterior (sagittal plane) and to the left (frontal plane) with respect to the center of the vertebrae).	100
Table 5.1: Spinal and pelvic parameters of the studied samples.....	103
Table 5.2: Pre- and post-operative spinal and pelvic parameters in a patient with a) thoracic deformity (patient1) and b) RT/LL curve (patient2).....	105
Table 5.3 : The average position of the pre- and post-operative biomechanical parameters (COM, COP_{SI}) in the studied groups.	106

LIST OF FIGURES

Figure 1.1: a) Frontal and b) sagittal views of the spine and its principal sections	5
Figure 1.2: Vertebrae and inter vertebra disks, facet joints and pedicles (Right), Spinal motion segment (left). Consulted on January 10 2012 from: http://www.ucneurosurgery.com/spinal.html	5
Figure 1.3: Six degrees of freedom of a functional unit (translations and rotations), White and Panjabi 1990	6
Figure 1.4: Pelvic bones: 1) Ilium 2) Sacrum 3) Sacroiliac joint 5) Coccyx 6) Pubis 7) Ischium 8) Pubic symphysis 9) Femoral/hip joint (Grey's anatomy 20 th edition)	7
Figure 1.5: Pelvic diameters from top view: 1- Diagonally, 2- antero-posterior, 3- medio-lateral and from inferior view 4- antero-posterior, 5- medio-lateral (Grey's anatomy 20 th edition) .	8
Figure 1.6: The sacrum anterior and top views (Gray's anatomy 20 th edition), Consulted on January 2012 from http://www.bartleby.com/107/24.html	8
Figure 1.7: Anterior and posterior view of the pelvic ligaments. Consulted on August 2011 from: http://home.comcast.net/~wnor/pelvis.htm	9
Figure 1.8: The anterior view of the trunk muscles position connecting to the pelvis. Consulted on December 2011 from: http://musclerad.blogspot.ca/2011/12/psoas-major-muscle.html .11	11
Figure 1.9: Measurement of the 1) Thoraco- lumbar curve Cobb angle, 2) kyphosis and 3) lordosis in a scoliotic subject (Saint- Justine University Hospital database)	13
Figure 1.10: Pelvic obliquity determined by contra-lateral ASIS in a subject thoracic deformity (Saint-Justine University Hospital database)	14
Figure 1.11: Pelvic rotation in the transverse plane presented as unequal ilium width on the antero-posterior radiograph (Saint-Justine University Hospital database.)	15
Figure 1.12: The presentation of the spiral path in pelvic rotation: upper part rotates clockwise while the pubic symphysis rotates counter clockwise (Boulay, 2006-a)	15
Figure 1.13: Sacroiliac parameters: pelvic tilt (PT), pelvic incidence (PI), sacral slope (SS) and femoral overhang.....	16

Figure 1.14: Spino-pelvic relative parameters in the sagittal balance used to describe postural equilibrium in subjects	19
Figure 1.15: a) Frontal and b) sagittal balance defined as the angle between line connecting the T1 and L5 and vertical line in frontal and sagittal planes respectively. Viewed in Clindexia software (Sainte Justine University Hospital, Montreal)	20
Figure 1.16: Position of the center of the femoral head vertical axis, trunk inclination, and C7 plumb-line. Clindexia software (Saint-Justine University Hospital, Montreal)	21
Figure 1.17: Kinematic analysis of the trunk-pelvic interaction by mean of motion capture systems in AIS during a) trunk movement (Pasha, 2010) and b) gait (Mahaudens, 2009) ..	23
Figure 1.18: Force plate with four force transducer. (X,Y) determines the COP position, F is the reaction force, and F_1 to F_4 determines the registered force at each corner.....	26
Figure 1.19: a) 3D reconstruction of the spine, pelvis and ribcage b) The corresponding FE model of the anatomical sections (Aubin, 1996).....	33
Figure 1.20: Biomechanical model of the spine and pelvis (MD ADAMS, 2010).....	33
Figure 1.21. Hybrid model of the spine (Gharbi, 2008).....	34
Figure 1.22 : Compressive stress distribution on the superior sacrum endplate (front (F) and back (b)) in spondylolisthesis subjects with different sacro-pelvic parameters (PI, SS, and slip percentage %) (Sevrain, 2012).....	35
Figure 3.1: (A) Marker configuration on the torso and pelvis; (B) Identification of movement onset and maximal range-of-motion (ROM_{max}).....	54
Figure 3.2: Sacro-pelvic morphological parameters: pelvic tilt (PT), pelvic incidence (PI) and sacral slope (SS)	54
Figure 3.3: Pelvic alignment in the three planes (sagittal, frontal and transverse) for each movement type at maximum range of motion.	55
Figure 3.4: Comparison between pelvic ROM (ROM_{pelvis}) and total ROM (ROM_{max}). (A) Pelvic contribution to total ROM for all movement types; (B) The interaction effect evident during left axial rotation.	56

Figure 3.5: Schematic illustrating the calculation of (A) pelvic frontal tilt ($pelvic_{FTilt}$) in the coronal plane and (B) pelvic axial rotation ($pelvic_{Rot}$) in the transverse plane.....	60
Figure 3.6: (A) Schematic representation of the possible pelvic orientation in the frontal and transverse planes (B) Illustration of the pseudo-sagittal projection of pelvic orientation in the frontal and transverse planes	61
Figure 3.7: Presentation of the pelvic orientation in (A) Right main thoracic (MT) (n=80) (B) Left thoracolumbar/lumbar (TL/L) (n=80), and (C) Controls (n=35). Angles are presented in degrees.....	63
Figure 3.8: A schematic illustrating the tendency of the spino-pelvic relative orientation in transverse and coronal planes in (A) MT and (B) TL/L. The values are the percentage number of cases (n=80 in both groups) with the demonstrated pelvic orientation.	64
Figure 3.9: The effect of the reconstruction error on the pelvic orientation in the MT group.....	66
Figure 4.1: Osseo- ligamentous finite element model of the trunk	85
Figure 4.2: Steps in computation of the stress distribution and the COP_{S1} position on the S1 endplate: a. Biplanar radiographs, b. 3D reconstruction of the spine and pelvis, c. Finite element simulation of the gravitational loads on the spine and pelvis, d. Compressive stress distribution on the S1 endplate (scaled between the minimum and maximum stress magnitude) and the position of the COP_{S1}	86
Figure 4.3: Distribution of the COP_{S1} position in the transverse plane in the three groups.	87
Figure 4.4: Distribution of the COM position in the transverse plane in the three groups	88
Figure 4.5: Cluster analysis of the stress distribution on the superior endplate of the sacrum in the three groups of subjects. The dashed line depicts the center line of the sacrum in the local coordinate system of the sacrum.	89
Figure 4.6: The origin and the axis orientation of the coordinate system on the force plate (first experimental setup).	92
Figure 4.7: a) The position of the calibration object on the pressure mat. b) The location of the feet and the COP on the pressure mat during the radiography acquisition.	95

Figure 4.8: The correlation between the COM and the COP positions: a) in postero-anterior direction, b) in the medio-lateral direction	98
Figure 4.9: a) Presentation of the bi-planar radiographs and the calibration object b) The 3D position of the vertebrae and the center of mass of each vertebra slice after optimization in the sagittal plane and c) in the frontal plane. (0, 0) is the position of the mid point of the femoral heads.....	99
Figure 4.10: Stress distribution on the superior plate of sacrum before and after optimization of the position of the center of mass	101
Figure 5.1: Biplanar radiographs and the location of the high and low stress areas on the sacrum endplate before and after surgery in a typical a) Lenke 1 and b) Lenke5 subject. The dash line separates the anterior and posterior parts of the sacrum	104

LIST OF SYMBOLS AND ABBREVIATIONS

2D	Two dimensional
3D	Tridimensional
AIS	Adolescent idiopathic scoliosis
ASIS	Anterior- superior iliac spine
C1-C7	Cervical vertebrae
CHVA	Center of the hip vertical axis
CNS	Central nervous system
COM	Center of mass
COP	Center of pressure
COP _{S1}	Barycenter of the stress distribution on the S1 endplate
DLT	Direct linear transformation
FEM	Finite element model
GL	Gravity line
L1-L5	Lumbar vertebrae
mm	millimetre
MT	Main thoracic
ROM	Range of motion
RT	Right thoracic
RTLL	Right thoracic with compensatory left lumbar curve
PSIS	Posterior-superior iliac spine
PI	Pelvic incidence
PSIF	Posterior spinal instrumentation and fusion
PT	Pelvic tilt

S1-S5	Sacral vertebrae
SIJ	Sacroiliac joint
SS	Sacral slope
T1-T12	Thoracic vertebrae
TL/L	Thoracolumbar/lumbar curve

INTRODUCTION

The human spine is a complex structure providing mobility and stability in different postures. In spinal deformities like scoliosis, the overall postural equilibrium and stability of the patients are affected (Chen, 1998; Nault, 2002; Beaulieu, 2009). The close interaction between the postural parameters and the stability in scoliosis makes the postural parameters analysis essential in the AIS evaluation.

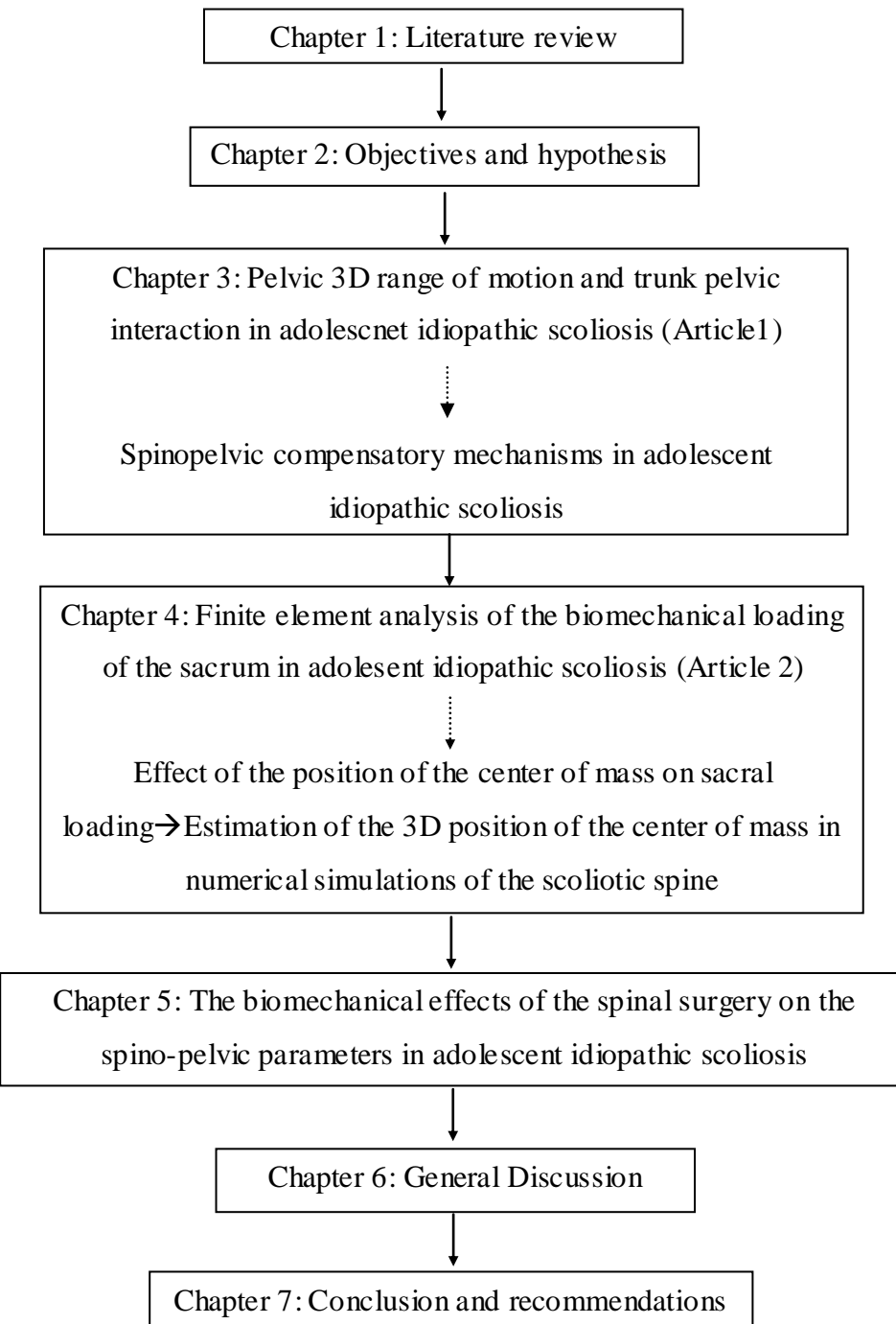
The pathology of scoliosis includes but is not limited to the anatomical abnormalities of the spine; thoracic and lumbar deformities in sagittal and frontal planes (King, 1983; Lenke, 2001), vertebral rotation in the transverse plane (Stokes, 1986; Lam, 2008), rib cage distortion (Grivas, 2006), pelvis asymmetry, rotation, and obliquity (Lucas, 2004; Gum, 2007), as well as alternations in the femoral heads position (Saji, 1995) have been reported in scoliosis cases. The relative orientation of the spine and pelvis in the sagittal plane is also affected in scoliosis and subsequently impacts the patient's sagittal balance (Berthonnaud, 2005; Berthonnaud, 2009). Moreover, the postural deformities resulting from scoliosis impact the kinematic of the movement (Mahaudens, 2005, Skalli, 2006) and muscular energy consumption (Feipel, 2002; Mahaudens, 2008). Postural deformities in AIS not only cause poor self- image in patients (Lonstein, 2006) but also, from a biomechanical point of view, are coupled with impaired postural balance and inefficient stability (Chen, 1998; Dalleau, 2011) which subsequently interferes with the patient daily life. Different studies have tried to characterize scoliotic deformities via postural analysis of the patients. However these methods are mainly limited to the postural analysis of the patients in the sagittal plane in static standing position (Upasani, 2007; Berthonnaud, 2009) and fail to provide information about the overall three-dimensional spino-pelvic deformities in scoliosis. Furthermore despite many literatures on the geometrical postural analysis of the AIS in the sagittal plane there is not much known about the biomechanics of the 3D spino-pelvic interaction and the differences due to various scoliotic spinal curves.

Bearing in mind the importance of the spino-pelvic postural analysis in scoliosis, characterization of the spino-pelvic interaction and its biomechanics in scoliotic subgroups were of interest of this Ph.D. thesis. The 3D relationship between the spinal and pelvic deformities in static, the kinematic of the spine and pelvis, and the biomechanical loading of the sacrum due to

the altered orientation of the spine and pelvis were investigated in scoliotic subgroups. The impact of the surgical spinal correction on the sacral loading and the transferred load between the spine and pelvis was also examined. The role of the pelvis in scoliosis was studied more closely in static and dynamic and the relationship between the morphological and biomechanical parameters of the spine and pelvis in the AIS subgroups were highlighted.

In the present document, after reviewing the pertinent literatures, the unreciprocated questions in the scoliosis postural analysis are listed. The objectives of the project are separately analyzed in five sections, including two scientific articles and three additional studies. Finally, a general discussion and conclusion highlight the important results and the clinical significance of the project.

The following flowchart presents the various steps of the project.



CHAPTER 1 LITERATURE REVIEW

1.1 Descriptive anatomy and functions of the normal trunk

1.1.1 Spine

The human spine contains five sections: cervical (7 vertebrae), thoracic (12 vertebrae), lumbar (5 vertebrae), sacrum (5 fused vertebrae), and coccyx (4-5 fused vertebrae) (figure 1.1). The vertebral size is different in each spinal section. Lumbar vertebrae are larger in size in comparison to thoracic and cervical vertebrae which make them more appropriate to carry the whole trunk weight. In the posterior part of the vertebrae, the spinous processes of two succeeding vertebrae are connected via the interspinous and supraspinous ligaments. The posterior facet joints (zygapophyseal joints) connect the articular facets of adjacent vertebrae. In the anterior part, the vertebrae are bounded with two adjacent intervertebral disks. Each intervertebral disk and its two adjacent vertebrae provide the kinematic component of the spine namely the motion segment (figure 1.2).

Intervertebral disks consist of the nucleus pulposus and the surrounding part namely annulus fibrosus. The ribcage is connected to the vertebral transverse processes and vertebral body, and contains 24 ribs, sternum, and costo-vertebral cartilaginous joints. The inferior part of the spine, the sacrum, is connected to the iliac bone on each side (Ellis, 2006). A detailed description of the pelvis is provided in the next section.

The spine normally appears as a straight line in the coronal plane. In the sagittal plane, the spine consists of 4 curves-two lordosis and two kyphosis curves: cervical lordosis, thoracic kyphosis, lumbar lordosis, and sacral kyphosis. In a normal spine, the curves magnitude vary by age and gender (Voutsinas, 1986; Fernand and Fox, 1985).

Groups of muscles provide flexion-extension (erector spinae, gluteus, and rectus abdominus), lateral bending, and axial rotation (erector spinae at ipsilateral side, rotatores and multifidus at the central- lateral side) of the spine. The co-contraction of these muscles provides spinal balance (White and Panjabi, 1990). Groups of spinal muscles connect different parts of the spine, as well as pelvis and lower extremities.

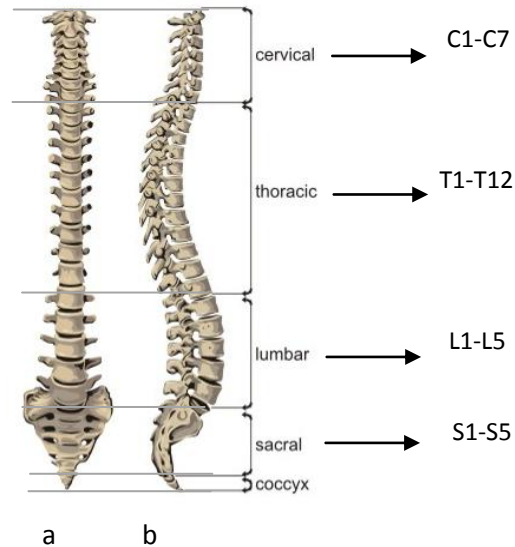


Figure 1.1: a) Frontal and b) sagittal views of the spine and its principal sections.

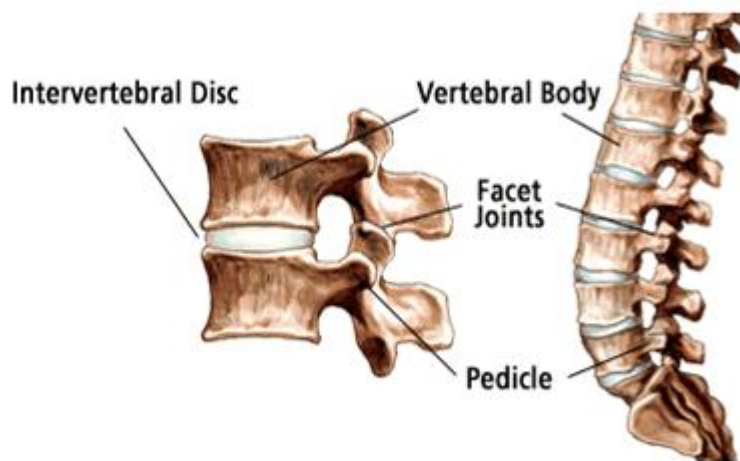


Figure 1.2: Vertebrae and inter vertebra disks, facet joints and pedicles (Right), Spinal motion segment (left). Consulted on January 10 2012 from: <http://www.ucneurosurgery.com/spinal.html>.

The motion of each vertebra is controlled by the synovial joints and pertinent muscles and ligaments. The translational and rotational motion of each vertebra is shown in figure 1.3. Each vertebra has six degrees of freedom. The range of motion (ROM) and the coupling mechanism of

the spinal vertebrae in 3D vary in thoracic and lumbar sections. The thoracic spine has limited movement due to its connection to the ribcage; its ROM decreases from T1 to T6 and increases from T6 to T12 during trunk flexion-extension. During lateral bending its ROM increases gradually from T1 to T12. The most important motion of the thoracic vertebrae is the axial rotation which gradually decreases from T1 to T12. The maximum range of motion of the thoracic vertebrae is about 9 degrees in adults (White and Panjabi 1990). The range of motion of the lumbar spine vertebrae increases from L1 to L5 during flexion-extension while its ROM is almost constant throughout the lumbar section during axial rotation (White and Panjabi 1990).

A coupling mechanism between axial rotation and lateral bending is observed in the thoracic and lumbar spine during trunk movement. The coupling mechanism is different in thoracic and lumbar sections (Harrison, 1999). While the axial rotation of the spinal vertebrae is in the direction of its lateral bending in the lumbar spine, the thoracic vertebrae rotate in the opposite direction of the lateral bending in the thoracic spine.

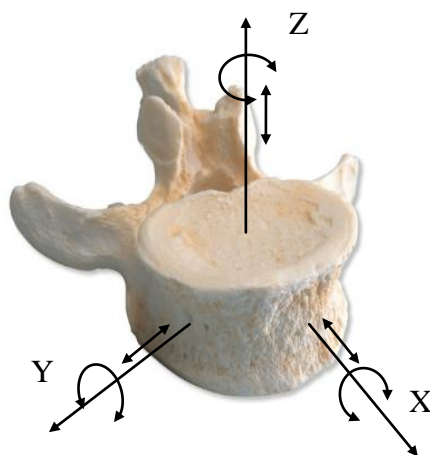


Figure 1.3: Six degrees of freedom of a functional unit (translations and rotations), White and Panjabi 1990.

1.1.2 Pelvis

The pelvic bony structure or pelvic girdle is one of the massive bony structures in the human body. The pelvis consists of 4 notable sections that form pelvic wall: 2 hip bones (ilium) (anterior and lateral parts), sacrum (posterior part), and pubic, and ischium (inferior part) (figure

1.4). Iliums are fused at the pubic symphysis and create the pubic arch. In the skeletal classification sacrum is considered as an axial skeleton similar to what is found in the skull, vertebrae, and thoracic cage. On the other hand, ilium is considered as a part of the appendicular skeleton similar to the lower and upper extremities bones and shoulder girdle (scapulas and clavicle). This skeletal classification is based on the role of the bony structure; while the axial bones are built to protect the sensitive members like brain and spinal cord, the appendicular bones are more involved in the movement (Gray 1918; Netter, 2010). The hybrid structure of the pelvis demonstrates both functions of the pelvic structure. While appendicular skeleton transfer the movement from the lower extremity via iliums and sacrum to the spine (axial skeleton) the axial skeleton has a protective role during pregnancy (Netter, 2010).

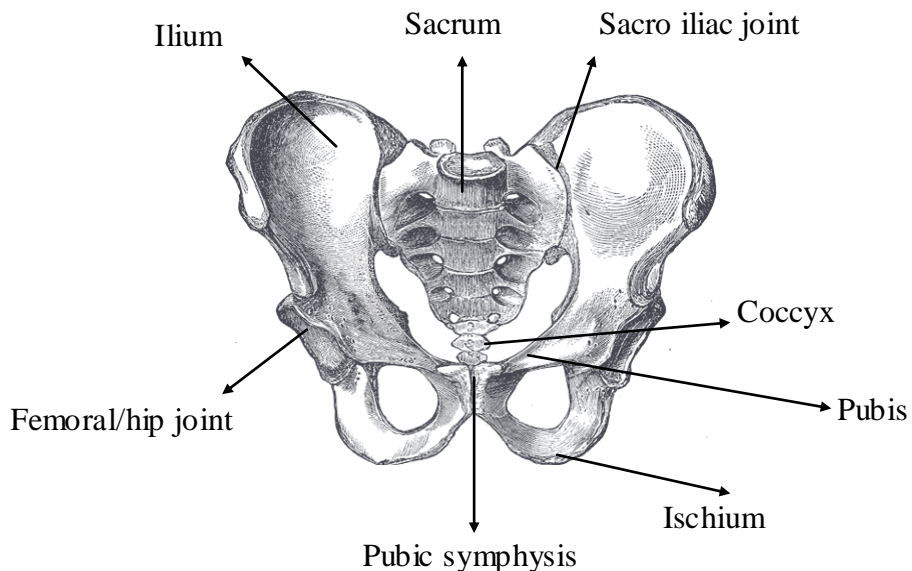


Figure 1.4: Pelvic bones: 1) Ilium 2) Sacrum 3) Sacroiliac joint 5) Coccyx 6) Pubis 7) Ischium 8) Pubic symphysis 9) Femoral/hip joint (Grey's anatomy 20th edition).

Three diametrical measurements, diagonally (oblique) (1), postero-anterior (2), and medio-lateral (3), are used to define the size of the pelvic cavity from the superior view (Gray, 1918). From the inferior view two diameters, postero- anterior (4) and medio- lateral (5) are used

to measure the pelvic cavity (figure 1.5). While these measurements are symmetrical in control subjects, in the scoliotic pelvis unequal radii in the pelvic cavity are reported (Boulay, 2006).

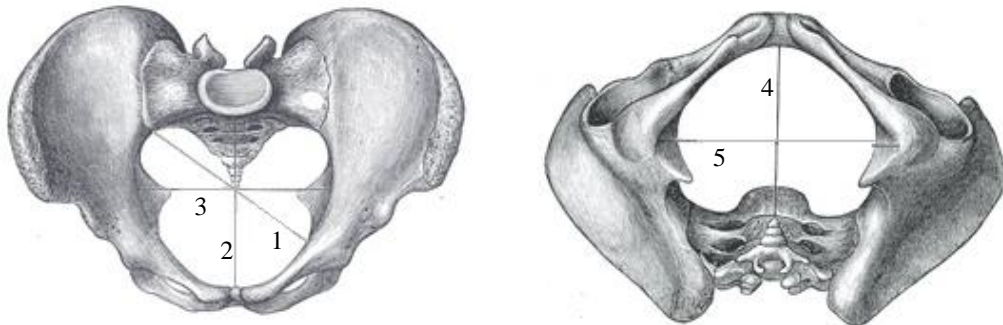


Figure 1.5: Pelvic diameters from top view: 1- Diagonally, 2- antero-posterior, 3- medio-lateral and from inferior view 4- antero-posterior, 5- medio-lateral (Grey's anatomy 20th edition).

1.1.3 Anatomy of the sacrum

Sacrum is a part of both spine and pelvis. More specifically, it contains of 5 fused vertebrae (figure 1.6). The sacrum movement with respect to the coccyx and between the sacrum bones is limited as a result of the specific shape and its restricted connection. Sacroiliac and iliolumbar ligaments keep the sacrum in its place. Consequently the main movement of the sacrum originates from the laxity and stretching of this group of ligaments (Gray, 1918).

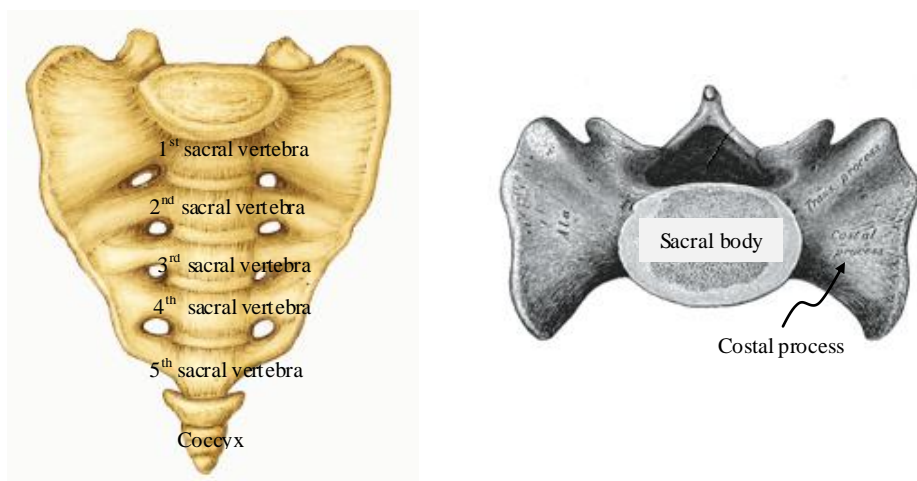


Figure 1.6: The sacrum anterior and top views (Gray's anatomy 20th edition), Consulted on January 2012 from <http://www.bartleby.com/107/24.html>.

1.1.4 Anatomy of the sacroiliac joint (SIJ)

The SIJ connects the ilium bones and sacrum in the posterior part of the pelvic ring. This joint is an amphiarthrodial joint, covered with cartilages. The SIJ is considered as two joints that connect the left and right sides of the sacrum to the left and right iliums respectively. The sacrum surface connects to the ilium via ligaments. This group of ligaments is divided in three parts based on their articulated section on the sacrum (Ellis, 2006) (figure 1.7). A detail description of this group of ligaments is presented shortly.

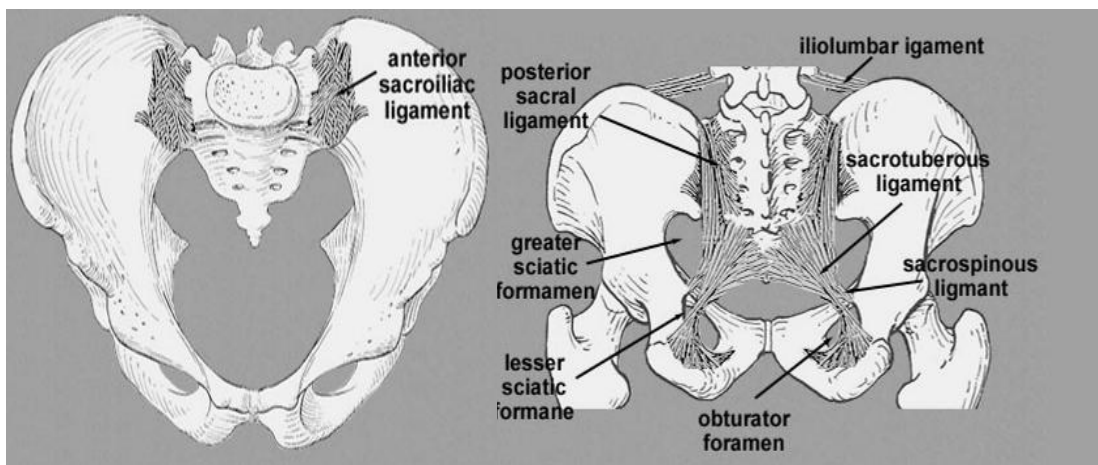


Figure 1.7: Anterior and posterior view of the pelvic ligaments. Consulted on August 2011 from: <http://home.comcast.net/~wnor/pelvis.htm>.

1.1.5 Sacroiliac joint function

The SIJ main function is the shock absorption between the pelvis and adjacent parts (Wilder, 1980; Lavignolle, 1983). The movement of this joint is limited and involves separation and elongation of the connecting ligaments (Wilder, 1980).

Another function of the SIJ is absorbing the shear force during gait (Wilder, 1980). The accelerating movement of the trunk and legs decelerates as the heel strike occurs. The changes in the movement acceleration cause a shear force at the SIJ which damps with SIJ ligaments (Wilder, 1980).

1.1.6 Sacroiliac joint ligaments

Sacroiliac ligaments guarantee the position of the sacrum with respect to the ilium. The range of motion of the sacrum is restrictedly dictated by these ligaments. The elongation of these ligaments makes the sacral motion possible. Sacrum is considered as a part of the spine as was explained in the section 1.1.1. Sacrum is also considered as a part of the pelvis (Gray, 1918) however its connection to the rest of the pelvis is ligamentous.

Three groups of ligaments connect different parts of the sacrum to the pelvis. This classification is based on the location of the origin point or direction of these ligaments on the sacrum.

a) Anterior sacroiliac ligament

Sacral anterior ligaments connect sacrum to ilium. Anterior sacroiliac ligament, iliolumbar ligament, and lumbosacral ligament connect to the sacrum and ilium superiorly. The sacrotuberous and sacrospinous connect the inferior part of the sacrum to the ilium (Gray, 1918).

b) Posterior sacroiliac ligament

Due to the specific shape of the sacrum and the load transmission between sacrum and ilium, the posterior ligaments are the most important group of ligaments in the sacrum-ilium junction. These ligaments are divided in two groups: 1. Lower part ligaments (long posterior sacroiliac ligament) which are aligned obliquely and attach the back of the lower part of the sacrum (third transverse tubercles) to the posterior superior part of the ilium, 2. The upper part ligaments (short posterior sacroiliac ligaments) which are aligned horizontally and attach the upper part of the sacrum (first and second transverse tubercles) posteriorly to the ilium (Gray, 1918).

c) Interosseous ligaments

This group of ligaments is deeply located at the posterior part of the sacrum and keeps the sacrum and ilium together (Gray, 1918).

Beside these three groups of ligaments, two more groups are linked between sacrum's parts or ilium sections only. Anterior longitudinal ligaments connect sacrum sections vertically. The Inguinal ligament connects the lower part of the ilium wing to the pubic bone anteriorly.

1.1.7 Pelvic muscles

Multiple pelvic muscles originate from various parts of the spine, pelvis, and lower extremities. Pelvic muscles originate from the pelvic ilium to lumbar spine (quadratus lumborum), thoracic spine (longissimus dorsi), the ribcage (iliocostalis lumborum), and inferiorly to the femur. Tables 1.1 and 1.2 summarize the origin-insertion and functionality of the muscle groups between the pelvis and lower extremities (Table 1.1) and between spine and pelvis (Table 1.2) (Ellis, 2006). Figure 1.8 depicts this group of muscles.

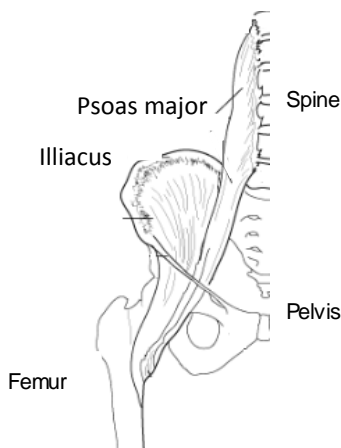


Figure 1.8: The anterior view of the Psoas and Iliacus muscles position. Consulted on December 2011 from: <http://musclerad.blogspot.ca/2011/12/psoas-major-muscle.html>.

Table 1.1 : Muscles originating from the pelvis and inserting in the lower extremities

Muscle	Origin	Insertion	Function
Internal and Extensor obturator	Obturator foramen	Trochanteric fossa	Hip external rotation
Quadratus femoris	Ischial tuberosity	Intertrochanteric crest	Hip external rotation , thigh and hip adduction
Superior and inferior gemelli	Ischial spine and ischial tuberosity (respectively)	Greater trochanter	Assist internal obturator

Table 1.2: Muscles connecting the pelvis to trunk

Muscle	Origin	Insertion	Function
Lattisimus dorsi	Posterior third of the iliac crest	Upper limb	Shoulder adduction, internal rotation.
Erector spinae Lateral superficial iliocostalis lumborum and longissimus thoracis	Posterior part of the sacrum and iliac crest	Spinous processes of T1 and T2 and cervical vertebrae	Spinal extension (bilateral action) Spinal lateral bending (unilateral)
Erector spinae Medial deep Straight and oblique	Sacrum	Spinal processes	Lateral bending Oblique spinal rotation Spinal extension
Abdominal muscle:Superficial (transversus and external oblique and internal oblique)	Ribcage	Iliac crest	Spinal axial rotation
Abdominal muscle deep (Rectus abdominis)	Rib cage 5 th , 7 th and sternum	Pubic crest	Trunk flexion
Quadratus lumborum	Iliac crest	12 th rib and lumbar vertebrae 1 to 4	Trunk lateral bending
iliopsoas (psoases minor and major)	Lesser trochanter and iliacus,	Iliac fossa	Flexes and externally rotates the hip joints. Trunk lateral bending and trunk flexion from the supine position.

1.2 Scoliotic spine and pelvis

The morphology of the spine and pelvis is subject to changes during the scoliotic progression. Various parameters and measurements are conventionally used in clinics to evaluate the scoliotic deformities in patients.

1.2.1 Scoliotic spine deformities

Spinal deformities in scoliosis appear in coronal, axial, and sagittal planes. The magnitude of the scoliotic curves in the coronal plane is calculated by the Cobb's angle, which represents the angle between the lines perpendicular to transitional vertebrae endplate of each curve (figure 1.9). The analytical Cobb angle is an alternate measurement and is defined by the lines perpendicular to the spinal curve at the location of its inflection points. Thoracic kyphosis and lumbar lordosis are measured in the sagittal plane. Vertebral rotation in the transverse plane and vertebral deformation (wedging) are also reported in scoliosis (Stokes, 2001).

Scoliotic spinal deformities can occur in one or many of the spinal sections including the cervical, proximal thoracic, main thoracic, thoraco-lumbar, lumbar and/or lumbo-sacral curves. Cervical and lumbar lordosis and thoracic and sacral kyphosis which are measured in the sagittal plane are also subject to change during the progression of scoliosis.

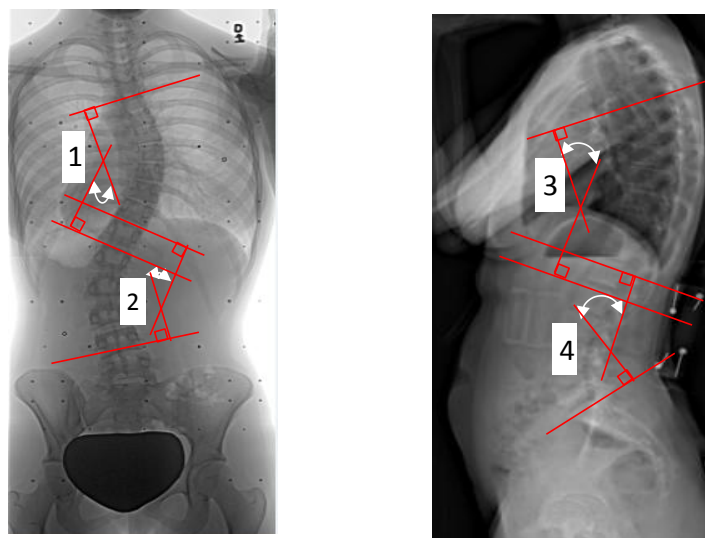


Figure 1.9: Traditional method in measurement of the 1) Thoraco-lumbar curve Cobb's angle, 2) kyphosis and 3) lordosis in a scoliotic subject (Saint- Justine University Hospital database).

The degree of the thoracic and lumbar spines rotation was explained in Stagnara's "Plan d'élection" (1985). A view of the spine in the transverse plane was developed to measure the orientation of the plane of maximum curvature in the scoliotic spine (Labelle, 2011).

1.2.2 Pelvic parameters in scoliosis

Scoliosis is associated with changes in the pelvic morphology and orientation (Boulay, 2006-a; Gum, 2007). Boulay (2006-a) measured unequal pelvic antero-posterior and medio-lateral diameters (figure 1.5). The position of the pubic bone, acetabulum, ischium, and the iliac crest width were measured on the radiographic images (Boulay, 2006-a; Gum, 2007). Unequal contra-lateral iliac crest wing width suggested a transversal rotation of the pelvis along with a torsion/ deformation of the pelvis in subjects. Gum (2007) showed that the pelvis is rotated in the direction of the major curve in the transverse plane. Also pelvic tilt in the frontal plane (pelvic obliquity) is reported in scoliotic subjects (figure 1.10) (Nault, 2002; Zabjek, 2005; Skalli, 2006).

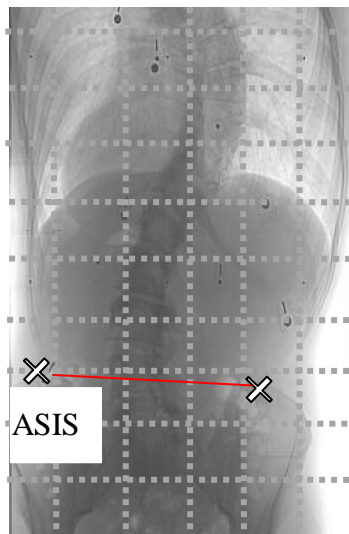


Figure 1.10: Severe pelvic obliquity determined by contra-lateral ASIS position in a subject with thoracic deformity (Saint-Justine University Hospital database).

3D measurement of the pelvic parameters showed that sacrum, iliac blade, iliac width, acetabulum, and the superior surface of the acetabulum are asymmetric in scoliosis (Boulay, 2006-a) (Figure 1.11). Also pelvic torsion was reported in this group of subjects: The upper part, measured from anterior and posterior contra-lateral iliac markers, rotates clockwise while the

pubic section rotated counter clockwise which consequently causes torsion in the pelvic body (Boulay, 2006-a) in non-scoliotic subjects (figure 1.12). It was suggested that pelvic rotation is more pronounced in scoliotic subjects and can be evaluated clinically by measuring the ASIS and PSIS orientation (Boulay, 2006-a). Similar results were reported in scoliotic subject with right thoracic deformity (Stylianides, 2012). The asymmetric iliac wing length was only significantly different in subjects with severe scoliotic deformities (Stylianides, 2012). However a recent study did not measure any asymmetry in the pelvic structure in scoliotic group and suggested that asymmetrical concave and convex sides iliac that appears on the antero-posterior radiographs are only due to the pelvic transverse rotation (Qiu, 2012)



Figure 1.11: Pelvic rotation in the transverse plane presented as unequal ilium width on the antero-posterior radiograph (Saint-Justine University Hospital database).

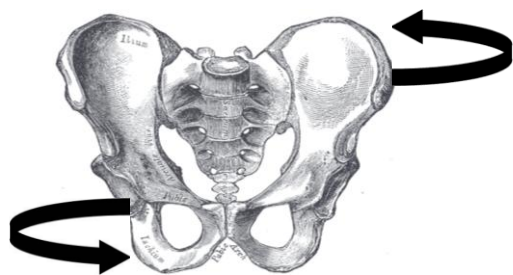


Figure 1.12: The presentation of the spiral path in pelvic rotation: upper part rotates clockwise while the pubic symphysis rotates counter clockwise (Boulay, 2006-a).

Furthermore sagittal pelvic parameters are defined by the relative alignment and orientation of the sacrum and femoral heads. Sacral slope (SS), pelvic incidence (PI), and pelvic tilt (PT) are the most widely used parameters in evaluation of the sagittal pelvic alignment in scoliotic and spondylolisthesis subjects. The relationship between these parameters and the sagittal profile of the spine is also investigated in pre- and post operative subjects.

More precisely, the SS is defined as the angle between the horizontal line and line parallel to the sacral endplate. PI is the angle between the line connecting the center of the femoral head to the center of the sacral endplate and the line perpendicular to the sacral endplate. Finally, PT is measured as the angle between the line connecting the center of the femoral head to the center of the sacral endplate and the vertical line. Equation 1.1 relates these three parameters. Furthermore pelvic overhang is used to measure the distance between the femoral head and the midpoint of sacrum in the sagittal plane (Labelle, 2005) (figure 1.13).

$$PI = PT + SS \quad \text{Equation 1.1}$$

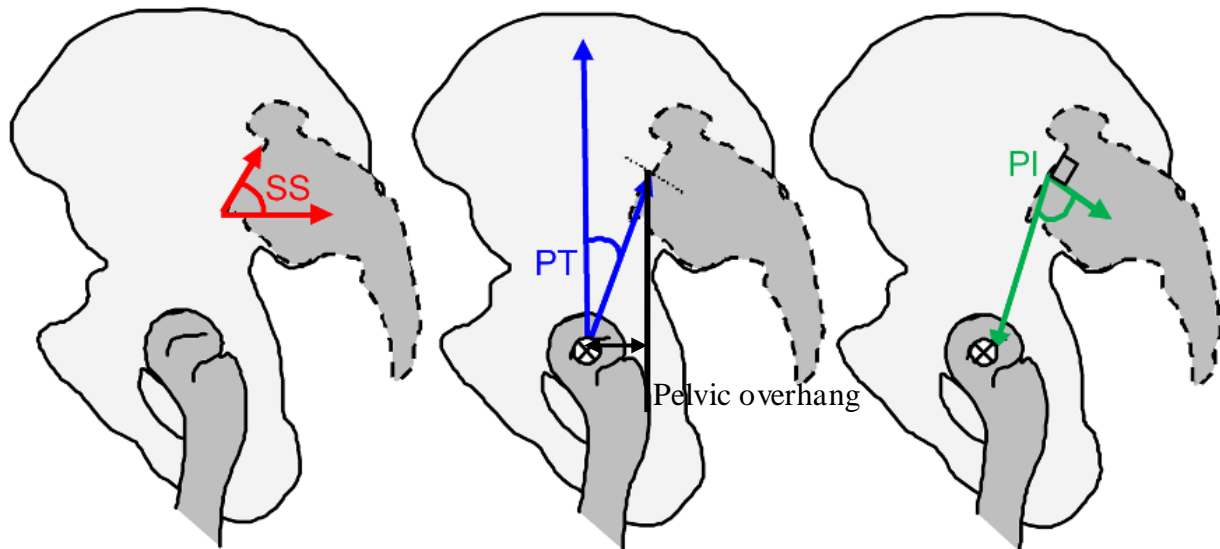


Figure 1.13: Sacro-iliac parameters: pelvic tilt (PT), pelvic incidence (PI), sacral slope (SS) and pelvic overhang.

1.3 Spino-pelvic relative alignment

The interaction between thoracic and lumbar spines and the pelvis is shown in controls and scoliosis (Mac-Thiong, 2003, Berthonnaud, 2005; Roussouly, 2005; Roussouly, 2011). It was observed that any variation in geometry or alignment of one section impacts the biomechanical behavior of the adjacent sections (Duval-Beaupère, 2004; Berthonnaud, 2005; Roussouly, 2011). This mechanism is more pronounced in subjects with musculoskeletal disorders such as in scoliosis (Mac-Thiong, 2003; Roussouly, 2011). Moreover the relative alignment of the spine and pelvis is essential to conduct the force between the spine and the pelvis and consequently to keep the upright position balance in humans (Jiang, 2006). This effect subsequently shows the importance of the relative spino-pelvic alignment in upright standing position.

1.3.1 Spino-pelvic alignment in controls

The pelvis is the bony connective structure between the spine and the lower extremities. Several studies have highlighted the importance of the pelvic alignment with respect to the spine in the standing postural balance (Snijders, 1998; Li, 2004; Jiang, 2006).

The correlation between the spinal and pelvic parameters particularly in the sagittal plane was measured in several studies. Guigui (2003) measured the angle between different vertebrae in thoracic and lumbar sections as well as the magnitude of the spinal curvature and trunk and pelvis inclinations. Significant correlations were found between the trunk inclination and SS, SS and lordosis, and SS and pelvic tilt. An independent linear correlation between pelvic inclination, sacral slope, lumbar lordosis, and thoracic kyphosis was reported. The same correlation between spinal and pelvic parameters was reported by (Vialle, 2005) wherein spinal and pelvic sagittal parameters in a group of healthy adults were measured.

Berthonnaud (2005) showed a significant correlation between each two adjoining shape parameters *i.e.* cervical lordosis, thoracic kyphosis, lumbar lordosis, PI, SS, and PT and orientation parameters *i.e.* the angle between the line connecting the two ends of each spinal section and the vertical line in a group of 160 asymptomatic adult sagittal radiographic images. PI and SS significantly were correlated to the lumbar tilt and lumbar lordosis while PT was only correlated to the lumbar tilt. A higher correlation was found between the lumbar and pelvic parameters in comparison to the correlation between the thoracic and lumbar parameters.

Considering the coefficient of the correlations, a strong relationship was found between the shape and orientation parameters in the most flexible parts of the spine *i.e.* lumbar and cervical spine. The results revealed the link between the spine and pelvis orientation and suggested the likelihood of the rearrangement of the each segment to compensate for alignment of the adjacent part. While this study established the linkage between several parameters in the sagittal plane any correlation between spinal and pelvic parameters in the frontal plane remains unclear for subjects with scoliotic deformities.

Considering the relationship between the spine and pelvic parameters in controls, Boulay (2006-b) in a study on 149 control subjects investigated the possibility of the existence of an equation that relates the lumbar lordosis and the sacro-pelvic parameters. A multivariate analysis using the lumbar lordosis as the predicted variable was used to formulate the lordosis as a function of kyphosis, sacro-pelvic parameters, T9, and L1 tilt (figure 1.14). The lordosis predictive equation was formulated in equation 1.2. The parameters are presented in degree.

$$\text{Lumbar lordosis} = -9.13 + 0.19 \times \text{Kyphosis} + 1.54 \times \text{SS} - 0.27 \times \text{PI} + 1.39 \times \text{T9}_{\text{tilt}}$$

Equation 1.2

A new factor that was brought out in the study by Boulay (2006-b) was the T9 tilt. The importance of this parameter can be explained by the correlation between T9 tilt and the position of the center of mass with respect to the coxo-femoral joint in the sagittal plane (Boulay, 2006-b). Boulay (2006-b) showed the role of the T9 tilt in prediction of the lumbar lordosis and its biomechanical impact on the position of the COM in asymptomatic subjects. Furthermore, this model was found to be robust in the prediction of the lumbar lordosis and can be used to define an “economic posture” during the bipedal standing position (Boulay, 2006-b).

Among pelvic parameters, the pelvic tilt modified the position of the gravity line (Roussouly, 2005). This study validated again the linear correlation between lumbar lordosis and sacral slope. Moreover Roussouly (2005) pointed out that since pelvic tilt is affected by the knee flexion, extra attention should be paid to keep the knees fully extended during the x-ray acquisition.

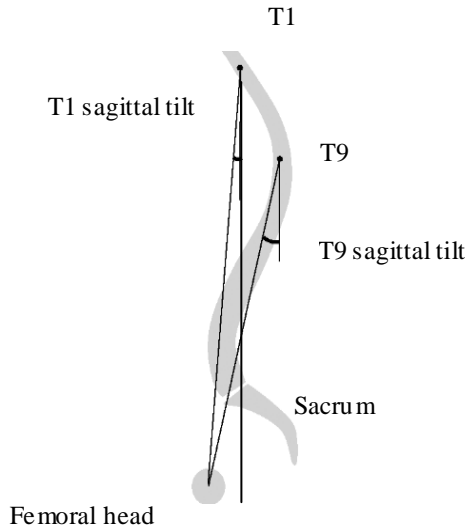


Figure 1.14: Spino-pelvic relative parameters in the sagittal plane used to describe postural equilibrium in subjects.

1.3.2 Spino-pelvic alignment in scoliosis

The spinal deformities in scoliosis affect the morphology and alignment of the shoulders, pelvis, and ribcage (Nault, 2002; Zabjek, 2005, Mahaudens, 2005; Gum, 2007; Mahaudens, 2008). To emphasize the biomechanical role of the pelvis in the spino-pelvic analysis Dubousset (1996, 1998) introduced the concept of the pelvic vertebra to show the close interaction between the spine and pelvis.

Moreover postural parameters in scoliosis have been associated with the postural balance in patients (Nault, 2002; Zabjek, 2005; Beaulieu, 2010) which highlights the importance of the postural analysis in AIS. Sagittal and frontal balances were introduced to assess the postural balance in AIS subjects and are defined as the angle between the vertical axis and the line connecting L5 and C7 in the sagittal and frontal plane respectively. These two parameters are shown in the anterior-posterior and sagittal views of the spine respectively in figure 1.15. Each dot shows the 2D position of the center of vertebra in the related anatomical plane.

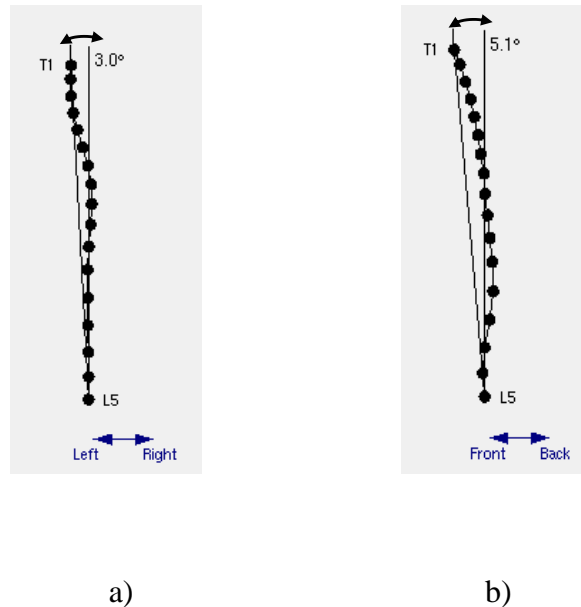


Figure 1.15: a) Frontal and b) sagittal balance defined as the angle between line connecting the T1 and L5 and vertical line in frontal and sagittal planes respectively. Viewed in Clinindexia software (Sainte Justine University Hospital, Montreal).

Legaye (1998) measured sacro-pelvic and sagittal spinal parameters on the radiographic images of the scoliosis subjects. These results suggested that pelvic incidence is an important anatomical parameter in regulating the spino-pelvic relative alignment in adults with scoliosis. Pelvic incidence is a determinant factor in the sagittal pelvic alignment and subsequently determines the lordosis magnitude.

Roussouly (2005) studied the correlation between the gravity line (calculated from the mean position of the center of pressure) and the plumb-line (vertical line passing through the center of C7 vertebra) in the sagittal plane. The results showed that the C7 plumb-line and the gravity line are not collinear in the sagittal plane. Hence the C7 plumb-line does not necessarily represent the sagittal equilibrium in patient. On the other hand the position of the gravity line was related to the postural parameters; the gravity line was located between the sacrum and the femoral heads and was related to the pelvic tilt. In other words, the pelvic tilt is in such way that minimizes the distance between the gravity line and the position of the femoral heads. Figure 1.16 shows the position of the CHVA, C7 plumb-line, and the trunk inclination in a patient.

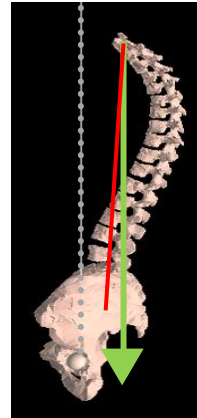


Figure 1.16: Position of the center of the femoral head vertical axis, trunk inclination —, and C7 plumb-line → . Clindexia software (Polytechnique Montreal and Saint-Justine University Hospital, Montreal).

Richards (2005) used the coronal spinal parameters to explain the relationship between the trunk and the pelvis in subjects with thoracic deformity. In this study coronal balance which was defined as the horizontal distance between C7 and the center of S1, lateral trunk shift and the apical thoracic vertebra shift were measured. A high correlation was found between these parameters in the frontal plane in main thoracic scoliotic subjects. The result suggested that in the thoracic subjects these three parameters are related.

Bearing in mind the relative alignment of the spine and pelvis in control subjects, Berthonnaud (2009) used spine and pelvis geometrical parameters to determine the stability in a limited number of scoliotic subjects. In this study C7, L5, femoral heads, and the center of the sacrum endplate were determined on the radiographic images. These parameters later were projected on the transverse plane. Four zones were defined based on the relative position of the femoral heads, sacrum, and C7 and the relative position of these parameters on the transverse plane was used to determine the different classes of stability.

Mac-Thiong (2003) and Mac-Thiong (2007) studied the spino-pelvic parameters in scoliosis and healthy adolescent controls. Although the magnitude of the spino-pelvic parameters varied between the two groups, the relationship between these parameters was similar. In other

words, the spino-pelvic relative alignment is in such a way that preserves the postural balance despite the spinal deformity. The relationship between the spino-pelvic alignment and the postural balance was highlighted in another study (Mac-Thiong, 2011).

Tanguay (2007) studied the relationship between the pelvic indices and lumbar parameters after surgery in AIS patients. The sagittal pelvic parameters were used to predict the lumbar lordosis after surgery. A high correlation was observed between lumbar lordosis and pelvic incidence in 272 healthy adolescents as following (equation 1.3):

$$\text{Lumbar lordosis} = 5.6 \times PI + 33.43 \quad \text{Equation 1.3}$$

The author suggested that the relationship between the lumbosacral parameters and lordosis should be considered during spinal instrumentation to sustain the spino-pelvic alignment.

The study by Schwab (2006) showed that the relative alignment and the position of the thoracic and lumbar deformities have an important role in patient health and should be considered in the treatment of the patients. This study also highlighted the regulative role of the pelvis in standing postural equilibrium. In another study lumbar lordosis also correlated to the balance and pelvic translation and rotation around the hip axis (Jackson, 1998). The result of this study was in line with the “Conus of economy” concept (Dubousset, 1994). This concept stated that not only the trunk and shoulders contribute in minimization of the muscles energy expenditure during standing but also the pelvis adjusts itself to control the muscle activation and provide postural balance.

Although the importance of the sagittal balance and its relationship to the spino-pelvic alignment is shown in different studies a protocol that relates the spino-pelvic parameters in 3D from a biomechanical point of view is not developed yet.

1.4 Kinematic of the spine and pelvic in scoliosis

The skeletal deformities in scoliosis are conspicuous and measurable on the patient's radiographs however the impact of these deformities on the kinematic function of the affected sections cannot be explored via these images.

The scoliotic spine kinematic is not investigated in detail *in vivo*, however the effects of the spinal disorders such as degenerative back pain on the kinematic of the movement has been

studied. Spinal disorders causing lower back pain impacts the spino-pelvic interaction (Marras, 1995; Lee and Wong 2002). Several studies have suggested a compensatory mechanism in the spino-pelvic interaction particularly in subjects with spinal disorders (Nelson, 1995; Granata, 2000; Milosavljevic, 2008). Scoliotic as a spinal deformity is not expelled from this conclusion; the compensative role of the pelvis in spinal kinematic has been observed during gait (Mahaudens, 2005) in scoliotic subjects (figure 1.17). Mahaudens (2005) measured pelvic parameters during static and gait in adolescent scoliotic subjects. These parameters were namely pelvic transverse rotation, pelvic obliquity, and pelvic inclination. Although these parameters were reported statistically different during quite standing, pelvic parameters were similar in control and scoliotic subjects during gait. This phenomenon was explained by increased spino-pelvic muscles energy expenditure and elongated muscle activation time in the AIS group.

Pelvic kinematic was compared post operatively (Skalli, 2006). Even though pelvis remains unfused in most surgical cases, its alignment is subject to change due to the spinal surgery (Skalli, 2006). In this study Skalli (2006) measured the pelvic alignment and range of motion in scoliotic subjects before and after operation using the reflective skin markers and motion capture system. Even though the shoulder and trunk alignment are improved significantly after operation, no single trend was reported in case of the pelvic realignment.



Figure 1.17: Kinematic analysis of the trunk-pelvic interaction by mean of motion capture systems in AIS during gait (Mahaudens, 2009).

One difficulty in interpreting the result of the studies by Skalli (2006) and Mahaudens (2005) originated from the studies sample; pelvic alignment in subjects with different types of the spinal deformities were measured and the average values were compared between scoliotic and control subjects. Considering that scoliotic subgroups present with different pelvic alignment (Gum, 2007) such analysis does not capture the intra scoliotic subgroups differences and may bias the interpretation of the results.

1.5 Center of pressure and center of mass

1.5.1 Center of pressure: Facts and measurement

The position of the center of pressure (COP) is dictated by the position of the whole body center of mass (COM) and the effect of the central nervous system (CNS) to keep the position of the COM within the base of support (Chen, 1998). A larger COP-COM difference is known to be related to the larger neuromuscular demand (Beaulieu, 2009). This difference consequently can be used to evaluate the standing balance and stability of the human subject. There are various methods to directly calculate the COM of the body segments *in vivo* and *in vitro*, however the correlation between the COP and the COM is also functional in predicting the COM position.

1.5.1.1 Direct measurement of the COM

Direct measurements of the position of the COM divide in two groups of *in vivo* and *in vitro* measurements. While the body segment's COM measurement *in vitro* (cadaver) is not available in different populations or subjects with musculoskeletal disease, *in vivo* measurement proposes methods and materials which can be applied in a wide range of population. Many experiences primarily were demonstrated on the animal subjects. Huang (1983) used the computerized tomography method (CT) on the porcine specimens and then validated the results on different body sections after scarification; the comparison between two methods was promising. Dual energy x-ray absorptiometry (DXA) also was a useful method to obtain segmental body mass parameters *in vivo* (Durkin, 2002). The direct measurement of the COM although reduced the assumptions made in calculation of the COM position in individuals, its application is limited due to the invasive nature of the method and potential health risks (Pearsall, 1994). For example Zatsiorsky (1983) used *in vivo* gamma-ray scanning. In this method the gamma-ray intensity at the source and the distance between the source and the subject were

known. The gamma-rays intensities before and after penetration were compared and the amount of absorption was used to determine the section mass. This method, although accurate, imposes high risk factor to the human subjects and limits the application of the method in clinic.

Duval-Beaupère (1987) and Duval-Beaupère (1992) used the barycentremeter method to determine the weight of the spine and pelvis. Also the center of mass of each trunk slice, divided at the level of each vertebra, was measured in reference to a fixed coordinate system *in vivo*. A gamma-ray scanner was used to determine the mass and the center of mass of each slice from head to the coxo-femoral joint *in vivo* human subjects. Although the movement of the section affects the mass and the location of the center of mass, the error is smaller than 500-600 grams for the mass and 1 cm for the location of the center of mass (Duval-Beaupère, 1987). Nevertheless the effect of the spinal deformity or curve stiffness in scoliosis was not encountered in this experience.

1.5.1.2 Indirect measurement of the COM: Measurement of the COM via the position of the COP

COP registration and data processing

One method in indirect calculation of the COM is based on the center of pressure oscillation. In this method the COP oscillation and the projection of the COM position on the transverse plane are related.

Multidirectional force transducers (figure 1.18) are used to register the ground reaction force (COP oscillation) during the quiet stance. Piezoelectric sensors also can be used in a pressure mat which permits to study the pressure distribution under the feet.

In a force plate four transducers are installed at its corners measure the reaction force in three dimensions. The position of the center of pressure measures as the barycenter of the registered forces at each corner (Winter, 2009). When the dimension of the faceplate is known the 2D coordinate of the COP calculates using equations 1.4:

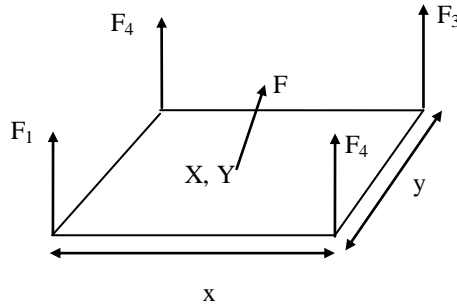


Figure 1.18: Force plate with four force transducers. (X,Y) determines the COP position, F is the reaction force, and F₁ to F₄ determines the registered force at each corner.

$$X = \frac{x}{2} \left(1 + \frac{(F_3 + F_4) - (F_1 + F_2)}{F} \right) \quad \text{Equations 1.4}$$

$$Y = \frac{y}{2} \left(1 + \frac{(F_3 + F_2) - (F_1 + F_4)}{F} \right)$$

where F is the sum of the registered forces by the transducers.

AMTI force plate is another kind of force place which is able to register 6 signals. Three force components F_x, F_y, and F_z and three moments M_x, M_y, and M_z are registered by a AMTI force plate. The position of the center of pressure in such force place calculates from equations 1.5:

$$X = -\frac{My + Fx * dz}{Fz} \quad \text{Equations 1.5}$$

$$Y = \frac{Mx - Fy * dz}{Fz}$$

where dz is the thickness of the face plate (41.3 mm).

The raw registered data should be processed before analysis. One goal of the data processing is noise reduction in the registered data. Curve fitting techniques and smoothing are of these methods. These techniques are based on the assumption that the signal follows a specific shape and the noise can be removed by finding the best fit for the registered data (Winter, 2009). Beside the curve fitting techniques, data filtering is also used to remove the noise from the signal. This method is based on distinguishing between the frequency content of the signals and noises. Once the signal frequency was determined the noise can be removed from the original signal.

Application of the COP data in determination of the COM position

The 2D position of the COP is used to define the projection of the COM on the transverse plane. The position of the body segment's center of mass can be calculated by measuring the position of the COP in two positions: standing position and lying on a simple bar or plate. One end of the bar is located on a force plate and the other end is fixed on the ground (reaction board). The COM of each section is calculated by the movement of the section and measuring the displacement of the COP (Pataky, 2003). The equilibrium equations are used to calculate the segment mass and the center of mass. The location of the joint should be fixed in reference to the force plate. This method can be repeated for all limbs. Although this concept is fairly simple it is rather time consuming and biased by the accuracy of the joint location and the whole body position. Damavandi (2009) used a modified version of this method by recording the COM in two positions (on the force plate and the reaction plate) with and without moving a segment. The results of this method were in line with the results of the COM position calculation via CT scans and MRI methods (Durkin, 2002).

Another method in calculating the COM by means of a force plate is the zero- to- zero point double integration technique. This method assumes that the projection of the COM on the transverse plane and the COP coincide in absence of the horizontal component of the ground reaction force. At the instance the COM can be calculated by double integration of the force in time intervals between two succeeding times when the horizontal component of the ground reaction is zero (Zatsiorsky and King, 1998). The modified version of this method which calculates a non-zero first and second constant was proposed by Zatsiorsky and Duarte (2000). The results were comparable with other methods presented in literature such as the segmental or MRI (Lafond, 2004).

Another proposed method in calculating the COM position is based on the correlation between COP and COM as a function of the oscillation frequency. Brenière (1996) showed that during standing the magnitude of the COP and COM positions with respect to each other changes by the same oscillation frequency. A discrete fast Fourier method was used to transform the COP time series into the frequency domain and multiplied by a low pass filter.

Where m is the body weight, g is the gravity, h is the COM height from the ankle, and I_A is the moment inertia of the whole body around the ankle. The range of the COP oscillation after passing the filter was assumed to be equal to the COM oscillation. Later an inverse fast Fourier transform was used to obtain the trajectory of the COM oscillation in the time domain. This method is more suitable in low frequency oscillation therefore its applicability is not evaluated in subjects with postural control deficiency.

Although different methods, as was explained, have been used to determine the personalized position of the COM, a method that estimates the position of the COM with respect to the center of vertebra and subsequently is applicable in numerical models of the scoliotic spine is not available yet. Such method is particularly important in biomechanical analysis of the scoliotic spine (Park, 2012).

1.5.2 Center of pressure related stability measurement in control and scoliosis

The CNS sustains the COM within the base of support during quiet stance (Zatsiorsky and Duarte, 2000). Increased COP oscillation has been reported in AIS (Beaulieu, 2009). An increased oscillation in the COP position can be explained by the CNS deficiency (Beaulieu, 2009) as well as postural and spinal deformity (Nault, 2002) in scoliotic subjects. The relationship between the postural parameters and COP oscillation has been used to explain the postural stability in AIS (Nault, 2002; Beaulieu, 2009; Dalleau, 2011).

Dalleau (2011) analyzed the oscillation of the COP and the position of the COM in control and scoliotic groups. The COM was calculated by the method explained in Damavandi (2009) and compared to the anterior-posterior and medial-lateral oscillation of the COP. The anterior-posterior offset of the COP (COP_{AP}) was anterior to the body COM in the control while COP_{AP} was posterior to the COM in the scoliotic group. In comparison to control subjects, the medio-lateral offset of the COM was lower and its antero-posterior offset was higher in scoliotic subjects. This effect was explained by the postural compensative mechanism in AIS; due to the spinal deformity head and trunk are tilted posteriorly which in turn causes an increase in the medio-lateral neuromuscular demand.

Nault (2002) showed decreased stability in adolescents with idiopathic scoliosis. The stability deficiency was characterized as the increased sway area of the COP and the COM as

well as a high difference between the COM and the COP oscillation. These findings suggested a higher neuromuscular demand to keep the standing balance despite the spinal deformity. Chen (1998) measured different COP related parameters such as COP sway area and radius and postural parameters in scoliotic subjects during quite stance and gait. An opto-electronic device was used to measure the range of motion of different body parts during gait. A higher COP sway area was measured in scoliotic subjects. The higher sway area interpreted as higher demands of the CNS and poor postural stability in scoliosis.

Schwab (2006) studied the postural parameters of asymptomatic and patients with back pain by using the gravity line. The result of this experiment showed the relationship between the spino-pelvic alignment and the postural equilibrium (Schwab, 2006). The results of studies by Steffen (2010), Schwab (2006), and Lafage (2008) showed that the relative position of the spino-pelvic parameters and the gravity line is significantly different in asymptomatic and patients with back pain. Postural parameters such as T1 and T9 sagittal tilts (figure 1.14), and sagittal and frontal balances (figure 1.15) were defined to assess the postural equilibrium by means of spino-pelvic parameters.

El Fegoun (2005) used the simultaneous radiograph and center of pressure acquisition to assess postural stability in scoliotic and control subjects. The main objective of this project was to validate the accuracy of the conventional plumb- line test and its correlation to the gravity line as a measure of the stability. The results showed a significant difference between the position of the gravity line and the plumb line in both sagittal and frontal planes in the scoliotic subjects while there was significant correlation in both sagittal and frontal plane in the control group. In addition the plumb line in the sagittal plane is affected by the shoulder position and knee flexion which is also a source of error in determination of the location of the plumb line via lateral x-ray images (Marks, 2003). The author suggested that the position of the gravity line is be a better index to determine the postural stability of the subject and is better to be replaced with the plumb-line method.

Several parameters that were explained in this section are used to assess the postural equilibrium and balance in scoliosis, an aspect that is known to be adversely affected during the progression of the scoliosis. In the next section the literature on the spinal equilibrium in scoliosis and other pathologies is summarized.

1.6 Spinal equilibrium in scoliosis

Spine has a key role in providing posture and movement in human body. Spinal stability is essential to guarantee and reinforce the posture. The effect of many spinal musculoskeletal or degenerative diseases on the overall stability of the patient has been reported (Panjabi, 1994; Panjabi 2003; Panjabi, 2007). Increased muscle activity duration and energy expenditure have been observed as a compensative mechanism that provides postural balance despite the postural deformities (Mahaudens, 2005).

From a mechanical point of view, stability is the optimal state of the equilibrium in a system. Considering the spine as a mechanical structure, Bergmark (1989) for the first time tried to formulate the spinal stability in human. Although the concept of the minimum potential energy and its correlation with the stability made it possible to quantify spinal stability in this study, high level of simplifications and assumptions in his model impacted the accuracy of the results. The concept of the minimum potential energy was applied in more detailed models and was combined with optimization methods to overcome the redundancy problem in calculation of the trunk internal forces (Cholewicki, 1997). Electromyography (EMG) assisted models were provided the model with more precise measurement of the agonist- antagonist muscle co-activation. The muscle co-contraction mechanism was observed as an important spinal stabilization mechanism (Gardner-Morse, 1995; Gardner-Morse, 1998; Granata 2001; Lee, 2002).

Although these models tended to formulate and estimate the spinal stability in different postures the spinal stiffness eventually interpreted as spinal stability. As an example some studies suggested that spinal stability is higher in high demanding tasks such as presence of an external load or during maximum trunk extension (Cholewicki and McGill, 1996; Marras, 1997; Lee, 2002) which are in contradictory with postural stability. These controversial results leave the exact definition of the spinal stability unanswered. Moreover scoliosis has been associated with vertebrae and intervertebral disk degeneration which in turn may cause local spinal instability (Adams, 2000). Detailed models of the spine have been able to assess local mechanical loading of the vertebral and intervertebral disk in patient-specific models of the spine. These biomechanical models have been developed to assess the spinal loading during brace treatment (Clin, 2009) and surgical correction (Wang, 2012).

1.7 Scoliotic spine modeling

Several methods exist to create spinal models. These methods each present with advantages and disadvantages and permit to study different aspects of the spine's mechanics and movement. Physical models create the geometry of the spine in 3D using different materials. One example of these models which specifically used to study scoliotic development was presented by Takemura (1999). In this model vertebrae were modeled by synthetic resin and intervertebral disks were modeled by silicon discs and were mounted on a metal frame. This model permitted to apply different force combinations to the spine to study the biomechanical origin of the scoliotic development. Application of the inorganic materials and simplifications in the manufacturing of the model made the applications of the model limited.

Kinematic models use the equation of the movement to derive the kinetic and dynamic of the body sections. The kinematic model of the lumbar spine by Van Deursen (2000) was able to measure the internal forces between the spine and pelvis due to the pelvic movement. Moreover the mathematical models were used to study the spine's dynamic. The commercial packages use forward kinematics and inverse dynamic technique to calculate the internal forces based on the kinematics of the movement in more complicated movements such as jumping (Opensim, CA, simtak.org and Lifemodele, CA, lifemodele.com).

Computer aided models of the scoliotic spine are used to assess the biomechanics of the scoliotic spine and simulate new treatment methods before application *in vivo*. Finite element (FE) models of the spine are used to determine the vertebral biomechanical loading. Different commercial softwares such as ANSYS and Abaqus can be used to provide a detailed model of the spine. Spinal sections are generated by appropriate element types. Materials properties are associated to each section from pertinent literatures. In the conventional method of the FE spinal modeling, the geometry of the spine is acquired from radiographic images. A 3D reconstruction technique is applied to calculate the 3D coordinates of the anatomical landmarks and finally these coordinates are used to create patient specific FE model of the anatomical parts such as spine, pelvis, and ribcage.

In addition to the skeletal geometry, muscles and soft tissues can be simulated in a FE model. Computed tomography (CT) scans, magnetic resonance imaging (MRI) and surface topography are used to obtain the geometry of the muscles and the trunk surface. MRI muscle

scan determines muscle cross section as well as origin and insertion of each muscle fascia and connective tissues (Parkkola, 1992).

The mechanical properties of the spinal components which subsequently impact the spinal stiffness are essential in biomechanical evaluation of the spinal forces. These parameters have been investigated *in vitro* (Panjabi, 1992; Stokes, 2001). Some studies have tried to personalize trunk stiffness (Perie, 2004; Petit, 2004; Lamarre, 2009) in human subjects. Lateral bending (Petit, 2004) and traction (Lamarre, 2009) are two methods that are used to determine the curve stiffness in AIS subjects pre-operatively. The lateral bending test is based on the degree of the correction of the spinal curve in the radiographic images while patient performs lateral bending. In this method the curve severity in standing position and lateral bending are compared in the anterior-posterior radiographic images. In the traction test the curve reduction during the suspension test is evaluated to assess the curve flexibility (Lamarre, 2009). Comparing these two methods *i.e.* lateral bending and suspension, the feasibility of the traction method was shown (Lamarre, 2009). This method was suggested to be used in evaluation of the spinal flexibility rather than the lateral bending test (Lamarre, 2009). However some parameters such as the position of the COM are not specifically personalized in numerical simulation of the scoliotic spine.

The 3D reconstruction of the spine and pelvis is used to determine the geometry of the spine from X-ray images (Cheriet 2002; Delorme 2003; Kadoury 2007-a). The precision of the spinal geometry depends on the quality of the X-ray images (Delorme, 2003). EOS system (Biospace, Paris) bi-planar radiography minimizes the patient movement in comparison to the conventional radiography techniques (Dubousset, 2004). In the 3D reconstruction of the X-ray images direct linear transformation (Delorme, 2003), non- stereo corresponding algorithm, and the free form morphing technique (Kadoury, 2007-a; Kadoury, 2007-b) are used. In addition to the x-rays images, computed tomography (CT) can be used to obtain the geometry of the spine by millimetric scans on the patient body. However this method is not usually applied in the standing position which subsequently impacts the geometry of the spinal deformity in the scoliotic spine (Duke, 2005). Detailed FE models are used to study the biomechanical effects of the brace treatment (Clin, 2007), patients positioning during surgery (Driscoll, C.R., 2011), and fusion-less spinal correction (Driscoll, M., 2009) in scoliosis (figure 1.19).

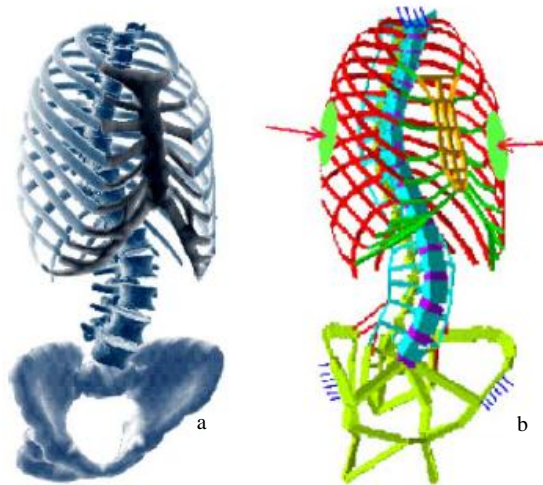


Figure 1.19: a) 3D reconstruction of the spine, pelvis and ribcage b) The corresponding FE model of the anatomical sections (Aubin, 1996).

The biomechanical multibody models of the spine are composed of rigid bodies and flexible elements for vertebra and intervertebral disks respectively. The force/ deformation nonlinear relationship was defined mathematically in this model. Personalized mechanical properties of the spine can be adapted to the model using the lateral bending test (Petit, 2004). This model particularly has assisted in surgical decision making process of the spine (Wang, 2012) (figure 1.20). Although the simulation time is reduced in these models, no local information about the vertebral biomechanical stresses is available.

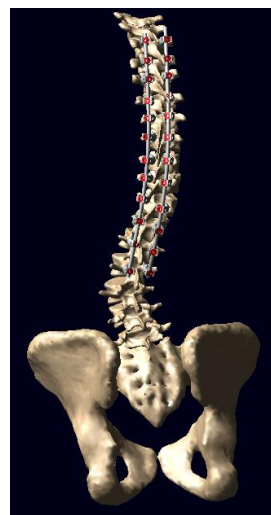


Figure 1.20: Biomechanical model of the spine and pelvis in MD ADAMS, 2010.

Hybrid models globally use a simplified geometry of the spine however refined properties are available for a specific section. In a model by Gharbi (2008) the back muscles in the finite element model of the spine, ribcage, and pelvis were included (figure 1.21). This model was refined in the low lumbar region (L4-pelvis region) to study the biomechanical factors involved in the development of spondylolisthesis. Two components of the sacral loading *i.e.* the shear and bending moments were of parameters that can result in development of spondylolisthesis. A similar FE model was used to study the effect of the pelvic parameters on the sacral loading such as compressive stress and sheer stress in different types of spondylolisthesis (Sevrain, 2012) (figure 1.22).

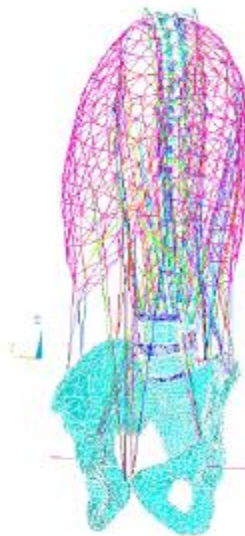


Figure 1.21: Hybrid model of the spine (Gharbi, 2008)

The simulation of the spinal muscles is accompanied by several assumptions. Co-contraction and agonist- antagonist muscle activation makes the simulation of the spinal muscle more intricate to solve. The concept of the follower load was used to simplify the application of the muscle forces in numerical models of the spine and solve the redundancy problem (Patwardhan, 1999; Rohlmann, 2001). Inverse and direct dynamic simulations are established to estimate the internal forces originated from numerous muscles and ligaments forces in the trunk (Gardner-Morse, 1995; Granata, 2001). Although these assumptions are vital to guarantee

the model convergence to a single solution but make the interpretation of the results limited and subject of discussion.

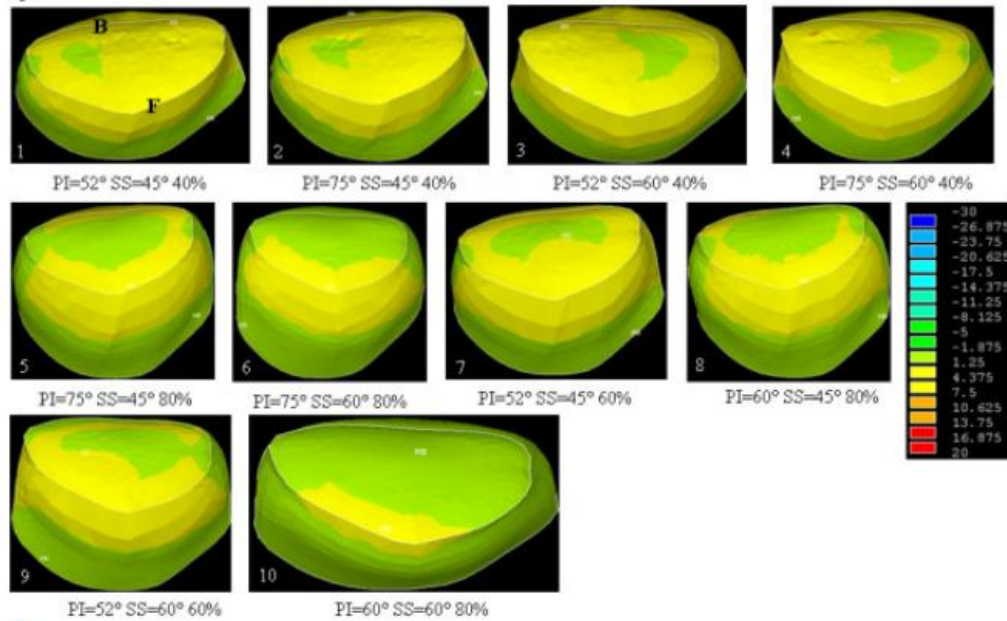


Figure 1.22 : Compressive stress distribution on the superior sacrum endplate (front (F) and back (b)) in spondylolisthesis subjects with different sacro-pelvic parameters (PI, SS, and slip percentage %) (Sevrain, 2012)

1.8 Scoliotic spine biomechanics before and after spinal fusion and instrumentation

The spinal instrumentation is applied to correct, control, and decrease the spinal deformity in scoliosis with a curvature higher than 40 degrees in frontal plane (Bridwell, 1999; Moen, 1999). Advanced instrumentation techniques are able to minimize the spinal deformity by segmental fusion (Hullin, 1991; McMaster, 1991). Various surgical methods and maneuvers are introduced and practiced among surgeons and the pros and cons of each method are determined (Lee, 2004; Majdouline, 2009). Although spinal surgery reduces the spinal deformity some complications have been reported post-operatively. Hypo-lordosis (flat back) (Bridwell, 1999; Umehara, 2000) and disk degeneration (Weiss, 2008) have been reported in post-operative

subjects. However the biomechanical origin of these problems has not been fully studied through comprehensive numerical models of the spine.

The effect of the different instrumentation devises on the biomechanical loading of the fused vertebrae has been studied (Wang, 2012). Finite element simulations were used to study the impact of the different spinal surgery methods on the spinal alignment in scoliosis (Stokes and Laible, 1999; Lafage, 2004). In FE model of the spine Lafage (2004) showed the effect of the instrumentation level on the spinal realignment and correction after spinal instrumentation. However the biomechanical impact of the spinal instrumentation on the distal unfused part of the spine is not well investigated in the patient-specific models of the AIS subgroups.

CHAPTER 2 OBJECTIVES AND HYPOTHESES

Although postural analysis is frequently used to evaluate skeletal deformities in scoliosis before and after treatment, the four following domains remain untouched or not fully explored:

- 1) The pelvic 3D orientation and its relationship with respect to the spinal deformities within different scoliotic types are not fully analyzed.
- 2) Although it is established that relative spino-pelvic alignment is affected in scoliotic subjects, the mechanism through which scoliotic parameters interfere with the biomechanical loading of the sacrum remains unknown.
- 3) A method to estimate the 3D personalized position of the center of mass which is applicable in numerical simulations of the scoliotic spine is not developed yet.
- 4) The impact of the surgical instrumentation of the spine on the biomechanical loading of the sacrum in scoliosis is not evaluated. Hence the way in which the correction of scoliosis impacts the position of the COM and the transferred load between the spine and pelvis through the sacrum is to be determined.

The general objective and four specific objectives were developed to address each of these problems separately:

General objective

The general objective of this Ph.D. thesis was to study the relationship between the spine and pelvic parameters in scoliotic subgroups. More particularly the objective was to investigate different aspects of the spino-pelvic interaction through different experimental setup in subjects with main thoracic and thoraco-lumbar deformities and to compare the results with an age-gender matched group of controls. To address this general objective, kinematic spino-pelvic interaction, the compensatory spino-pelvic alignment, and the biomechanical interaction between the spine and pelvis before and after operation were studied in the selected samples of the AIS subjects.

More specifically this main objective of this project was fulfilled through the four following specific objectives:

Objective 1

Study the 3D spino-pelvic range of motion during simple trunk movements in scoliotic subgroups and age-gender matched control subjects.

➤ Hypothesis 1

Scoliotic patients exhibit different spino-pelvic range of motion as compared to the controls in the 3 anatomical planes. Spino-pelvic range of motion is significantly different within the scoliotic groups and between AIS and controls ($p<0.05$).

Objective 2

Study the 3D orientation of the pelvis in static with respect to the spinal parameters in scoliotic subgroups and age-gender matched control subjects.

➤ Hypothesis 2

In addition to the spino-pelvic relationship in the sagittal plane, the pelvic orientation in scoliotic subjects is also related to spinal deformities in transverse and frontal planes. A statistically significant relationship exists between the pelvic 3D orientation (pelvic obliquity and pelvic axial rotation) and spinal parameters (thoracic and lumbar Cobb angles) in scoliotic subgroups in frontal and transverse planes ($p<0.05$).

Objective 3

Study the load transfer to the pelvis, and more specifically the compressive stress distribution on the sacral superior endplate in AIS subgroups and controls.

➤ Hypothesis 3

The position of the barycenter of the compressive stress distribution on the sacrum endplate is significantly different between subjects with different scoliotic types as well as between AIS subgroups and controls $p<0.05$.

Objective 4

Study the postural parameters and the biomechanical loading of the sacrum in AIS subjects with different curve types before and after posterior spinal instrumentation and fusion.

➤ Hypothesis 4

The compressive stress distribution on the sacrum is more equilibrated in scoliotic subjects after surgical spinal instrumentation as compared to the sacral loading before the operation. The position of the compressive stress distribution barycenter with respect to the center of the femoral heads is significantly different between pre- and post- operative patients and pre-operative patients and controls ($p<0.05$) while no such difference is observed between the post-operative and control subjects ($p>0.05$).

CHAPTER 3 PELVIC 3D KINEMATIC AND ORIENTATION IN ADOLESCENT IDIOPATHIC SCOLIOSIS

This chapter focuses on the pelvic parameters using kinematic analysis and radiographic measurements. Although it is established that sagittal spino-pelvic relative alignment is different from asymptomatic control in scoliotic subjects (Mac-Thiong, 2003, Berthennoud, 2005) it is not known to what extent the kinematic of the movement is affected by the skeletal deformities in scoliosis. More particularly the pelvic kinematic and the spino-pelvic interaction during trunk movement is not analyzed in AIS subjects with different curve types closely. In the current literature, the relative spino-pelvic alignment is defined with sacro-pelvic parameters which do not characterize the 3D orientation of the pelvis with respect to the spine.

To address the spino-pelvic interaction in AIS first parameters that define the global pelvic orientation should be identified. In this chapter, 3D pelvic parameters were defined to study the pelvic range of motion via kinematic analysis of the motion and later the same parameters were used to characterize the 3D spino-pelvic alignment in static in scoliotic subgroups.

Therefore this chapter consists of two sections: the first part of this chapter focuses on the 3D assessment of the spino-pelvic interaction in scoliotic subgroups during simple trunk movements (objective and hypothesis 1). Although kinematic data was registered throughout the experiment only explicit parameters were selected to characterize the spino-pelvic kinematic interaction at the maximum range of movement. Once the importance of the pelvic orientation in the spino-pelvic motion was shown kinematically, driven parameters in the first section were used to study the pelvic orientation in the second part of this chapter. Using this approach, the 3D orientation of the pelvis with respect to the spinal deformities in static in AIS subgroups was analyzed more closely (objective and hypothesis 2). This sequence (kinematic analysis before static analysis) was selected to first define the pelvic parameters affected by different motion types through the first manuscript and then apply these parameters in static evaluation of the spino-pelvic orientation.

3.1 Presentation of the first article

The analysis of the pelvic kinematic in two different scoliotic groups is presented in the first manuscript. This article addresses the first objective and hypothesis presented in this thesis.

The article “Characterizing pelvis dynamics in adolescent with idiopathic scoliosis” was published in August 2010 in the Spine Journal. The contribution of the first author in preparation and edition of the article is evaluated at 85%.

3.2 First article: Characterizing pelvis dynamics in adolescent with idiopathic scoliosis

^{1,2} Saba Pasha, ^{1,2}Archana P. Sangole, ^{1,2} Carl-Eric Aubin, ² Stefan Parent, ² Jean-Marc Mac Thiong, ² Hubert Labelle

1. École Polytechnique de Montréal

Dept. Mechanical Engineering

P.O. Box 6079, Station “Centre-ville”

Montréal (Québec)

H3C 3A7 CANADA

2. Research Center, Sainte-Justine University Hospital Center

3175, Cote Sainte-Catherine Road

Montréal (Québec)

H3T 1C5 CANADA

Running Head: Pelvic dynamics in AIS

Submitted to: Spine

Submitted on: August 2009

Corresponding author: Carl-Eric Aubin, PhD,

e-mail: carl-eric.aubin@polymtl.ca

Tel: (514) 340-4711 ext. 2834, Fax: (514) 340-5867,

École Polytechnique, Dept of Mechanical Engineering,
P.O. Box 6079, Station “Centre-ville”, Montréal (Québec), H3C 3A7 CANADA

3.2.1 Abstract

Study design. Pelvic dynamic analysis in adolescents with idiopathic scoliosis (AIS).

Summary of background data. Although studies have examined spine and pelvis postural differences between female adolescents with and without scoliosis much is still unknown about the dynamics of pelvis in trunk-pelvic interaction and how the type of scoliosis compromises pelvic mobility consequently impacting the overall dynamics of the trunk-pelvis kinematic chain.

Methods. 25 female adolescents with idiopathic scoliosis (18 right thoracic: RT and 7 right thoracic-left lumbar: RT-LL) and 12 controls were recruited. Reflective markers were placed on the trunk and pelvis and their trajectories were recorded using a 5-camera motion capture system. Subjects performed various trunk-pelvis movements (flexion-extension, lateral bend and axial rotation on the either sides), 3 trials each.

Results. Pelvic alignment in the three planes were significantly different for all movement types ($p<0.001$), with distinct differences in pelvic sagittal tilt and transverse plane rotation, particularly during lateral bending and axial rotation in patients with right thoracic and left lumbar curves ($p=0.035$, $p=0.006$ respectively). A majority of the patients from the two scoliotic groups had the pelvis rotated to the side of the major curve (right). While RT subjects had similar dynamic pelvic responses as the controls, the RT-LL patients had relatively more pelvic sagittal tilt during lateral bending and axial rotation towards the major curve.

Conclusion. In AIS, the initial 3D alignment of the pelvis (sagittal and frontal tilt, transverse plane rotation) plays an essential role in dictating the biomechanics of the pelvis for any movement type. A spatial concurrency in pelvic alignment was noted wherein a change in one parameter will impact the remaining two. Increased pelvic sagittal tilt in the RT-LL subjects was substituted by more pelvic rotation in the RT subjects during trunk flexion-extension. Differences in pelvic dynamics in AIS are not evident in discrete parameters e.g. total ranges-of-motion but more so in its biomechanics during the movement which in turn is dictated by the initial alignment of the pelvis.

Key words: scoliosis, pelvis, dynamic parameters, motion analysis.

Acknowledgements This study was funded by the Natural Sciences and Engineering Research Council of Canada (NSERC) and Fonds quebecois en recherche en nature et technologie (FQRNT).

3.2.2 Introduction

The sacrum and the pelvis represent the foundation of the spine¹. Both together serve as the connecting link between the lower extremities and the trunk. The concept of ‘pelvic vertebra’ in the scoliotic spine was introduced by Dubousset²⁻⁴, and later referenced by Skalli⁵, wherein the notion was to integrate the pelvis as a vertebral body in the treatment of extreme pelvic obliquity. From a biomechanical standpoint, it may be regarded as the unit of balance in this multi-link system, while also contributing to overall postural stability⁶. Pelvic mis-alignment⁷ and morphological asymmetry⁸⁻⁹ has been linked to the skeletal deformity in the scoliotic spine. These factors will impact its dynamical role in trunk-pelvis interaction.

Radiographic analyses have shown that the spinal deformity may cause the iliac wing/crest to appear wider on the side of the major curve in posterior-anterior radiographs indicating that the pelvis may be rotated in the direction of the thoracic deformity⁷. Skeletal asymmetry aside from that in the spine *e.g.* increased femoral neck-shaft angles on the opposite side of the structural spinal curve alter the loading characteristics in the pelvis¹⁰. Altered loading at the pelvis may be attributed to the coupled effect of transverse pelvic rotation in the direction of the major (thoracic) curve and increased femoral neck-shaft angles on the side opposite to the major curve.

Significant correlations between sagittal spine parameters (kyphosis and lordosis) and the sacro-pelvic morphological parameters: pelvic incidence, sacral slope and pelvic tilting have been reported¹¹. These parameters however are sagittal anatomical characterizations at the junction of the sacrum and pelvis which remain constant irrespective of the trunk-pelvis dynamics. They therefore cannot reflect any alterations/adaptations in the biomechanical role of the pelvis.

No significant difference in pelvic alignment was observed during gait¹² and quite standing stance¹³. One possible explanation may be the inclusion of patients with different scoliotic sub-types (thoracic, thoraco-lumbar and lumbar) thus masking any variability in pelvic

orientation, if it were present. Although radiographic measurements were different between the controls and subjects with scoliosis¹², no significant difference was observed in 3D kinematics. This may be attributed to the experimental protocol which did not isolate the pelvic dynamics specifically and perhaps gait-related parameters that were measured *e.g.* cadence, speed and stance-phase did not characterize adaptation/compensation that may be occurring at the pelvic level.

Although there are post-operative postural improvements such as decreased thoracic and lumbar Cobb angles and decreased shoulder rotation there is no reportable trend in post-surgical changes in pelvic alignment and range-of-motion⁵. In some patients the pelvis is retroverted before surgery and became anteverted after surgery. This clearly emphasizes the need to assess trunk and pelvic motion before surgery in order to retain as much pelvic range-of-motion (ROM) as possible since that of the spine is decreased⁵. This requires knowledge about the initial alignment of the pelvis relative to the spine in order to ensure reversing the pre-surgical pelvic alignment.

Although it is documented that scoliosis affects pelvic orientation it is unclear how pelvic orientation impacts the biomechanical role of the pelvis during trunk-pelvis dynamics. Knowledge of pelvic movement and its overall role in trunk-pelvis interaction could assist in determining surgical parameters particularly those related to mobility *e.g.* identifying lower end vertebra during spinal fusion. In addition, there are no specific protocols that address pelvic alignment while positioning the patient for surgery, much of the emphasis is on reducing the spinal deformity in the major curve. We hypothesize that there is an association between 3D spinal deformities and pelvic dynamic parameters. This can only be examined in an experimental set-up that specifically emphasizes on spine-pelvic interactive movement *e.g.* bending movements.

The study investigates pelvic orientation during different trunk movements in right thoracic and right thoracic left lumbar adolescent scoliotic subjects. The objective is to evaluate how AIS impacts the dynamics of the pelvis by examining correlations between the spinal deformity and pelvis biomechanics. We anticipate that correlations may be attributed to the compensatory role of the pelvis.

3.2.3 Materials and Methods

3.2.3.1 Subjects

Twenty-five female adolescents (mean age 14.4 yrs, range 10-17 yrs) with scoliosis participated in the study, of which, 18 were right thoracic (mean Cobb angle 22°, range 10°-45°) and 7 were right thoracic with compensatory curve at lumbar (mean Cobb angle thoracic 26° range 15°-57°, lumbar 27° range 12°-65°). Twelve adolescents (female, mean age 13.8 yrs, range 10-17 yrs) with no history of any musculoskeletal disorders, were recruited as controls. Participation of all subjects was voluntary and all were signed consent forms approved by ethics committee of CHU Sainte-Justine, Montréal.

Experiment set-up:

Seven reflective markers (10 mm diameter) were placed on the anterior (ASIS) and posterior (PSIS) iliac spine (left and right sides), C7 (7th cervical vertebra), shoulder acromion (left and right). Subjects were asked to perform three types of bending movements: flexion and extension, lateral bending and rotation on the either sides, 6 movements in total, 3 trials each. Every movement was performed starting from initial position to the maximum possible comfortable range and then return to the initial position. To minimize variability in overall posture while performing the movements subjects were asked to cross their arms in front of their torso while lightly touching their shoulders. Variability due to subject positioning was minimized by using a jig to set the subject's foot-stance and that of start-end position was controlled by requesting the subject to look at a fixed target on the wall which was adjusted to the subject's eye-level. A 5-camera motion capture system (Motion Analysis Corp, CA, USA) was used to record marker trajectories during the movement.

Data recording and motion analysis parameters:

The raw kinematic data was filtered using a 2nd order Butterworth filter (Matlab, Mathworks, Natick, MA, USA) with a cut-off frequency of 60 Hz. Movement onset ($M_{initial}$) was determined as the instance when the tangential velocity of the C7 marker exceeded 5% of its peak velocity and maximum trunk range-of-motion (ROM_{max}) was identified as the instance when the first maximal peak is attained. For axial rotation, the contralateral shoulder marker was used. For example, tangential velocity of the left shoulder was used to determine movement onset and

maximal ROM during axial rotation to the right. Figure 3.1 illustrates the marker configuration (Fig. 3.1A) and the identification of movement onset and max ROM (Fig. 3.1B). Only the movement segment to attain maximal ROM was analyzed in this paper.

Insert figure 3.1 near here

Pelvic alignment (sagittal, frontal and transverse) was defined as the relative orientation of the four pelvic markers ASIS and PSIS (left and right) with respect to the pelvic centroid (P_c) (Eqn 3.1). The three planar components of pelvic alignment were defined as the change in the orientation of a vector connecting the pelvic centroid (P_c) to the respective point as indicated below (Eqns 3.2a-3.2c), throughout the movement. Change in orientation was computed relative to the initial alignment.

$$\text{Pelvic centroid } (\overrightarrow{P_c}) = \frac{\text{ASIS}_{left} + \text{ASIS}_{right} + \text{PSIS}_{left} + \text{PSIS}_{right}}{4} \quad (3.1)$$

$$\text{Pelvic sagittal tilt: } P_c \rightarrow \frac{\text{ASIS}_{left} + \text{ASIS}_{right}}{2} \quad (3.2a)$$

$$\text{Pelvic frontal tilt: } P_c \rightarrow \frac{\text{ASIS}_{right} + \text{PSIS}_{right}}{2} \quad (3.2b)$$

$$\text{Pelvic transverse orientation: } P_c \rightarrow \text{ASIS}_{right} \quad (3.2c)$$

Maximal ROM for trunk flexion-extension and lateral bending was calculated as the angle between the initial and final position (ROM_{max}) of the vector connecting P_c to C7. For trunk axial rotation the contralateral shoulder acromion marker was used instead of C7. The pelvic parameters computed from the kinematic data for every movement type are continuous data and were normalized to ROM_{max} of each subject to facilitate inter-subject comparisons.

3.2.3.2 Statistical analysis

In the analysis, correlations between: pelvic initial alignment (parameters averaged over the time prior to movement onset (approx. 5 secs, $M_{initial}$) and sacro-pelvic radiographic parameters, kinematically derived pelvic parameters and scoliosis type were examined. For each subject, a 3D reconstruction of the spine was obtained from calibrated bi-planar radiographs [14]. The sacro-pelvic radiographic parameters (see Figure 3.2), pelvic tilt (PT), pelvic incidence (PI) and sacral slope (SS), were calculated from the 3D spine reconstructions.

Insert figure 3.2 near here

In summary, for each movement type, the following analyses were done:

- (1) Correlations between pelvic initial alignment and sacro-pelvic morphological parameters.
- (2) Correlations between pelvis alignment in the sagittal, frontal and transverse planes and movement type between groups.
- (3) Comparisons between ROM_{pelvis} and ROM_{max} .
- (4) Timing of pelvic involvement (sagittal, frontal and transverse).

3.2.4 Results

- (1) Correlation between pelvic initial alignment (derived from kinematic data) and sacro-pelvic morphological parameters (estimated from radiographs).

On examining the initial pelvic alignment, prior to movement onset, it was observed that patients with RT-LL scoliosis had a transversely rotated pelvis (in the direction of the major curve) while patients with RT scoliosis showed a similar pelvic alignment as the controls. A strong correlation ($r = 0.88$) was found in the RT-LL group between the kinematically derived pelvic frontal tilt and radiographic PT compared to that in the RT group ($r = -0.45$).

- (2) Correlations between pelvic alignment in the sagittal, frontal and transverse plane for each movement type between groups.

Both scoliotic groups had increased pelvic rotation during movements performed to the side opposite to the major curve *i.e.* lateral bending and axial rotation to the left, as compared to the same performed to the side of the major curve. In contrast, the control group showed more pelvic rotation during lateral bending and axial rotation to the right as compared to the same movement to the left. There was however no difference in the ROM_{max} between the same movements performed on each side, for all three groups. In general, for all movements, subjects with right thoracic scoliosis (RT group) were more similar to the controls in terms of planar contribution of the pelvis to the total ROM as compared to the right thoracic-left lumbar group.

Figure 3.3 illustrates the planar contribution of the pelvis at ROM_{max} for all movement types. As an example, consider lateral bending to the right. As seen in the figure, there is more sagittal pelvic tilt in the RT-LL group as compared to the RT and control group. This reflects a

spatial concurrency in the pelvic 3D alignment parameters (sagittal and frontal tilt, transverse plane rotation). A change in one parameter will consequently impact the remaining two parameters.

Insert figure 3.3 near here

Pelvic parameters derived from the kinematic data were significantly influenced by the movement type ($p<0.001$). There was a significant difference between groups in pelvic sagittal tilt and pelvic rotation ($p=0.035$ and $p=0.006$ respectively). The RT-LL subjects showed significant differences in pelvic sagittal tilt when compared to the RT subjects ($p=0.016$). The RT subjects showed significant differences in pelvic rotation as compared to the control group ($p=0.011$), particularly during axial rotation movement to the left. Both scoliotic groups exhibited pelvic frontal tilt comparable to the controls, for all movements with slightly increased tilt during axial rotation to the side of the major curve (right).

(3) Comparison between pelvic ROM (ROM_{pelvis}) and total ROM (ROM_{max})

In order to examine how much the pelvis contributed to the overall range-of-motion and whether the type of spinal deformity impacted this contribution pelvic ROM (ROM_{pelvis}) was compared with max ROM (ROM_{max}) (see Figure 3.4A). Pelvic ROM (ROM_{pelvis}) was estimated as the maximum 3D spatial movement of the pelvis for each movement type. This was resolved into its respective planar components (sagittal tilt, frontal tilt and transverse plane rotation). Although there was a significant difference in pelvic contribution to ROM_{max} between each movement type ($p < 0.005$) there was only a marginally significant difference ($p = 0.05$) between group types. There was however an interaction effect (see Figure 3.4B) particularly evident during axial rotation to the left *i.e.* opposite to the side of the major curve. There is less pelvic contribution in the RT subjects which remarkably increases in the RT-LL.

Insert figure 3.4 near here

(4) Timing of pelvic involvement (sagittal, frontal and transverse)

The kinematically derived pelvic parameters are continuous in nature and are computed throughout every movement type. Therefore every pelvic parameter (sagittal, frontal, transverse) is a trajectory over time for the duration of the movement. Thus the timing of pelvic involvement in a specific plane was identified as the instance when the movement in the respective plane

exceeded 5% of its maximal movement. For example, involvement of pelvic sagittal tilt towards achieving ROM_{max} was defined as the instance when the value of pelvic sagittal tilt exceed 5% of the maximal sagittal tilt for that movement. Table 3.1 lists the sequence of pelvic involvement in the three planes. Although a significant difference was found in the timing of pelvic involvement and movement type ($p<0.001$) no general trend was observed between groups. However, it was observed that during axial rotation to the left both the control and the RT group initiated pelvic involvement with pelvis transverse plane rotation while the RT-LL group initiated it with pelvic sagittal tilt.

Insert table 3.1 near here

3.2.5 Discussion

This study examined pelvis biomechanics during different trunk-pelvis movements in patients with right thoracic (RT) and right thoracic-left lumbar (RT-LL) scoliosis. Our findings showed that patients with RT-LL scoliosis had a transversely rotated pelvis (in the direction of the major curve) while patients with RT scoliosis showed a similar alignment as the controls. This may be attributed to the compensatory lumbar curve in the RT-LL group suggesting its increased influence on global pelvic alignment wherein the pelvis is oriented in the direction opposite to the lumbar curve in an attempt to maintain spinal balance. The kinematically derived pelvic frontal tilt captures the orientation of the pelvis as influenced not only by the lumbar spinal segment but also that of the proximal and main thoracic segments. The weak correlation between the kinematically derived pelvic tilt and radiographic PT Cobb in the RT group indicates that the sacro-pelvic parameters are local to the pelvis and are thus more influenced by the spinal deformity in the lumbar segment. From a computational standpoint, one possible explanation for the weaker correlation in the RT group is the manner in which the kinematic pelvic tilt is calculated. The kinematic tilt measure is derived from the inclination of the pelvic plane which in essence is influenced not only by the spinal deformity in the lumbar segment but also that in the proximal and main thoracic segments. Evaluating pelvic 3D alignment at maximal range of motion reflected a spatial concurrency in the parameters wherein a change in any one parameter consequently impacted the remaining two parameters thus changing the pelvis dynamics during the movement. Within this context, if the initial alignment of the pelvis is in the path of the movement, it continues along the same path thereby further increasing the inclination in three

planes during the course of the movement. On the other hand, if the initial pelvic alignment is not along the path of movement, the pelvis needs to first be re-oriented thus impacting pelvic orientation in the three planes. Our findings in the two scoliotic groups showed that the initial alignment of the pelvis plays an essential role in dictating the biomechanics of the pelvis for any movement type. A majority of the patients from the two scoliotic groups had the pelvis rotated to the side of the major curve (right). As a result during movements in the direction opposite to the major curve they used more pelvic rotation to the left to compensate to the initially rotated pelvis in the opposite direction. Differences between the two scoliotic groups indicate that the compensatory lumbar curve in the RT-LL group limits the rotation of the pelvis in the direction of the lumbar curve or opposite to the direction of the major curve. The overall findings suggest a need to take into account pelvic initial alignment during surgical planning. Knowledge of the initial pelvic alignment and the consequent biomechanical impact on trunk-pelvis dynamics could provide insights to define protocols or guidelines addressing pelvic alignment while positioning the patient during surgery. Although the timing of pelvic involvement was not entirely conclusive in terms of showing specific trends within the three groups the subtle differences does suggest that pelvic dynamics is impacted. This influence on pelvic dynamics is not evident in discrete parameters such as total ranges-of-motion but more so its biomechanics during the movement which in turn is dictated by the initial alignment of the pelvis.

Other studies such as that by Skalli⁵ showed that although the pelvis is not fused in the spinal instrumentation surgery its mobility changes due to increased spinal rigidity which consequently results in decreased total ROM. Their findings also demonstrate a close correlation between spine and pelvis dynamics which suggests more investigation about pelvic dynamic in scoliosis and the importance of the considering pelvic alignment during surgery. Our findings indicated that there is less pelvic contribution in the RT subjects which is remarkably increased in the RT-LL subjects. The increased pelvic contribution may be attributed to the compensatory lumbar curve which causes the lumbar segment and the pelvis to operate as a rigid link. This suggests that more inferior the spinal deformity greater is the compromise in the integrity of pelvic mobility because then it operates as a rigid link with the lumbar segment.

While the interpretation of our results is limited by the small number of subjects the findings do provide evidence that pelvic initial alignment needs to be considered during surgical planning. Furthermore, a majority of the patients that participated in the study had moderate

curves and very few were severe. Nevertheless, the findings of the study highlight how the dynamics of the pelvis is impacted by the spinal deformity in two groups of patients. The analyses, in its current form, may not necessarily be used as a clinical pre-surgical test. It is a first step towards demonstrating that pelvic dynamics is impacted by the spinal deformity and is characterized by initial pelvis mal-alignment. A more detailed experimental protocol involving activities of daily living (ADLs) is required to specifically investigate how and what percentage of spine-pelvis movement will be affected when subjects with AIS perform everyday activities requiring trunk-pelvis involvement.

3.2.6 Conclusion

Different initial pelvic alignment and pelvic dynamics between the two scoliotic groups may be attributed to the compensatory lumbar curve in the RT-LL group suggesting that the more inferior the deformity greater is the impact on the pelvic parameters. In scoliosis, increased pelvic tilt during lateral bending suggests an initial transversely rotated pelvic orientation. This rotation towards the major curve is more prominent in right thoracic-left lumbar patients. Although the compensatory lumbar curve decreases this effect in the initial position is further exaggerated during trunk movements by increased pelvic tilt. While the results presented in this paper provide evidence that pelvic dynamics in AIS is impacted by the spinal deformity and is characterized by initial pelvis mal-alignment, the findings are limited in specifically commenting on how to align the pelvis during surgical positioning, which is the eventual goal. A better understanding of pelvic alignment and its dynamics in scoliosis will provide additional insights that may assist in considering pelvic position during surgical planning. This study is the first to explicitly demonstrate the dynamics of pelvis in trunk-pelvic interaction and how the type of scoliosis compromises pelvic mobility consequently impacting the overall dynamics of the trunk-pelvis kinematic chain. A retrospective study with more severe cases and requiring pre- and post-operative pelvic initial alignment evaluation is required to further understand how different surgical strategies impact spine-pelvic biomechanics.

3.2.7 References

1. Artlet V. Surgical anatomy of the sacrum and pelvis. In: Dewald, R. ed. Spinal Deformities: The comprehensive text. NY, Thieme Medical Publishers 2003, 2-13.
2. Dubousset J. Importance de la vertèbre pelvienne dans l'équilibre rachidien. In : Application à la chirurgie de la colonne vertébrale chez l'enfant et l'adolescent Pied, équilibre et rachis. Paris: Frison –Roche; 1998: 141-148.
3. Dubousset J. Pelvic obliquity correction. In: Margulies JY, Floman Y, Farcy JP, Neuwirth M eds. Lumbosacral and spino-pelvic fixation. NY, Lippincott-Raven 1996: 39-49.
4. Dubousset J. Three dimensional analysis of the scoliotic deformity. In: Weinstein, S.L., ed. The Pediatric Spine: Principles and Practice, NY, Raven Press 1995: 479–495.
5. Skalli W, Zeller RD, Miladi L, Bourcereau G, Savidan M, Lavaste F, Dubousset J. Importance of pelvic compensation in posture and motion after posterior spinal fusion using CD instrumentation for idiopathic scoliosis. Spine 2006; 31(12): E359-366.
6. Jiang Y, Nagaski S, You M, Zhou J. Dynamic studies on human body sway by using a simple model with special concerns on the pelvic and muscle roles Asian Journal of Control 2006; 8(3): 297-306.
7. Gum JL, Asher MA, Burton DC, Lai S-M, Lambart LM. Transverse plane pelvic rotation in adolescent idiopathic scoliosis: Primary or compensatory? European Spine Journal 2007; 16:1579-1586.
8. Burwell, R.G., Freeman, B.J., Dangerfield, P.H., Aujla, R.K., Cole, A.A., Kirby, A.S., Polak, F., Pratt, R.K., Webb, J.K., Moulton, A., 2006. Etiologic theories of idiopathic scoliosis: Neurodevelopmental concepts of maturational delay of the CNS body schema ('body-in-the-brain'). *Studies in Health and Technology Informatics*. 123 pp. 72-79.
9. Schwender JD, Denis F. Coronal plane imbalance in adolescent idiopathic scoliosis with left lumbar curves exceeding 40 degrees. The Role of the Lumbosacral Hemicurve. Spine 2000; 25 (18): 2358-2363.
10. Saji M, Upadhyay S, Leong J. Increased femoral neck-shaft angles in adolescents idiopathic scoliosis. European Spine Journal 1995; 7: 99-103.

11. Legaye J, Duval-Beaupère G, Hecquet J, Marty C. Pelvic incidence: a fundamental pelvic parameter for three-dimensional regulation of spinal sagittal curves. European Spine Journal 1998; 7:99-103.
12. Mahaudens P, Thonnard J-L, Detrembleur C. Influence of structural pelvic disorders during standing and walking in adolescents with idiopathic scoliosis. The spine Journal 2005; 5:427-433.
13. Zabjek KF, Leroux MA, Coillard C, Rivard CH, Prince F. Evaluation of segmental postural characteristics during quiet standing in control and Idiopathic Scoliosis patients, 2005, Clinical Biomechanics; 20:483-490.
14. Delorme S, Petit Y, de Guise JA, Labelle H, Aubin CÉ, Dansereau J. Assessment of the 3D reconstruction and high-resolution geometric modeling of the human skeletal trunk from 2D radiographic images. IEEE Transactions on Biomedical Engineering 2003; 50(8): 989-998.

3.2.8 Figures and Tables

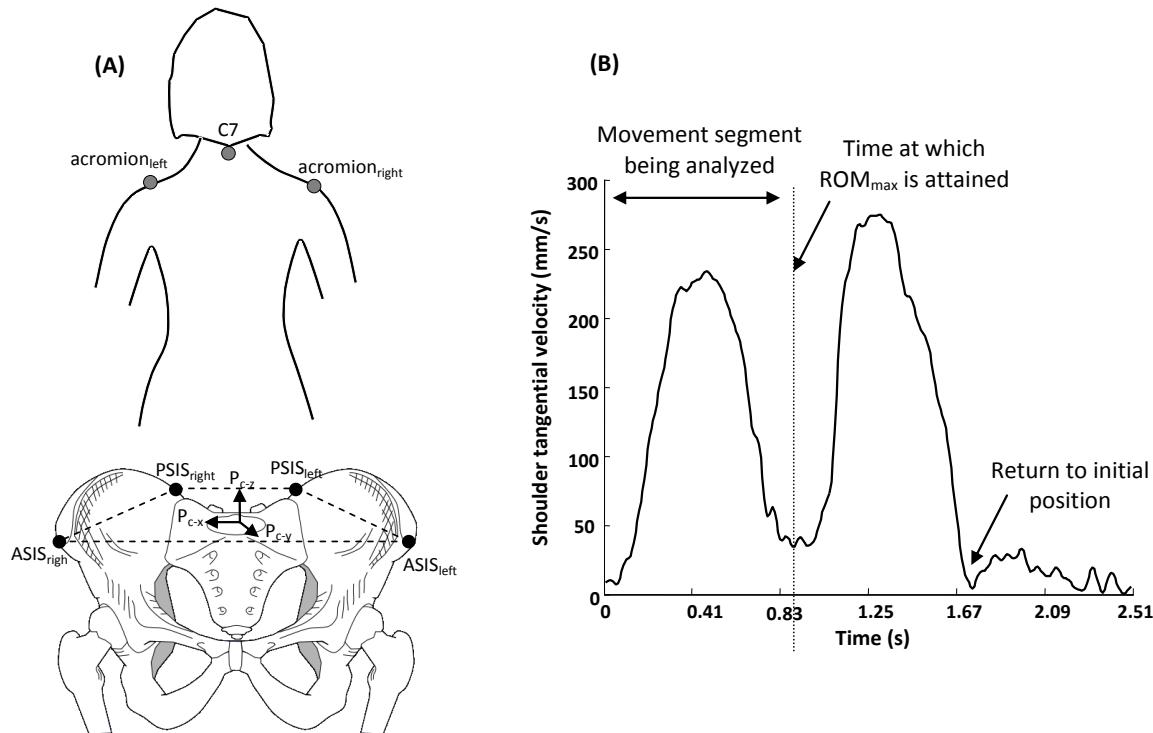


Figure 3.1: (A) Marker configuration on the torso and pelvis; (B) Identification of movement onset and maximal range-of-motion (ROM_{max}).

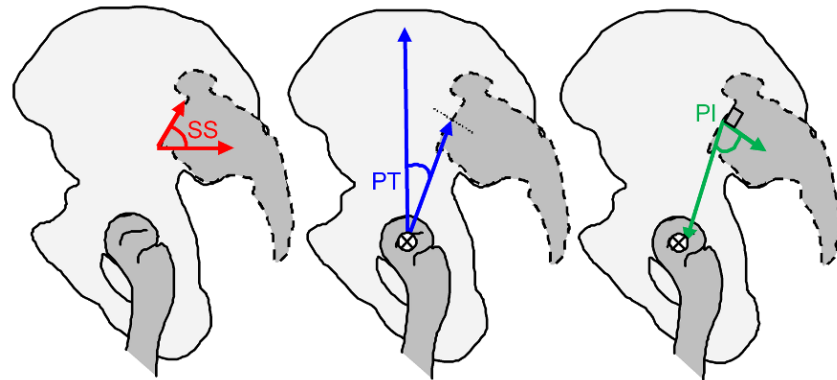


Figure 3.2: Sacro-pelvic morphological parameters: pelvic tilt (PT), pelvic incidence (PI) and sacral slope (SS)

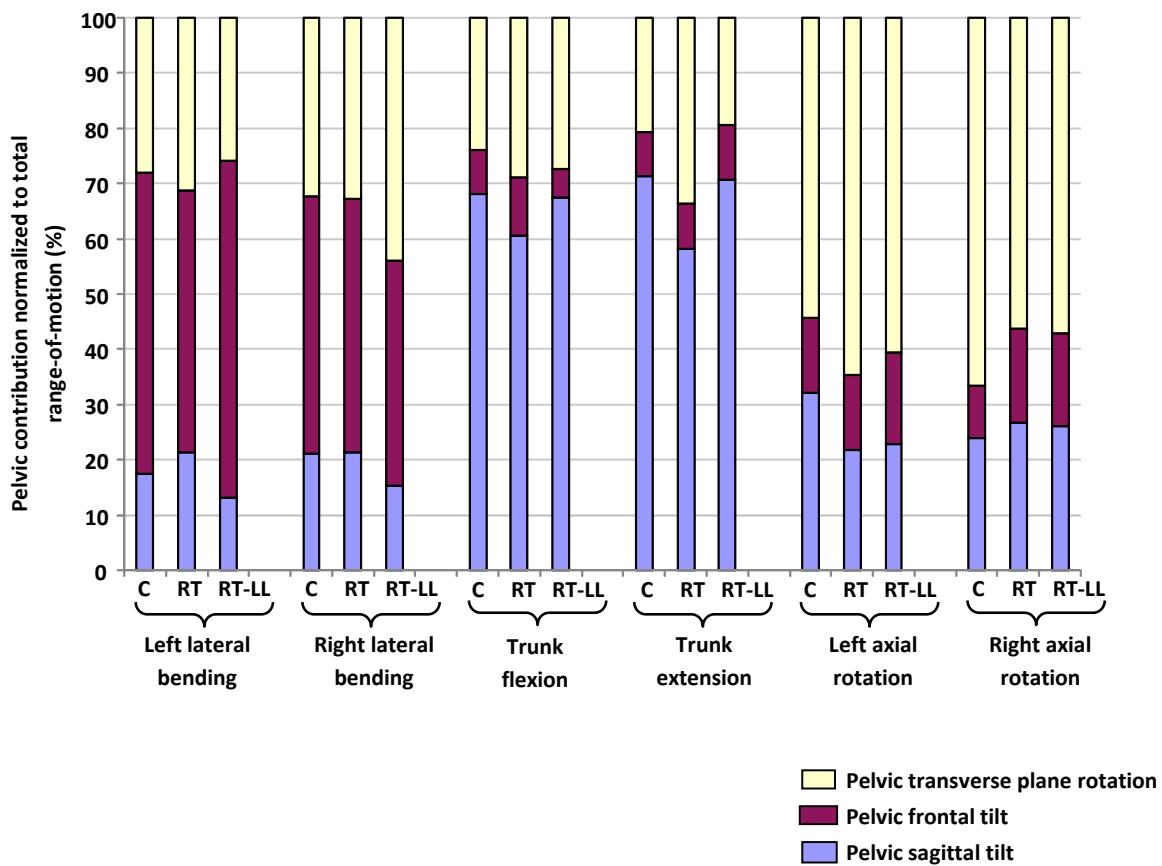


Figure 3.3: Pelvic alignment in the three planes (sagittal, frontal and transverse) for each movement type at maximum range of motion.

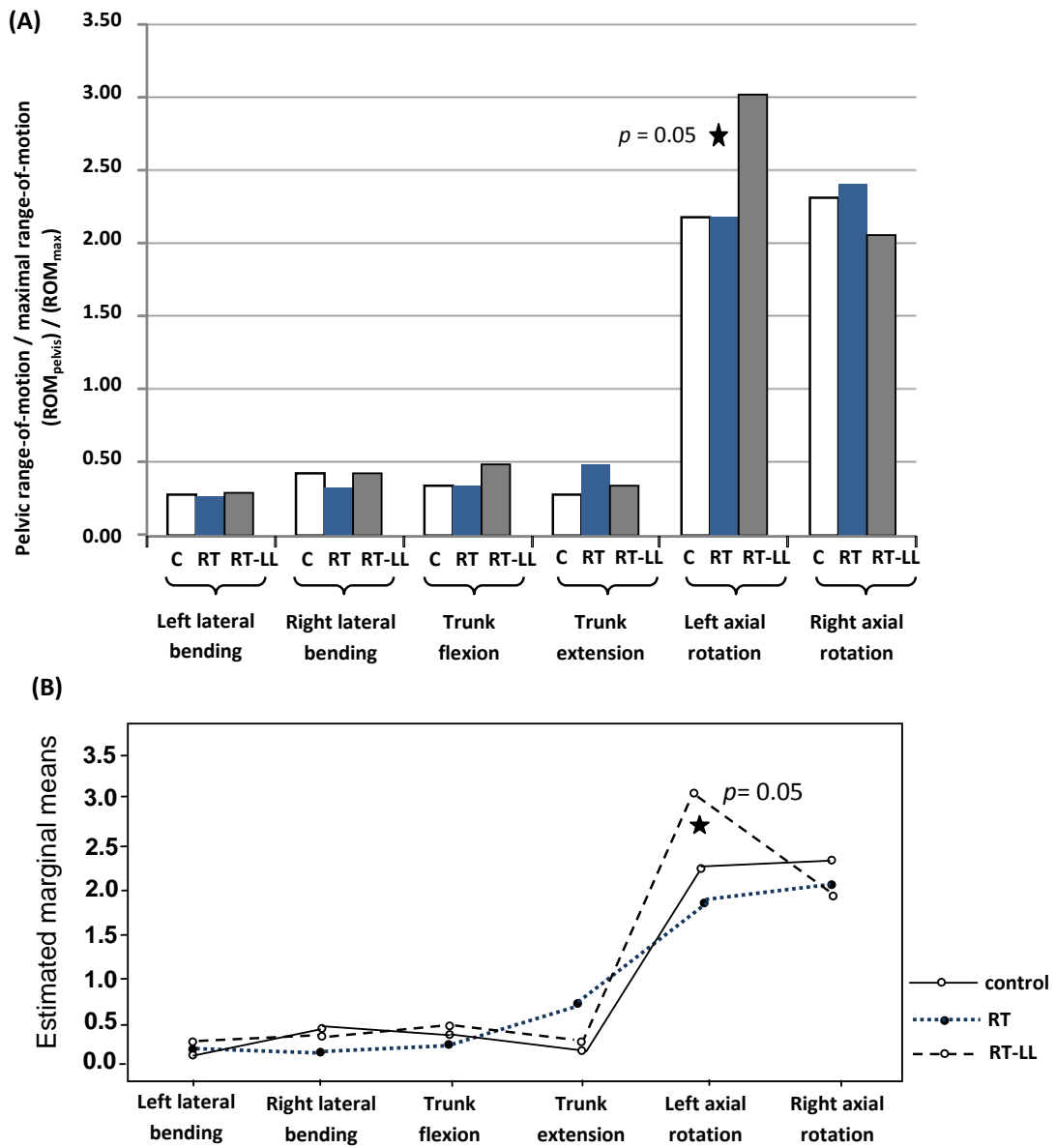


Figure 3.4: Comparison between pelvic ROM (ROM_{pelvis}) and total ROM (ROM_{max}). (A) Pelvic contribution to total ROM for all movement types; (B) The interaction effect evident during left axial rotation.

Table 3.1: Pelvic dynamics established sequentially by resolving pelvic 3D alignment into its three planar components: sagittal tilt (P_S), frontal tilt (P_F) and transverse plane rotation (P_T). The parentheses indicate compound movement of the pelvis.

Movement type	Control	RT	RT-LL
Left lateral bending	$P_S \rightarrow P_F \rightarrow P_T$	$(P_S \rightarrow P_T) \rightarrow P_F$	$(P_S \rightarrow P_F) \rightarrow P_T$
Right lateral bending	$P_S \rightarrow P_F \rightarrow P_T$	$P_S \rightarrow (P_T \rightarrow P_F)$	$P_T \rightarrow P_S \rightarrow P_F$
Trunk flexion	$(P_S \rightarrow P_F) \rightarrow P_T$	$P_S \rightarrow P_F \rightarrow P_T$	$P_F \rightarrow (P_T \rightarrow P_S)$
Trunk extension	$P_F \rightarrow P_T \rightarrow P_S$	$(P_T \rightarrow P_F) \rightarrow P_S$	$(P_S \rightarrow P_F \rightarrow P_T)$
Left axial rotation	$(P_T \rightarrow P_F) \rightarrow P_S$	$P_T \rightarrow P_F \rightarrow P_S$	$P_S \rightarrow P_T \rightarrow P_F$
Right axial rotation	$P_T \rightarrow P_F \rightarrow P_S$	$(P_T \rightarrow P_F) \rightarrow P_S$	$P_T \rightarrow (P_S \rightarrow P_F)$

3.3 Analysis of the spino-pelvic relative orientation in scoliotic subgroups in the standing posture

As it was shown in the previous section pelvic range of motion and its interaction with spinal movement varies in AIS subgroups. In this section parameters describing the relative 3D spino-pelvic orientation were used in two scoliotic subgroups to study the spino-pelvic interaction in standing position. The relationship between the pelvic orientation in different anatomical planes and spinal parameters was used to analyze the 3D spino-pelvic compensatory mechanisms in AIS subgroups.

It is known that scoliosis affects the spine and pelvis morphology and their relative orientation (Lucas, 2004; Gum, 2007). However pelvic parameters which have been developed to explain the pelvic orientation are mainly defined in the sagittal plane while the relative spino-pelvic orientation in the frontal and transverse plane is less emphasized in scoliosis. For instance, the orientation of the sacrum endplate and its position with respect to the femoral heads is used to characterize the spino-pelvic alignment in scoliosis and spondylolisthesis (Vaz, 2002, Mac-Thiong, 2003). However the mechanism through which the 3D pelvic orientation relates to the thoracic and lumbar spines in scoliosis subgroups was not systematically analyzed.

3.3.1 Materials and Methods

3.3.1.1 Subjects

Eighty AIS patients with a right main thoracic curve (MT) and 80 with a thoracolumbar/lumbar curve (TL/L) were randomly selected and studied retrospectively. No criteria in terms of the curve severity (brace or surgery cases) were considered in sample selection. 35 asymptomatic control subjects, with no history of spinal disease and showing no spinal deformity on full spine radiographs examined by a spine surgeon and were added as the asymptomatic control group. The sample sizes were verified by a small-scale preliminary study (pilot study) for this study. Ethic approval was obtained from our institution to use the radiographic images and patient's medical chart for this study. The average age at the time of the visit was 14 ± 3 years for the MT group and 15 ± 2 years for the TL/L. A curve was mathematically fitted to the center of the vertebrae. Thoracic and lumbar Cobb angles were measured as the angle

between the perpendiculars to the tangents at the inflection point of the curve in the coronal plane. The kyphosis was measured between T4-T12 and lordosis was measured between L1-L5 vertebrae. Table 3.2 lists the average values of the different spine and pelvic parameters in each studied group.

Table 3.2: Spinal and pelvic parameters of the studied sample

	MT Cobb (°)	TL/L Cobb (°)	Kyphosis (°)	Lordosis (°)	PI (°)	PT (°)	SS (°)
Control N=35	-	-	44±8	32±15	48±9	12±7	38±12
MT N=80	45±11	25±25	27±12	36±12	50±12	8±8	42±8
TL/L N=80	24±11	37±12	34±12	37±13	52±11	12±7	41±10

3.3.1.2 Pelvic orientation in the global coordinate system

Three radiographic images (lateral and postero-anterior views) were used to create the three-dimensional reconstruction of the spine and pelvis applying the direct linear transformation (DLT) algorithm (Delorme, 2003). The average accuracy of the reconstruction technique was 3.3 mm (SD 3.8 mm) with a maximum 5mm error in measurement of the pelvic landmarks (Delorme, 2003). Since patients positioning with respect to the radiograph apparatus during the radiographic acquisition slightly varied, a rotation matrix around the vertical axis was used to align the 3D reconstruction models in such way that the bi-femoral head axis was placed in the coronal plane. The reconstructed model was used to determine the 3D coordinates of four pelvic landmarks *i.e.* left and right anterior (ASIS) and posterior (PSIS) superior iliac spine.

The global reference coordinate system was defined using the Scoliosis Research Society (SRS) convention (Stokes, 1994) wherein: X-axis was oriented anteriorly, Y-axis was medio-lateral (to the left), and Z-axis was ascending vertically. The method to determine the pelvic orientation was described in section 3.2.2 and is summarized in figure 3.5. $\mathbf{v}_{\text{pelvis}}$ was defined as the vector connecting the midpoint of the lines joining the ipsilateral ASIS and PSIS (figure 3.5). Pelvic frontal tilt (pelvic_{FTilt}) was defined as the angle between the $\mathbf{v}_{\text{pelvis}}$ and Y-axis in the frontal

plane. Pelvic axial rotation ($pelvic_{Rot}$) was defined as the angle between the v_{pelvis} and Y-axis in the transverse plane.

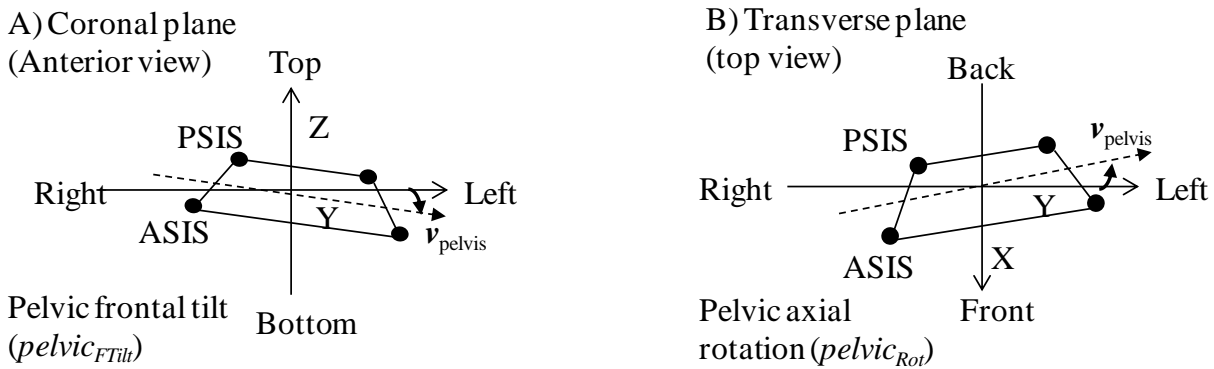


Figure 3.5: Schematic illustrating the calculation of (A) pelvic frontal tilt ($pelvic_{FTilt}$) in the coronal plane and (B) pelvic axial rotation ($pelvic_{Rot}$) in the transverse plane.

There are two possible directions of pelvic rotation (from top view) and pelvic frontal tilt (from anterior view) in each plane: clockwise (-) as the example shows in Figure 3.5A and counter-clockwise (+) as is shown in Figure 3.5B. Combination of these two possible directions of the $pelvic_{FTilt}$ and $pelvic_{Rot}$ in coronal and transverse planes results in 4 possible pelvic orientations (Figure 3.6A). Table 3.3 lists these four pelvic orientations.

The pelvic orientation *i.e.* $pelvic_{Rot}$ and $pelvic_{FTilt}$ was calculated for the 80 patients of each scoliotic subgroup and the 35 asymptomatic controls separately. A illustration of the pelvic orientation ($pelvic_{Rot}$ and $pelvic_{FTilt}$) with the magnitude of the ‘pelvic axial rotation’ determined on the x-axis and the magnitude of the ‘pelvic frontal tilt’ shown on the y-axis was used to present these two parameters in a single plot for each patient (Figure 3.6B).

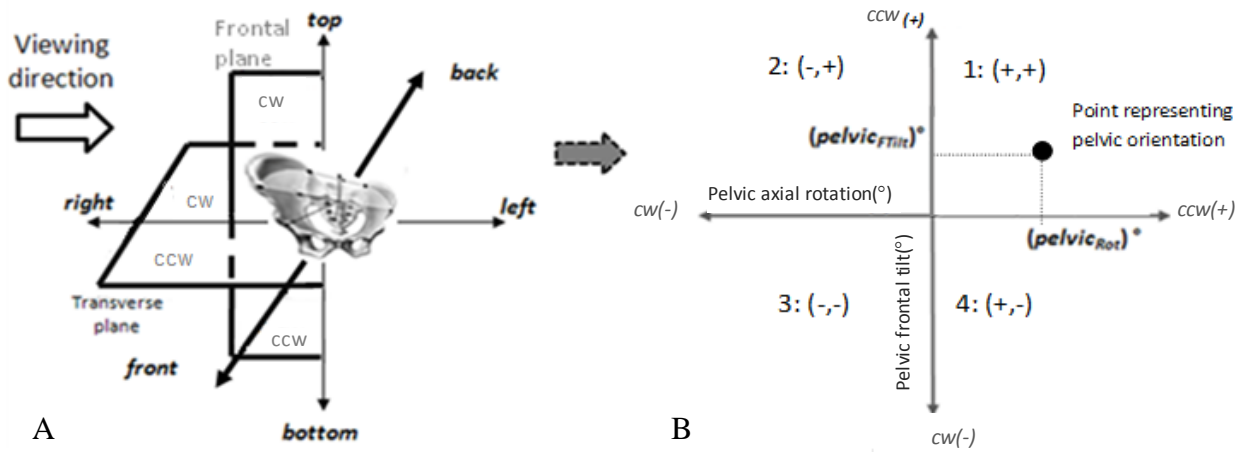


Figure 3.6: (A) Schematic representation of the possible pelvic orientation in the frontal and transverse planes (B) Illustration of the 2D representation of the pelvic orientation.

Table 3.3: Four possible pelvic orientations in the frontal and transverse planes.

Pelvic orientation groups	1	2	3	4
$pelvic_{Rot}$	$pelvic_{Rot}$ ccw(+)	$pelvic_{Rot}$ cw(-)	$pelvic_{Rot}$ cw(-)	$pelvic_{Rot}$ ccw(+)
$pelvic_{FTilt}$	$pelvic_{FTilt}$ ccw(+)	$pelvic_{FTilt}$ ccw(+)	$pelvic_{FTilt}$ cw(-)	$pelvic_{FTilt}$ cw(-)
Pelvic orientation ($pelvic_{Rot}$, $pelvic_{FTilt}$)	(+,-)	(-,+)	(-,-)	(+,-)

3.3.1.3 Pelvic orientation with respect to the thoracic and lumbar spinal deformities

The coronal and transverse views of the spine and pelvis were used to study the pelvic orientation *i.e.* $pelvic_{FTilt}$ and $pelvic_{Rot}$ with respect to the thoracic and lumbar spinal deformities in the MT and TL/L groups. In this study the direction of the $pelvic_{FTilt}$ and $pelvic_{Rot}$ *i.e.* clockwise

or counter clockwise was related to the position of the spinal deformities in antero-posterior and top views of the spine and pelvis.

3.3.1.4 Impact of the reconstruction error on the pelvic orientation: a sensitivity analysis

A maximum error of 5mm was reported in the measurement of pelvic anatomical landmarks in the 3D reconstruction of the pelvis (Delorme, 2003). The effect of the reconstruction error on the results of the current study was studied in the MT group. This group was selected because subjects in this group had relatively smaller pelvic orientation angles in comparison to the TL/L group and subsequently the measured angles were more affected by the reconstruction error.

Considering the reconstruction error, a normally distributed noise was added to the coordinates of the ASIS and PSIS in the frontal and transverse planes. The pelvic orientation after was calculated for 100 trials for each patient and the standard deviation of the pelvic orientation was calculated in a commercial software (MATLAB R2008a, The MathWorks Inc., Natick, MA, 2008) for each patient. This process was repeated for all the subjects in the MT group and the average standard deviation was calculated. Subjects with different pelvic orientations were selected and the initial and 100 generated pelvic orientations were plotted.

3.3.2 Results

3.3.2.1 Pelvic orientation in the global coordinate system

The average of the absolute $pelvic_{FTilt}$ was calculated at $2.6^\circ \pm 2.3^\circ$, range $[-6^\circ, 5^\circ]$ in MT subjects and at $3.2^\circ \pm 1.1^\circ$, range $[-8^\circ, 4^\circ]$ in TL/L subjects. $Pelvic_{Rot}$ was $3.8^\circ \pm 2.1^\circ$, range $[-7^\circ, 8^\circ]$ in MT group and $4.4^\circ \pm 2.7^\circ$, range $[-10^\circ, 10^\circ]$ in TL/L. In controls $pelvic_{FTilt}$ was $1.8^\circ \pm 0.7^\circ$, range $[-3^\circ, 4^\circ]$ and $pelvic_{Rot}$ was $1.5^\circ \pm 1.1^\circ$, range $[-4^\circ, 5^\circ]$. All controls had either $pelvic_{FTilt}$ or $pelvic_{Rot}$ smaller than four degrees.

The distribution of the pelvic orientation in each group of subjects was shown in figure 3.7: MT (figure. 3.7A), TL/L (figure. 3.7B), and controls (figure 3.7C). More specifically, of the 80 MT patients, 8% were placed in the first quadrant (1), 33% in the second (2), 51% in the third (3), and 8% in the fourth quadrant (4) (Figure 3.7A). The TL/L subjects (80 patients) were distributed 34% in the first quadrant, 45 % in the second quadrant, 10% in the third quadrant, and

11% in the fourth quadrant (Figure 3.7B). In the control group 11% (n=4) were in the first quadrant, while the other subjects were almost equally distributed (26%- 31%) in the quadrants 2 (n=11), 3(n= 11), and 4 (n=9) (Figure 3.7C).

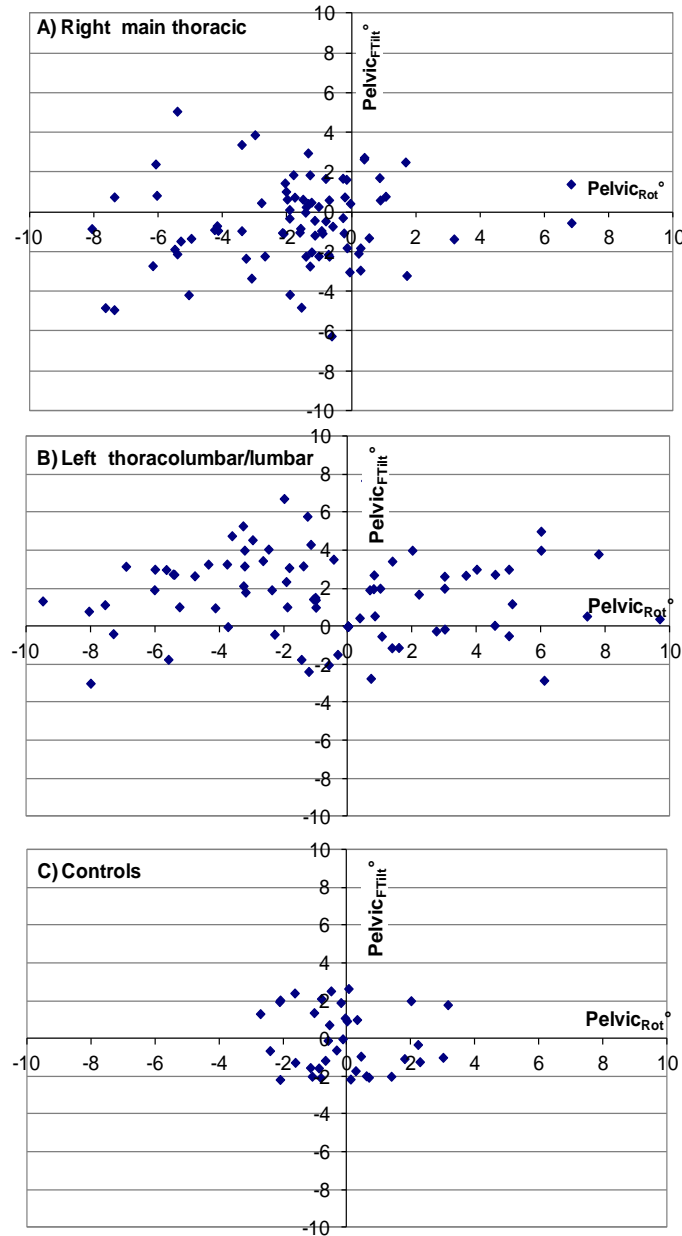


Figure 3.7: Presentation of the pelvic orientation in (A) Right main thoracic (MT) (n=80) (B) Left thoracolumbar/lumbar (TL/L) (n=80), and (C) Controls (n=35). Angles are presented in degrees.

3.3.2.2 Pelvic orientation with respect to the thoracic and lumbar spinal deformities

Figure 3.8 shows the relative spino-pelvic alignment in the frontal and transverse views. 59% of the MT had $pelvic_{FTilt}$ toward the convex side of the major curve *i.e.* thoracic curve and 79% of TL/L patients had $pelvic_{FTilt}$ toward the convex side of the major curve *i.e.* lumbar curve (figure 3.8). In a view from the top, a majority of the patients in the MT group (84%) had the clockwise $pelvic_{Rot}$ while this percentage was decreased to 55% in the TL/L (figure 3.8).

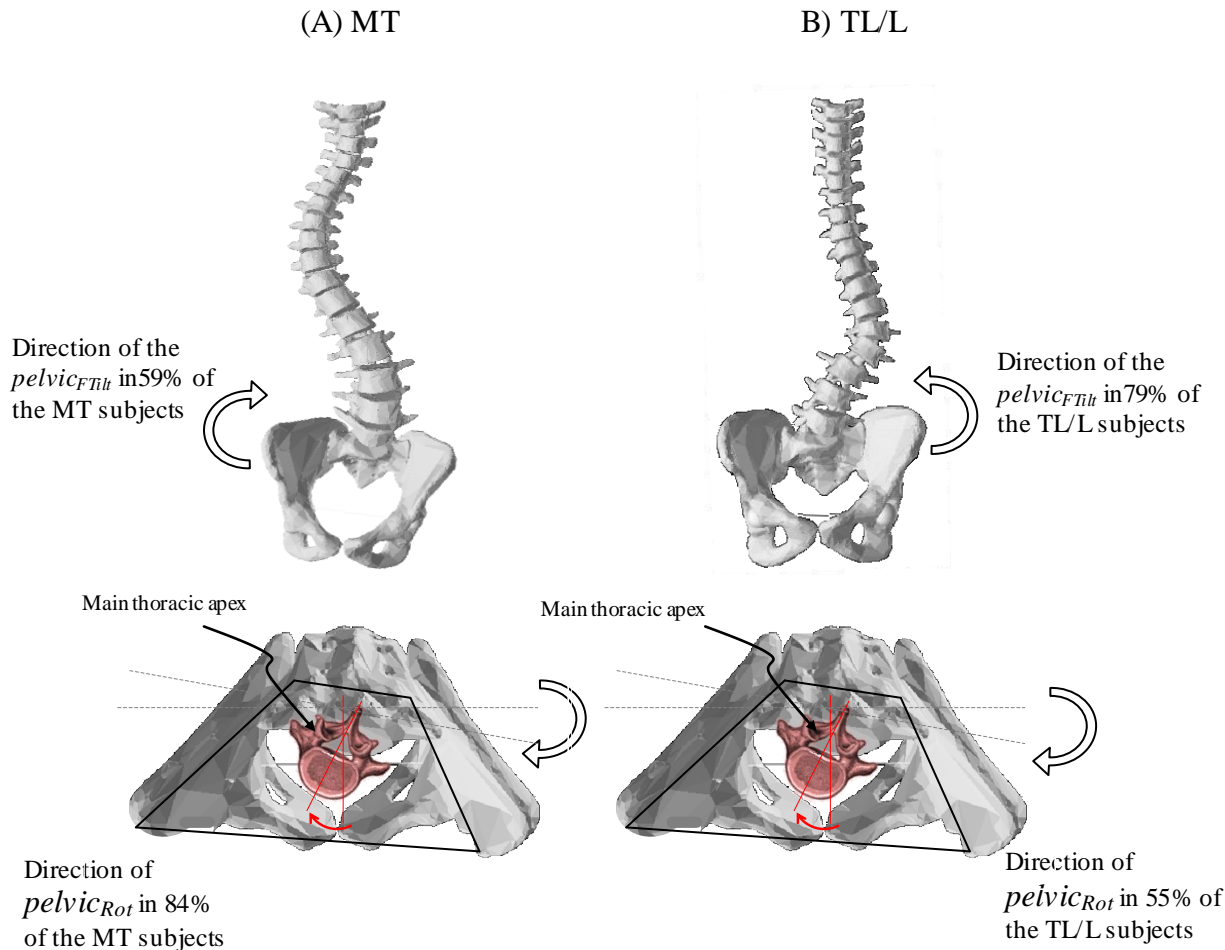


Figure 3.8: A schematic illustrating the tendency of the spino-pelvic relative orientation in transverse and coronal planes in (A) MT and (B) TL/L. The values are the percentage number of cases (n=80 in both groups) with the demonstrated pelvic orientation.

3.3.2.3 Impact of the reconstruction error on the pelvic orientation: a sensitivity analysis

The effect of the reconstruction error on the measured parameters was studied in the MT group. Figure (3.9) showed the initial pelvic orientation and the 100 generated pelvic orientations after adding the error for six cases with different pelvic orientation. While the presentation of all subjects was not possible due to the close position of the pelvic orientation in many cases, the selected cases were representative of the impact of the reconstruction error on the different magnitude of the $pelvic_{Rot}^{\circ}$ and $pelvic_{FTilt}^{\circ}$. Table 3.4 listed the initial pelvic orientation ($pelvic_{Rot}$ and $pelvic_{FTilt}$), the average of 100 generated pelvic orientations, and the standard deviation of the generated pelvic orientations for each presented case in the figure 3.9.

Table 3.4: The initial, average and standard deviation of the generated pelvic orientation

	Initial $pelvic_{Rot}^{\circ}$	Initial $pelvic_{FTilt}^{\circ}$	Average of generated $pelvic_{Rot}^{\circ}$	Average of generated $pelvic_{FTilt}^{\circ}$	SD $^{\circ}$
Case1	3.2	-1.2	3.4	-1.3	0.86
Case2	-2.5	-2.8	-2.6	-2.8	1.08
Case3	0.2	1.3	0.3	1.1	0.96
Case4	-2.0	0	-2.1	-0.1	1.21
Case5	-5.3	1.9	-5.1	2.3	0.75
Case6	-6.2	5.2	-6.3	5.2	1.03

Average standard deviation of the generated pelvic orientations ($pelvic_{Rot}^{\circ}$, $pelvic_{FTilt}^{\circ}$) was $\pm 1.05^{\circ}$ for the cohort of MT subjects.

Subjects with pelvic orientation ($pelvic_{Rot}^{\circ}$ and $pelvic_{FTilt}^{\circ}$) less than 1.05° were excluded from the study and the percentage of subjects who have placed in each quadrant was recalculated. 7% of the subjects were placed in the first quadrant (versus originally 8%), 29% were placed in the second quadrant (versus originally 33%), 57% were placed in the third quadrant (versus originally 51%), and 7% were placed in the fourth quadrant (versus originally 8%).

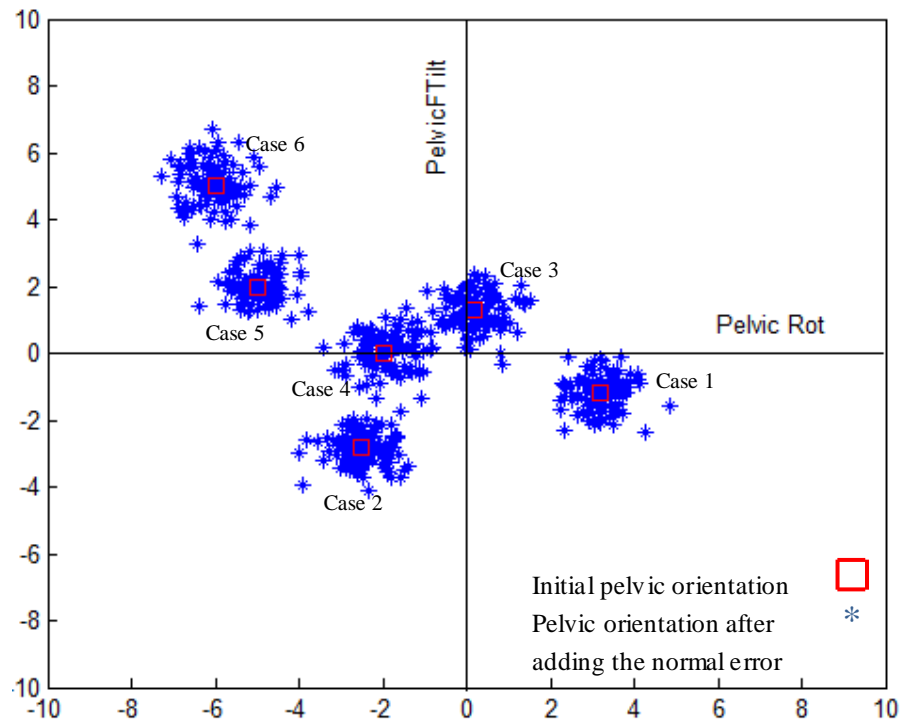


Figure 3.9 : The effect of the reconstruction error on the pelvic orientation in the MT subjects

CHAPTER4 FINITE ELEMENT ANALYSIS OF THE BIOMECHANICAL LOADING OF THE SACRUM IN ADOLESCENT IDIOPATHIC SCOLIOSIS

As it was shown in the previous chapter, the 3D pelvic alignment with respect to the spine varies in scoliotic subgroups. However the mechanism through which the spino-pelvic alignment in subjects with different curve types interferes with the transferred load between the spine and pelvis is not fully determined. Among different postural parameters the position of the trunk center of mass (COM) that can vary due to the scoliotic deformities impacts the transferred load between the spine and pelvis. The importance of the position of the COM in biomechanical assessment of the human spine was highlighted previously (Park, 2012). However a method that estimates the position of the COM in numerical models of the scoliotic spine is not developed yet.

Hence this chapter consists of two studies: The first study focuses on the biomechanical analysis of the spino-pelvic alignment (Objective and hypothesis 3). Since the sacrum is part of both spine and pelvis the mechanical loading of this vertebra was used to assess the impact of the different spino-pelvic configurations on the transferred load between the spine and pelvis. The compressive stress on the upper sacral endplate was studied in two scoliotic groups, main right thoracic and left thoracolumbar/lumbar curves and compared to a group of controls using a detailed finite element model (FEM). To verify the sensitivity of the FE model to the COM position the impact of the COM position on the sacral loading was analyzed in the second part of this chapter. A mathematical technique was developed to first determine the COM position in scoliotic subjects and then study the impact of the position of the COM on the biomechanical loading the sacrum in the patient specific FE models of the spine that was generated in the previous section.

4.1 Presentation of the second article

The biomechanical analysis of the sacral loading was presented through the second manuscript. This article addresses the third objective and hypothesis presented in this thesis.

The article “Biomechanical Loading of the Sacrum in Adolescent Idiopathic Scoliosis” was submitted to the European Spine journal in June 2012. The contribution of the first author in preparation and edition of the article is evaluated at 85%.

4.2 Second article: Biomechanical loading of the sacrum in adolescent idiopathic scoliosis

Saba Pasha^{1, 2}, Carl-Eric Aubin^{1, 2, 3}, Stefan Parent^{2,3}, Hubert Labelle^{2, 3}, Jean-Marc Mac Thiong^{2, 3, 4}.

1. Dept. Mechanical Engineering
École Polytechnique de Montréal,
P.O. Box 6079, Station “Centre-ville”
Montréal (Québec)
H3C 3A7 CANADA
2. Research Center, Sainte-Justine University Hospital Center
3175, Cote Sainte-Catherine Road
Montréal (Québec)
H3T 1C5 CANADA
3. Department of Surgery
Université de Montréal
C.P. 6128, station “Centre-ville”
Montréal (Québec)
H3C 3J7 CANADA
4. Division of Orthopedic Surgery
Hôpital du Sacré-Coeur de Montréal
5400 Gouin Ouest
Montréal (Québec)
H4J 1C5 CANADA

Running Head: biomechanical loading of the sacrum in AIS

Submitted to: European Spine Journal

Submitted in: June 2012

Corresponding author: Carl-Eric Aubin

École Polytechnique, Dept of Mechanical Engineering
 P.O. Box 6079, Station “Centre-ville”,
 Montréal (Québec), H3C 3A7 CANADA
 e-mail: carl-eric.aubin@polymtl.ca
 Tel: (514) 340-4711 ext. 2836, Fax: (514) 340-5867

4.2.1 Abstract

Background The pelvis maintains an important role in transferring loads from the upper body to the lower extremities and hence contributes to the body postural balance. Even though changes in spino-pelvic relative alignment are involved in the pathophysiology of scoliosis, the mechanism through which the transferred load between the spine and pelvis is related to the spinal deformities and sacro-pelvic parameters in different scoliotic curve types is not well understood.

Purpose The objective of this study was to analyze the transferred load between the spine and pelvis through the biomechanical loading of the sacrum in AIS subjects with two different curve types as compared to asymptomatic subjects.

Method A personalized finite element (FE) model of the spine and pelvis was constructed for 34 AIS subjects (11 with right main thoracic (MT) curves, 23 with left thoracolumbar-lumbar (TL/L) curves), and 12 asymptomatic controls. The compressive stress distribution on the sacrum endplate was computed and normalized to the patient’s weight for each subject. The sacro-pelvic parameters (pelvic tilt, pelvic incidence, and sacral slope) were computed using the 3D reconstruction from the patient’s biplanar radiographs. Both the position of the stress distribution barycenter on the S1 endplate (COP_{S1}) in reference to the central hip vertical axis (CHVA) and of the trunk center of mass (COM) were projected on the transverse plane and compared between scoliotic subgroups and controls.

Results The medio-lateral position of the COP_{S1} was significantly different between the scoliotic subgroups and controls ($p<0.05$). The COP_{S1} was located at the right side of the CHVA in 82% of the MT and to the left side of the CHVA in 91% of TL/L. In both controls and right MT subjects the stress distribution on the sacrum endplate was medio-laterally symmetric in the S1 local coordinate system. Subjects with TL/L curves showed higher stress at the left side of the sacrum in comparison to the right side ($p<0.05$). The position of the COP_{S1} was significantly correlated to the sacro-pelvic parameters in both AIS subgroups and controls ($p<0.05$).

Conclusion The transferred load to the sacrum was related to both spinal and pelvic parameters and thus was different between scoliotic subgroups and controls. Analysis of the transferred load to the sacrum provided insight into the biomechanical interaction between the spine and pelvis in 3D.

4.2.2 Introduction

In humans the pelvis maintains an important role in transferring loads between the lower extremities and spine [20]. With this in mind, Dubousset [11, 12] introduced the concept of the pelvic vertebra to emphasize the biomechanical role of the sacrum and pelvis relative to the spine. The relative spino-pelvic alignment was believed to ensure postural stability and help minimize energy expenditure in the bipedal kinematic chain [2, 3].

In scoliosis, both the kinematics [37] and morphology [5, 19] of the pelvis are subject to changes with varying curve types and severity. The relationship between pelvic and lumbar parameters has been measured in the static position particularly in the sagittal plane in both asymptomatic [3, 18, 35] and scoliotic subjects [23, 43]. Sacro-pelvic parameters *i.e.* pelvic incidence (PI), pelvic tilt (PT), and sacral slope (SS) were introduced to explain the orientation of the sacrum and its position with respect to the center of the femoral heads in the sagittal plane [4, 23]. The correlations between these parameters and lumbar lordosis remained similar within pre- and post-operative scoliotic groups [42]. This finding emphasized the significance of the relative spino-pelvic alignment in providing postural balance despite the spinal deformity [2, 3]. The importance of preserving this correlation in scoliosis surgery to protect the patient's postural balance was highlighted in AIS [42]. Moreover the adaptive spino-pelvic alignment impacts the kinematic of the movement pre- and post-operatively [37,41] which consequently interferes with the muscle activation and energy consumption of the patient [30].

To date, most studies have analyzed the geometrical aspects of the spino-pelvic alignment; however the biomechanical interaction in terms of forces transferred between the spine and pelvis was not investigated in scoliotic subgroups. Since mechanical loading of the sacrum represents the conducted force between the pelvis and the spine, from a biomechanical point of view, study of the sacral loading could be important in the postural evaluation of the AIS. Several studies focused on the biomechanical loading of the sacrum in isthmic spondylolysis and spondylolisthesis [31, 39] and reported abnormal stress distribution on the sacrum as well as a relationship between the sacral loading and sacro-pelvic parameters such as sacral slippage and pelvic incidence [39]. However the main interest in biomechanical analysis of the scoliosis is focused on the thoracic and lumbar vertebral loading [7, 9, 44]. To our knowledge, no study has focused on the differences between mechanical loadings of the sacrum in subjects with different scoliotic types. This paper aimed to analyze and compare the load patterns transferred to the sacrum based on the morphology and relative orientation of the sacrum and spine between controls and scoliotic subjects with two different curve types.

4.2.3 Materials and methods

4.2.3.1 Subjects

23 scoliotic patients with a left thoraco-lumbar/lumbar (TL/L) curve and 11 with a right main thoracic (MT) curve were selected randomly from our institution database. Inclusion criteria consisted of a diagnosis of adolescent idiopathic scoliosis, with no previous surgical spinal correction, and a Cobb angle exceeding 20° for the main thoracic or lumbar scoliosis. In addition, 12 asymptomatic control subjects, examined by a spine surgeon, with no history of spinal disorder were included in this study. The sample size for each group was determined based on a power analysis ($p<0.05$ and Type II error of 20%). All participants were female adolescents. The research proposal was accepted by the ethic committee of our institution.

4.2.3.2 Measurement of the patient's morphological parameters

The 3-dimensional reconstruction of the spine, pelvis, ribcage, and the position of the femoral heads were created from digitized landmarks on the postero-anterior and lateral x-rays using a 3D reconstruction and self-calibration method [6, 21, 22]. A detailed atlas of the spine and pelvis along with a freeform deformation technique were used to create a comprehensive

geometry of the spine, pelvis, and ribcage. In applying this method, an average error of 1.2 mm (S.D. 0.8 mm) was calculated on the vertebral body and 1.6mm (S.D. 1.1mm) on the pedicles. Average variations of 1° and 7° were reported in the calculation of the spinal curves in the coronal and sagittal planes respectively when results from the 3D reconstruction were compared to the 2D measurements on the radiographs by clinicians [8, 24].

The spinal parameters (thoracic and lumbar Cobb angles, kyphosis, and lordosis) and sacro-pelvic parameters *i.e.* PI, PT, and SS were determined. Kyphosis and lordosis angles were computed between T4-T12 and L1-S1 respectively. The 3D coordinates of the center of the femoral heads were determined on the 3D reconstructions. Central hip vertical axis (CHVA) was defined as the vertical line passing through the midpoint of the line joining the center of the femoral heads [38].

4.2.3.3 Finite element modeling and simulation

An osseo-ligamentous finite element (FE) model of the spine from T1 to S1, ribcage, and pelvis was constructed using ANSYS 11.0 FE package (ANSYS Inc., Canonsburg, PA, USA). A detailed version of this model is described elsewhere and the main components are summarized here. Elastic beam elements of appropriate mechanical properties [7] were used to present the different components of the spine, ribcage and pelvis. Intercostal and intervertebral ligaments were modeled with tension-only spring elements while zygapophyseal joints were modeled using non-linear contact and shell elements. The abdominal cavity wall was created by interpolating the nodes of the ribcage, pelvis, and vertebrae. A model of the trunk surface and external soft tissues was approximated by the 3D coordinates of these interpolated nodes. The external surface was defined by hexahedral solid elements [7]. Different components of the model are presented in figure 4.1.

Insert Figure 4.1 near here

The weight of the trunk slices, head, neck, and arms were determined as a percentage of the total body weight. The position of the center of mass (COM) of each trunk slice was set at the center of each vertebral body in the frontal plane. In the sagittal plane the COM of the trunk slices at the level of each vertebra was determined from literature [13, 14, 26]. A rigid beam was used to connect the COM of each trunk slice to the center of the vertebrae. The weight of the head and neck were associated with that of the trunk slice at T1 vertebra level. The weight of the

arms was distributed at T3-T5 vertebrae levels by the method described by El-Rich and Shirazi-Adl [15]. 17 nodes with associated weights were determined from T1 to L5 to represent the center of gravity of the head, neck, arm, and trunk in the FE model. The 3D position of the global trunk COM was calculated as the weighted sum of the COM of all these sections [15].

The gravitational force (F_i) was applied at the COM of each vertebral level as following:

$$F_i = m_i \times g, \quad i=1:17$$

where m is the mass associated with each vertebral level, g is the standard gravity (9.81 m/s^2), and i is the vertebral level (12 for thoracic spine and 5 for lumbar spine). In order to retain the actual geometry of the spine following application of the gravitational force (weight), an optimization method was used during the course of the simulation. The simulation was performed in two steps: the first step of the simulation consisted of applying the associated force (weight) at the level of each vertebra in the opposite direction of the gravity *i.e.* upward to obtain the spine under no-gravity condition (zero-gravity model) [7]. Subsequently the stresses calculated at the spinal vertebrae at the end of this step were reset to zero. In the second step of the simulation gravitational forces were applied in the true direction *i.e.* downward on the zero-gravity model. Afterward, the outcome geometry of the FE model due to the gravitational forces was compared to the geometry of the spine from the 3D reconstructions. The applied forces in the first step of the simulation were modified, using a minimization optimization method, until the differences between the resultant geometry of the FE model and the 3D reconstruction of the radiographs were minimized. In applying this method, the original geometries of the spine and pelvis were preserved [7].

The FE model was used to compute the compressive stress distribution on the S1 endplate. In order to make the comparison between subjects possible, the magnitudes of the compressive stress on the S1 endplate were weight normalized and scaled between the maximum and minimum values for each subject (Figure 4.2-d). Considering the stress distribution on the S1 (S_i) and the radius of the sacrum (r_i) in each subject, the barycenter of the stress distribution on the S1 endplate (COP_{S1}) was calculated (Figure 4.2-d). The position of the COP_{S1} was presented with respect to the CHVA in the global coordinate system. The 2D coordinates of the CHVA on the transverse plane were set as the origin of the coordinate system using a commercial software package (MATLAB R2008a, The MathWorks Inc., Natick, MA, 2008). The coordinates of the

spine and pelvis, position of the trunk COM, and the position of the COP_{S1} were modified accordingly. In this coordinate system, the X axis is oriented anteriorly, the Y axis is oriented from right to left, and the Z axis is pointing upward.

Insert figure 4.2 near here

4.2.3.4 Statistical analysis

A Shapiro-Wilk normality test was used to determine if the computed geometrical and biomechanical parameters were normally distributed in the cohort of subjects. These parameters are listed as: the projection of the COM and COP_{S1} on the transverse plane, PI, PT, SS, thoracic and lumbar Cobb angles, kyphosis, and lordosis.

For each group of subjects, the average of all the computed data was calculated and compared between groups. ANOVA test (PAWS statistics 18.0, SPSS Inc., Chicago, IL) was used to compare the average value of the measured parameters. A post-hoc test (Dunnett's T3, PAWS statistics 18.0) with assumption of unequal variance in the three groups was performed on the parameters to determine significant differences between the studied groups. The relationship between pelvic and spine morphological and biomechanical parameters was determined by univariate correlation analysis. A clustering technique (K-means cluster, PAWS statistics 18.0) was used to divide the resulting distributions of compressive stress measured on the S1 endplate in two clusters (low and high stress regions) based on the average normalized stress magnitudes in the three groups of subjects separately.

While the position of the COM was personalized in the sagittal plane using the Pearsall (1996) method, there was not enough information available about the COM position in the frontal plane for the scoliotic subjects. The position of the COM at the level of each vertebra was shifted 1cm to the either sides of the vertebra center in the frontal plane to study the sensitivity of the results to the COM position in the TL/L group. This group was selected because the location and severity of the spinal curve varied more in this cohort of subjects. The stress distribution on the superior endplate of the sacrum and the position of the COP_{S1} were calculated and were compared as the COM position changed. Statistical test (T-Test, PAWS statistics 18.0, SPSS Inc., Chicago, IL) was performed to determine the differences in the sacral loading as the COM position varies. Moreover, the spinal stiffness was modified to verify if it impacts the general trend of the stress distribution and the position of the COP_{S1} on the sacrum endplate in the studied

group. The mechanical properties of the intervertebral disks were multiplied by 0.5 and 2 to simulate flexible versus rigid spine respectively. The sacral loading was compared when different material properties were used in the FEM (T-Test, PAWS statistics 18.0, SPSS Inc., Chicago, IL).

4.2.4 Results

4.2.4.1 Subjects

The subjects' age range was 10-17 years at the time of the radiographic acquisition (average: 15.8 ± 2.4 years). Subjects' weight was also registered (controls: 53 ± 5 kg, MT 50 ± 8 Kg, TL/L 52 ± 12 Kg). The average, standard deviation, and range of thoracic and lumbar Cobb angles in subjects with a main right thoracic deformity were $51.2 \pm 14.1^\circ$ [range: $37^\circ, 76^\circ$] and $32.1^\circ \pm 12.2^\circ$ [$15^\circ, 47^\circ$] respectively. In subjects with a main left TL/L deformity, Cobb angles were measured at $24^\circ \pm 7.6^\circ$ [$11^\circ, 42^\circ$] in thoracic and $40.5^\circ \pm 11.7^\circ$ [$17^\circ, 61^\circ$] in thoracolumbar/lumbar curves. Table 4.1 summarizes the spinal and pelvic parameters in the two scoliotic groups and controls.

Insert Table 4.1 near here

4.2.4.2 Statistical analysis

The Shapiro-Wilk normality test confirmed that the measured and computed morphological and biomechanical parameters were normally distributed.

4.2.4.3 Spine and pelvic parameters in the global coordinate system

The position of the COM and COP_{S1} in both medio-lateral and postero-anterior directions were reported in table 4.2 for the three groups. The medio-lateral position of the trunk COM and the medio-lateral position of the COP_{S1} were significantly different between the two scoliotic groups and controls ($p < 0.05$). In 82% of the MT subjects the COP_{S1} was placed to the right side of the sagittal plane passing through the CHVA, while in 91% of the TL/L the COP_{S1} was at the left side of this plane. In controls, the COP_{S1} is mostly close to the sagittal plane (Figure 4.3). In the three studied groups, no significant relationship was observed between the 2D position of the trunk COM and the COP_{S1} however similar to the general trend of COP_{S1} distribution, the

position of the COM was mostly at the right side of the CHVA in MT subjects (91%) and at the left side (100%) in TL/L group (Figure 4.4).

Insert Table 4.2 near here

Insert Figure 4.3 near here

Insert Figure 4.4 near here

In controls, the postero-anterior position of the COP_{S1} was correlated with the PI ($r= -0.79, p< 0.05$) and SS ($r= -0.91, p< 0.05$). In MT subjects, the postero-anterior position of the COP_{S1} was correlated with the SS ($r= -0.66, p< 0.05$). In TL/L subjects, the postero-anterior position of the COP_{S1} was correlated with the PI ($r= -0.44, p< 0.05$) and SS ($r= -0.47, p< 0.05$).

A higher lateral shift in the position of the COP_{S1} was observed as the lumbar lordosis was increased ($r= 0.44, p< 0.05$) in TL/L. The medio-lateral position of the COP_{S1} was correlated with the lumbar Cobb in the TL/L subjects ($r= 0.5, p< 0.05$). The medio-lateral ($r= 0.61, p< 0.05$) and postero-anterior ($r= 0.37, p< 0.05$) positions of the COP_{S1} were correlated with the TL/L Cobb angle when these parameters were compared in the cohort of the scoliotic subjects. No relationship was observed between these two parameters in the control and MT groups.

Among the sacro-pelvic parameters, the SS and the PI were significantly higher in MT and TL/L when compared to controls ($p<0.05$).

4.2.4.4 Sacral loading in the local coordinate system of the sacrum

Although the compressive stress distribution on the S1 endplate was symmetric in the MT group and in the controls in the local coordinate system of the sacrum, in TL/L subjects higher stress was observed in the left side of the sacrum as compared to the right side $p<0.05$ (Figure 4.5). The cluster analysis (K-means cluster) identified low and high stress regions on the S1 endplate based on the average weight-normalized and scaled compressive stress magnitude in each studied group. While these two areas are located postero-anteriorly in controls and main thoracic subjects, in TL/L subjects the anterior left side of the sacrum is under higher compressive stress as compared to the right side $p<0.05$ (Figure 4.5). The average, scaled, weight-normalized compressive stress was 8%, 15%, and 11% higher in the high stress cluster than the low stress cluster in control, MT, and TL/L respectively.

Insert Figure 4.5 near here

Higher stress was observed at the anterior part of the sacrum in MT subjects when compared to controls ($p<0.05$) while it was not significantly different between MT and TL/L

subjects ($p<0.1$). The average magnitude of the weight-normalized compressive stress at the anterior part of the S1 endplate was 24% higher in the MT group than in the controls while it measured 6% higher in TL/L subjects as compared to controls. The post-hoc test (Dunnett's T3) showed significantly different stress at the left side of the sacrum between TL/L subjects and controls ($p<0.05$).

Although the magnitude of the compressive stress slightly varied when different spinal stiffness were applied in the model the overall trend of the weight-normalized and scaled stress distribution on the sacrum did not change significantly ($p<0.05$). The position of the COP_{S1} slightly changed as the position of the trunk slices COM varied however these changes were not statistically significant ($p>0.05$). The position of the high and low stress areas on the superior S1 endplate did not vary as a result of the 1cm shift in the COM position.

4.2.5 Discussion

This study focused on the biomechanical and geometrical parameters of the sacrum in two scoliotic subgroups as compared to asymptomatic controls. Although the relationship between spinal and pelvic parameters in the sagittal plane has been explored previously [23, 25, 28, 29, 42, 43] the method proposed herein allows analysis of the spino-pelvic 3D relationship in consideration of both the spino-pelvic geometrical and biomechanical indices. Biomechanical loading of the sacrum varied between subjects with different spino-pelvic configurations thus suggesting the effect of both spinal and pelvic parameters on the COP_{S1} position. The patient-specific FE model, although not sensitive to a small shift in the COM position, was able to show significant differences in the sacral loading between the studied groups as well as the associations between the sacral loading and curve severity within each group.

This study is the first to simulate possible loading mechanisms at the level of the sacrum in subjects with different types of AIS. The normal stress distribution on the sacrum varied more between subjects with a main thoracolumbar/lumbar curve and controls as compared to the differences between subjects with a main thoracic curve and controls. This finding is most likely explained by the fact that the pelvis is adjacent to the spinal deformity in subjects with thoracolumbar/lumbar deformities while it is more distant from the spinal deformity in subjects

with main thoracic curves. The results highlighted the relationship between the location and severity of the spinal deformities and mechanical loading of the sacrum in the studied groups.

Higher compressive stress was observed on the sacrum endplate at the same side of the lumbar deformity in left TL/L subjects. As discussed, this finding relates spinal deformity and sacral loading in these patients. In the MT group, higher stresses were measured in the anterior part of the sacrum as compared to the two other groups. This result can be explained by the fact that the COM is slightly shifted anteriorly in the MT studied sample (Figure 4.4 and Table 4.2). As a result, significantly increased stress on the anterior part of the sacrum was observed in this group of subjects. While sagittal pelvic configurations are not related to the scoliotic types [28], biomechanical loading of the sacrum appears to be associated to the spinal deformity and spino-pelvic alignment. Moreover since mechanical loading of the vertebra and intervertebral disks is linked to disk degeneration and reduced mobility of the affected section, [1, 10] study of the biomechanical loading of the sacrum in scoliosis is potentially important in identifying subjects who present with a high or abnormal compressive stress of the sacrum before or after operation and consequently are prone to further disk degeneration [1]. The proposed method and the notion of the COP_{S1} made it possible to identify patients with high or asymmetric stress distribution on the S1 endplate and relate it to the curve severity. It is suggested that biomechanical parameters such as distance between the COP_{S1} and CHVA and position of the COP_{S1} in the local coordinate system of the sacrum could be considered as additional parameters to further analyze spino-pelvic alignment especially before and after a surgical treatment in AIS.

The position of the COP_{S1} in the global coordinate system was related to the position of the sacrum in reference to the CHVA. However, a strong relationship was reported between the position of the COP_{S1} and sacro-pelvic parameters which was not the case when the 2D position of the sacrum endplate center and sacro-pelvic parameters were compared. This result suggests that the position of the COP_{S1} is not only related to the 2D position of the center of the S1 endplate but also is modified by the relative 3D orientation of the S1 endplate and pelvis in reference to the CHVA and trunk COM.

Although asymmetric contra-lateral muscular forces, particularly in scoliotic subjects [16], have an impact on the vertebral loading [17], the current study only focused on the sacral loading in AIS subgroups in consideration of the COM position due to the skeletal deformities

and spino-pelvic relative alignment. Despite the exclusion of the muscle forces in the model, the FE model is balanced. The reaction forces at the boundary levels, although not excessively significant (<35N), varied between subjects to assure the model equilibrium. While exclusion of the muscles and external forces such as the ground reaction force prohibits us from calculating the absolute magnitude of the sacral loading, it still permits us to compare the normalized and scaled sacral loading in different spino-pelvic configurations in an equilibrated patient-specific FEM. Moreover since the treatment of the AIS is mainly based on the geometrical skeletal correction, analysis of the spino-pelvic interaction in a skeletal model with no assumption about the local muscle forces provides an acceptable picture to assess the impact of the spinal deformities on the sacral loading. Study of the effect of the asymmetrical muscle forces on equilibrating the vertebral loading was not included in the current article and should be the subject of another study.

Due to the limitations of the model the relative analysis and comparison between normalized, scaled parameters rather than comparison between the absolute values of the sacral compressive stress was considered as an appropriate alternative to analyzing the specific effect of the gravitational loads and spinal deformity on the sacral loading. The model showed the impact of the altered position of the COM due to spinal deformities on the biomechanical loading of the sacrum in subjects with thoracic or lumbar deformities. The role of the sacro-pelvic parameters as a geometrical factor affecting the sacral loading was accentuated in this study.

The effects of the variation in the position of the COM on the FEM simulation results were tested. The compressive stress on the S1 endplate did not significantly change by repositioning of the COM at the level of each vertebra within a simulated span of 1cm. This result suggests that the proposed parameter *i.e.* COP_{SI} is more sensitive to the differences in spino-pelvic geometry as was observed in scoliotic subgroups and not to the small changes in the position of the COM. However the personalized COM position both in the frontal and sagittal planes can contribute to better characterization of the sacral loading in patient-specific models of the spine and pelvis. The changes in the mechanical properties of the spine did not adversely impact the results of the study. In summary, the presented results in this study are representative of the impact of the spine and pelvic geometry and their relative alignment on the sacral loading and are not affected by the tested design parameters.

4.2.6 Conclusion

This study verified the role of the relative spine and pelvic alignment on the biomechanical loading of the sacrum in AIS subgroups and controls. The biomechanical analysis of the sacrum shows in addition to the location of the structural curve of the spine, the sacral loading was a characteristic of each scoliotic subgroup. This finding was potentially important in explaining the 3D spine and pelvic biomechanical interaction and assessment of the transferred load between the spine and pelvis in AIS subgroups.

4.2.7 References

- 1 Adams MA, Freeman BJC, Morrison HP, Nelson IW, Dolan P (2000) Mechanical initiation of intervertebral disc degeneration. *Spine* 25:1625-1636.
- 2 Berthonnaud E, Dimnet J, Hilmi R (2009) Classification of pelvis and spinal postural patterns in upright position. Specific cases of scoliotic patients. *Comput med imag grap* 33:634-643.
- 3 Berthonnaud E, Dimnet J, Roussouly P, Labelle H (2005) Analysis of the sagittal balance of the spine and pelvis using shape and orientation parameters. *J spinal disord tech* 18:40-47.
- 4 Boulay C, Tardieu C, Hecquet J, Benaim C, Mouilleseaux B, Marty C, Prat-Pradal D, Legaye J, Duval-Beaupère G, Pélissier J (2006) Sagittal alignment of spine and pelvis regulated by pelvic incidence: standard values and prediction of lordosis. *Eur Spine J* 15:415-422.
- 5 Boulay C, Tardieu C, Benaim C, Hecquet J, Marty C, Prat-Pradal D, Legaye J, Duval-Beaupère G, Pélissier J. (2006) Three-dimensional study of pelvic asymmetry on anatomical specimens and its clinical perspectives. *J Anat* 208:21-33.
- 6 Cheriet F, Remaki L, Bellefleur C, Koller A, Labelle H, Dansereau J (2002) A new X-ray calibration/reconstruction system for 3D clinical assessment of spinal deformities. *Stud Health Technol Inform* 91:257-261.
- 7 Clin J, Aubin C-É, Lalonde N, Parent S, Labelle H (2011) A new method to include the gravitational forces in a finite element model of the scoliotic spine. *Med Biol Eng Comput* 49:967-77.

8 Delorme S, Petit Y, de Guise JA, Labelle H, Aubin C-É, Dansereau J (2003) Assessment of the 3D reconstruction and high-resolution geometric modeling of the human skeletal trunk from 2D radiographic images. *IEEE Trans biomed Eng* 50:989-998.

9 Driscoll M, Aubin CE, Moreau A, Villemure I, Parent S (2009) The role of spinal concave-convex biases in the progression of idiopathic scoliosis. *Eur Spine J* 18(2):180-187.

10 Duance VC, Crean JKG, Sims TJ, Avery N, Smith S, Menage J, Eisenstein SM, Roberts S (1998) Changes in Collagen Cross-Linking in Degenerative Disc Disease and Scoliosis. *Spine* 23:2545-2551.

11 Dubousset J (1996) Pelvic obliquity correction ed. NY: Lippincott-Raven.

12 Dubousset J (1994) Three dimensional analysis of the scoliotic deformity ed. New York: Raven Press.

13 Duval-Beaupère G, Legaye J (2004) Composante sagittale de la statique rachidienne. *Rev Rhum* 71:105-119.

14 Duval -Beaupère G, Cosson P (1992) A barycentric study of the sagittal shape of spine and pelvis, The condition required for an economic standing position. *Ann Biomed Eng* 20:451-462.

15 El-Rich M, Shirazi-Adl A (2005) Effect of load position on muscle forces, internal loads and stability of the human spine in upright postures. *Comput Methods Biomed Engineering* 8: 359-368.

16 Feipel V, Aubin C-É, Ciolofan OC, Beauséjour M, Labelle H, Mathieu PA (2002) Electromyogram and kinematic analysis of lateral bending in idiopathic scoliosis patients. *Med Biol Eng Comput* 40(5): 497-505.

17 Goel V, Kong W, Han J, Weinstein JN, Gilbertson LG (1993) A combined finite element and optimization investigation of lumbar spine mechanics with and without muscles. *Spine* 18: 1531-1541

18 Guigui P, Levassor N, Richards BS, Wodecki P, Cardinne L (2003) Valeur physiologique des paramètres pelviens et rachidiens de l'équilibre sagittal du rachis. *Rev Chir Orthop* 89:496-506.

19 Gum JL, Asher MA, Burton DC, Lai SM, Lambart LM (2007). Transverse plane pelvic rotation in adolescent idiopathic scoliosis: Primary or compensatory? *Eur Spine J* 16:1579-1586.

20 Jiang Y, Nagasaki S, You M, Zhou J (2006) Dynamic studies on human body sway by using a simple model with special concerns on the pelvic and muscle roles. *Asian Journal of Control* 8:297-306.

21 Kadoury S, Cheriet F, Dansereau J, Labelle H (2007) Three-dimensional reconstruction of the scoliotic spine and pelvis from uncalibrated biplanar x-ray images. *J Spinal Disord Tech* 20:160-167.

22 Kadoury S, Cheriet F, Laporte C, Labelle H (2007) A versatile 3D reconstruction system of the spine and pelvis for clinical assessment of spinal deformities. *Medi Biol Eng Comput* 45: 591-602.

23 Labelle H, Roussouly P, Berthonnaud E, Dimnet J, O'Brien M (2005) The importance of spino-pelvic balance in L5-S1 developmental spondylolisthesis. *Spine* 30:S27-S34.

24 Labelle H, Dansereau J, Bellefleur C, Poitras B, Rivard CH, Stokes IA, de Guise J (1995) Comparison between preoperative and postoperative three-dimensional reconstructions of idiopathic scoliosis with the Cotrel-Dubousset procedure. *Spine* 20: 2487-2492.

25 Legaye J, Duval-Beaupère G, Hecquet J, Marty C (1998) Pelvic incidence: a fundamental pelvic parameter for three-dimensional regulation of spinal sagittal curves. *Eur Spine J* 7:99-103.

26 Liu YK, Laborde JM, Van Buskirk WC. (1971) Inertial properties of a segmented cadaver trunk: their implications in acceleration injuries. *Aerosp Med* 42:650-657.

27 Mac-Thiong J-M, Roussouly P, Berthonnaud E, Guigui P (2011) Sagittal parameters of global spinal balance: normative values from a prospective cohort of seven hundred nine Caucasian asymptomatic adults. *Spine* 35:E1193-E1198.

28 Mac-Thiong J-M, Labelle H, Charlebois M, Huot MP, de Guise JA. (2003) Sagittal plane analysis of the spine and pelvis in adolescent idiopathic scoliosis according to the coronal curve type. *Spine* 28:1404-9.

29 Mac-Thiong J-M, Labelle H, Berthonnaud E, Betz RR, Roussouly P (2007) Sagittal spino-pelvic balance in normal children and adolescents. *Eur Spine J* 16: 227-234.

30 Mahaudens P, Detrembleur C, Mousny M, Banse X (2009) Gait in adolescent idiopathic scoliosis: energy cost analysis. *Eur Spine J* 18:1160-1168.

31 Natarajan RN, Garretson RB, Biyani A, Lim TH, Andersson GB, An HS (2003) Effects of slip severity and loading directions on the stability of isthmic spondylolisthesis: a finite element model study. *Spine* 28:1103-1112.

32 Pearsall DJ, Reid JG, Livingston LA (1996) Segmental inertial parameters of the human trunk as determined from computed tomography. *Ann Biomed Eng* 24:198-210.

33 Pearsall DJ, Reid JG, Ross R. (1994) Inertial properties of the human trunk of males determined from magnetic resonance imaging. *Ann Biomed Eng* 22:692-706.

34 Perie D, Aubin C-É, Lacroix M, Lafon Y, Labelle H (2004) Biomechanical modeling of orthotic treatment of the scoliotic spine including a detailed representation of the brace-torso interface. *Med Biol Eng Comput* 42:339-344

35 Roussouly P, Gollogly S, Berthonnaud E, Dimnet J (2005) Classification of the normal variation in the sagittal alignment of the human lumbar spine and pelvis in the standing position. *Spine* 30:346-353.

36 Roussouly P, Pinheiro-Franco JL (2011). Biomechanical analysis of the spino-pelvic organization and adaptation in pathology. *Eur Spine J* 20 (Suppl 5):S609-S518.

37 Pasha S, Sangole AP, Aubin C-É, Parent S, Mac-Thiong JM, Labelle H (2010) Characterizing pelvis dynamics in adolescent with idiopathic scoliosis. *Spine* 35:E820-E826.

38 Sangole AP, Aubin C-É, Labelle H, Lenke L, Jackson R, Newton P, Stokes IA; Scoliosis Research Society 3D Scoliosis Committee (2010) The central hip vertical axis: a reference axis for the Scoliosis Research Society three-dimensional classification of idiopathic scoliosis. *Spine* 35(12): E530-534.

39 Servain A, Aubin C-É, Gharbi H, Wang X, Labelle H (2012) Biomechanical evaluation of predictive parameters of progression in adolescent isthmic spondylolisthesis: a computer modeling and simulation study. *Scoliosis* 7(1):2.

40 Shufflebarger H, Suk S-I, Mardjetko S. (2006) Debate: Determining the upper instrumented vertebra in the management of adult degenerative scoliosis: stopping at T10 versus L1. *Spine* 31: S185-S94.

41 Skalli W, Zeller RD, Miladi L, Bourcereau G, Savidan M, Lavaste F, Dubousset J (2006) Importance of pelvic compensation in posture and motion after posterior spinal fusion using CD instrumentation for idiopathic scoliosis. *Spine* 31: E359-366.

42 Tanguay F, Mac-Thiong JM, de Guise JA, Labelle H (2007). Relation between the sagittal pelvic and lumbar spine geometries following surgical correction of adolescent idiopathic scoliosis. *Eur Spine J* 16:531-6.

43 Upasani VV, Tis J, Bastrom T, Pawelek J, Marks M, Lonner B, Crawford A, Newton PO (2007). Analysis of sagittal alignment in thoracic and thoracolumbar curves in adolescent idiopathic scoliosis. *Spine* 32:1355-9.

44 Villemure I, Aubin CE, Dansereau J, Labelle H (2002). Simulation of progressive deformities in adolescent idiopathic scoliosis using a biomechanical model integrating vertebral growth modulation. *J Biomech Eng* 124(6):784-790.

4.2.8 Figures and Tables

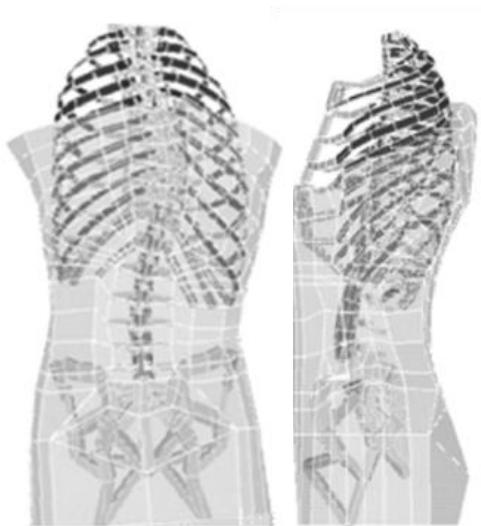


Figure 4.1: Osseo- ligamentous finite element model of the trunk.

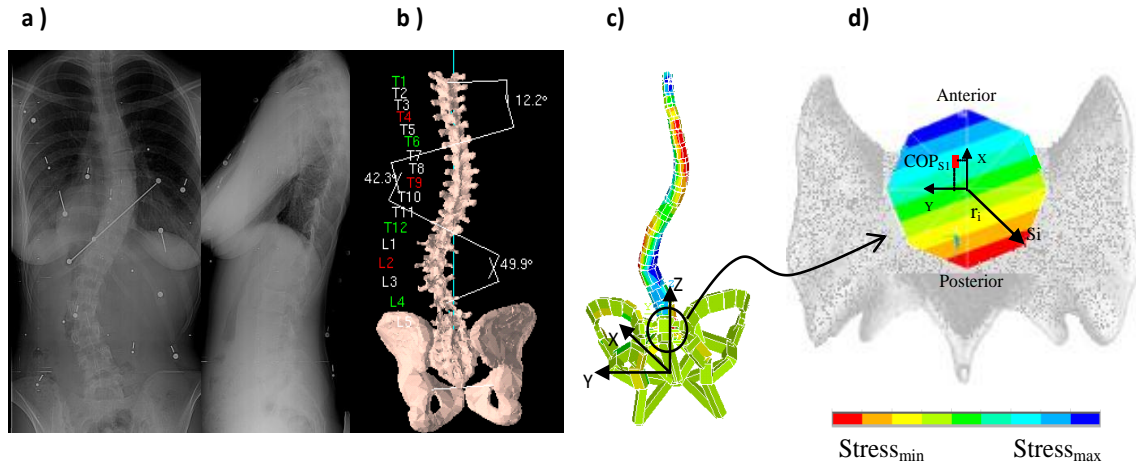


Figure 4.2: Steps in computation of the stress distribution and the COP_{S1} position on the S1 endplate: a. Biplanar radiographs, b. 3D reconstruction of the spine and pelvis, c. Finite element simulation of the gravitational loads on the spine and pelvis, d. Compressive stress distribution on the S1 endplate (scaled between the minimum and maximum stress magnitude) and the position of the COP_{S1} .

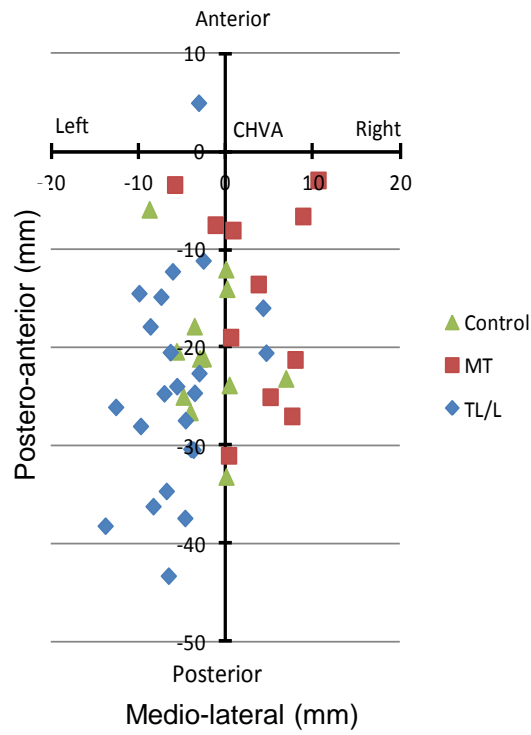


Figure 4.3: Distribution of the COP_{SI} position in the transverse plane in the three groups.

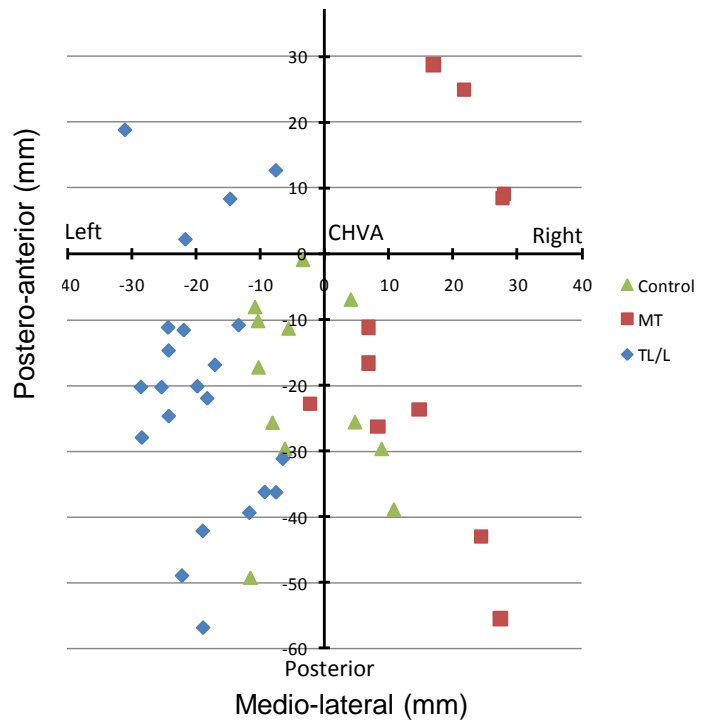


Figure 4.4: Distribution of the COM position in the transverse plane in the three groups.

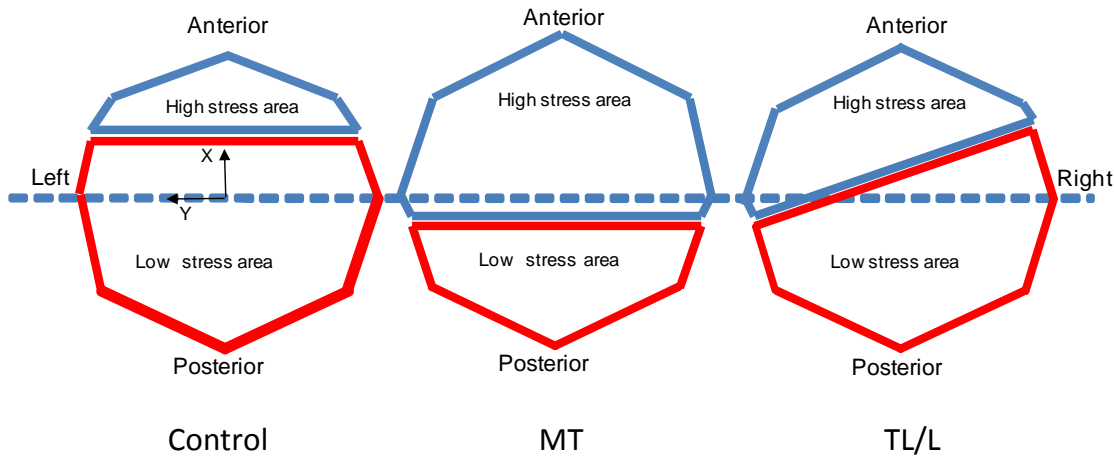


Figure 4.5: Cluster analysis of the stress distribution on the superior endplate of the sacrum in the three groups of subjects. The dashed line depicts the center line of the sacrum in the local coordinate system of the sacrum.

Table 4.1: Average and standard deviation of the geometrical parameters in the three studied groups: controls, subjects with main right thoracic (MT) deformity and subjects with left thoraco-lumbar/lumbar (TL/L) deformity.

Subjects	Thoracic Cobb (Right)	Kyphosis	Lumbar Cobb (Left)	Lordosis	PI	PT	SS
Control	-	47°± 10°	-	-58°± 8° 7°	44°± 8°	10°± 7°	35°± 5°
MT	51°±14°	37°± 18°	-32°± 12°	-67°± 13°	50°± 5°	8°± 7°	43°± 8°
TL/L	24°±7°	33°± 10°	-40°± 11°	-65°± 11°	50°± 8°	15°± 7°	36°± 7°

Table 4.2: The average and standard deviation of the position of the COM and COP_{SI} in the transverse plane.

Subjects	COM (mm)		COP _{SI} (mm)	
	Medio-lateral	Postero-anterior	Medio-lateral	Postero-anterior
Control	-3±8	-21±14	-2±3	-20±7
MT	16±10	-11±26	3±5	-14±8
TL/L	-19±8	-20±15	-7±4	-25±10

4.3 The effect of the position of the center of mass (COM) on the biomechanical loading of the sacrum: Sensitivity analysis and validation of the position of COM in the FE model

In the current study two experimental techniques were designed to estimate the COM position in AIS in such way that the personalized COM position is applicable in patient specific FE models of the spine. The first experiment was designed to find an equation that relates the COP position and projection of the COM on the transverse plane in scoliotic subjects with moderate spinal curves. The second experiment used this equation to transfer the location of the COP to the COM in the synchronized COP-radiographic images in another group of AIS subjects with moderate spinal curves. This new position of the COM was used to estimate the position of the trunk slices COM at the level of each vertebra with respect to the vertebrae center through an optimization process in the second group of subjects. This hybrid method allowed to estimate the personalized 3D position of the trunk slices' COM. Later the sensitivity of the FE model to the position of the COM was tested in the patient specific FE models of the spine and pelvis to quantify the impact of the personalized COM position on the sacral loading.

It is established that the COM position impacts the biomechanical loading of the spine (Park, 2012) which suggests the importance of the personalized COM position in numerical models of the spine and pelvis. Although several techniques have been developed to estimate the COM position the applicability of these techniques in numerical simulation of the scoliotic spine is not tested yet.

4.3.1 First experiment: study the relationship between the position of the COP and the COM in AIS

A total number of 21 AIS female subjects including 17 main right thoracic subjects and 4 right main thoracic with compensatory left lumbar curve were randomly selected. The exclusion criteria of receiving any treatment by brace or surgery was applied. All patients participated voluntarily and a consent form was signed by the participants and their parents. The project was approved by the ethics committee of our institution.

The average age of the subjects was 13.8 ± 2.1 years at the time of data collection. The mean height was measured at 158.3 ± 5.3 cm and the mean weight was 50.1 ± 6.2 kg. Mean Cobb angle in subjects with a main right thoracic curve was 32° (range: 20° – 57°). Subjects with right thoracic and compensatory left lumbar curve had a mean thoracic Cobb angle of 42° [20° – 52°] and a mean lumbar Cobb of 32° [23° – 45°].

Subjects were asked to stand on a force plate (AMTI, Newton, MA) for 30 seconds. The ground reaction forces and moments were registered throughout the experiment. The point of application of the resultant force presented the COP position (AMTI, Newton, MA). A jig was fixed on the force place to determine the heel position for all subjects (figure 4.6). Three trials were recorded for each subject. The collected data were filtered using a second order Butterworth filter (MATLAB R2008a, Mathworks, Natick, MA) with the sampling frequency of 64 Hz (Allard, 2004). The force plate local coordinate system is depicted in figure 4.6. The origin of the force plate was transferred to the midpoint between two heels.

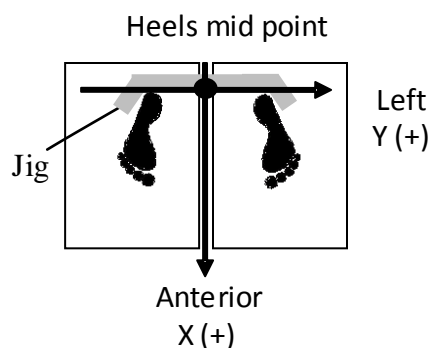


Figure 4.6: The origin (●) and the axis orientation of the coordinate system on the force plate (first experimental setup).

The modified version of the zero-to-zero point double integration technique and the equilibrium point (Zatsiorsky and Duarte, 1999; Zatsiorsky and Duarte, 2000) was applied on the filtered data. This technique is based on the assumption that the COP position and the COM coincide when the horizontal component of the ground reaction force is equal to zero. Therefore when the horizontal component of the ground reaction force (F_H) is equal to zero, the F_H was double integrated to calculate the projection of the COM on the transverse plane (COM_{2D}) (Zatsiorsky and Duarte, 1999, 2000). The first and second constants of the integration respectively were the position of the COP and the COP oscillation velocity at the time that $F_H=0$ ($T_{F_H=0}$).

In the kinematic of a particle the instantaneous position of the particle $X(t)$ is defined by equation (4.1):

$$X(t) = \int \int a(t) dt + v_0(t) + x_0 \quad \text{Equation 4.1}$$

Wherein a is the acceleration, v_0 is the initial velocity, and x_0 defines the initial position of the particle. v_0 is calculated as follow:

$$v_0 = v(t) - \int a(t) dt \quad \text{Equation 4.2}$$

where v defines the velocity of the particle as a function of time. Likewise, in case of the trunk oscillation, when the body mass (M) oscillates during t seconds of quite stance COM_{2D} is calculated as:

$$COM_{2D} = \int \int (F_H/M) dt + V_0(t) + COP_{T_{F_H=0}} \quad \text{Equation 4.3}$$

V_0 is the second constant of the integration which calculates from:

$$V_0 = (COP(t_{i+1}) - COP(t_i)) / \Delta t - \int (F_H/M) dt \quad \text{Equation 4.4}$$

t_i and t_{i+1} are two consequence time when $F_H=0$.

With digital registration of the ground reaction force, the exact time when $F_H=0$ ($T_{F_H=0}$) is not necessarily accessible throughout the experience. Thus a 2D local interpolation technique (cubic Spline, Matlab, Mathworks, Natick, MA, 2008) was used to approximately determine the

time when the polarity of the F_H changes *i.e.* when $F_H=0$ ($T_{FH=0}$). The position of the COP at this moment ($COP_{T_{FH=0}}$) is the first integration constant.

The filtered COP oscillation was used in equations 4.3 and 4.4 and the COM_{2D} was calculated in the cohort of subjects.

The position of the COM_{2D} (equation 4.3) was compared to the average position of the COP in the group of subjects. A regression line was fitted to the scatter points of the COM_{2D} and the average position of the COP to formulate the relationship between the COP and COM_{2D} in medio-lateral and antero-posterior directions separately in the studied group. Subsequently two regression equations were derived to formulate the COP-COM relative position in the medio-lateral and antero-posterior directions.

4.3.2 Second experiment: Optimization of the COM position at the level of each vertebra

In the second experiment a piezoelectric pressure mat with devoted software (Trubalance 1.0) was placed in a low dose 3D radiography system (EOS system, Biospace, Paris) available at our institution. The position of the COP was automatically calculated as the point of application of the resultant reaction forces in the Trubalance software. A calibration object was attached to the pressure mat (figure 4.7-a). The position of this object was used to transfer the position of the COP to the radiographs' coordinate system. 9 scoliotic subjects (7 with single right thoracic and 2 with right thoracic and left thoracolumbar/lumbar) participated in the second part of the experiment. All subjects were participated voluntarily. The project was approved by the ethics committee of our institution,

The mean age 14.5 ± 5.6 years, weight 54.0 ± 8.3 kg, and height 165.0 ± 10.1 cm of the participants were registered at the time of radiography acquisition. Spinal parameters were measured as following: thoracic Cobb angle $30^\circ \pm 24^\circ$ [15° - 68°], lumbar Cobb angle $24^\circ \pm 11^\circ$ [15° - 42°], thoracic kyphosis $30^\circ \pm 15^\circ$ [7° - 45°], and lumbar lordosis $35^\circ \pm 12^\circ$ [23° - 57°]. The subjects stayed on the pressure map after the radiograph acquisition to complete 30s of the COP oscillation registration. Since the pressure mat only calculates the position of the COP and no information about the reaction force is available, the regression equation from the first

experiment was used to transfer the position of the COP to the 2D projection of the COM on the transverse plane for each subject (COM_{regression}).

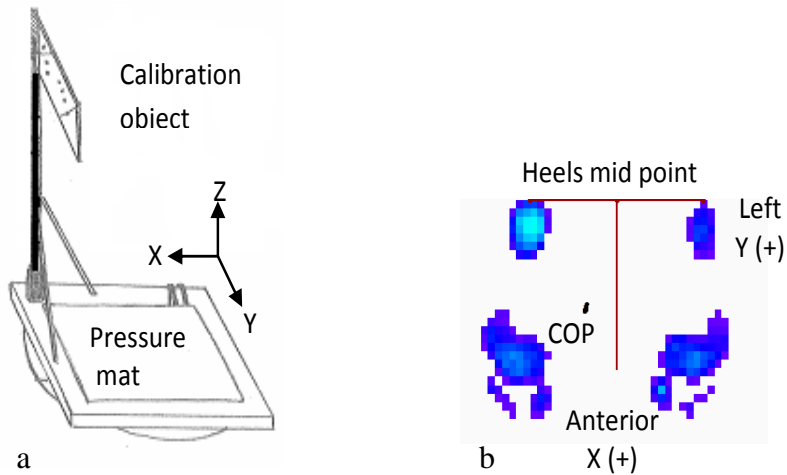


Figure 4.7: a) The position of the calibration object on the pressure mat. b) The location of the feet and the COP on the pressure mat during the radiography acquisition.

The 3D position of the vertebral endplates' center was determined from digitized x-rays in EOS system (Biospace med, Paris) using the method explained by Humbert (2009). In this method the upper endplate of T1, lower endplate of L5, and the spinal curvature are determined to create a parametric model of the spine. Later a detailed model of the spine and an interpolation method were used to create the 3D parametric model of the spine using limited number of parameters on the radiographic images. These parameters are described by the spinal curve length (length of the curve connecting T1 to L5 which passes through the vertebral bodies centers), the depth and width of the vertebrae and their position along the spinal curve. The precision of the spinal parameters was determined between 1.2° and 5.6° (Humbert, 2009).

The position of the trunk slices' COM at the level of each vertebra was determined in the sagittal and frontal planes: the antero-posterior position of the COM in the sagittal plane (x_i) was determined from literature (Liu, 1971; Pearsall, 1994; Pearsall, 1996). In the frontal plane the 2D position of the vertebral endplates' center was determined as the COM position (y_i). The center of masses of the head, neck, and arms were associated with the COM of the T1, T3, T4, and T5 vertebrae (El-Rich, 2005). The 2D position of the COM at the level of each vertebra (x_i, y_i), as the primarily estimation of the COM in the optimization process, was multiplied by optimization

parameters in sagittal (α) and frontal (β) planes separately (Equation 4.5). These optimization parameters were calculated during the optimization process to determine the position of the COM at the level of each trunk slice with respect to the vertebral center. Equations 4.5 to 4.7 formulate this procedure. $XCOM_{sagittal}$ and $YCOM_{frontal}$ are the predicted location of the COM at the level of each vertebra in the sagittal and frontal planes respectively. At this step of the optimization procedure $XCOM_{sagittal}$ and $YCOM_{frontal}$ are presented as a function of the optimization parameters. A total number of 40 optimization parameters (17 for spinal vertebrae, and 3 for the COM of head, neck, and arms in each plane) were used in the optimization process to optimize the position of the COM of the head, neck, arms, and trunk slices from T1 to L5 in sagittal and frontal planes ($i=1\dots40$). The optimization parameters (α and β) determined the distance between the center of each vertebral endplate and the COM in mm in the sagittal and frontal planes for each trunk slice respectively.

$$\begin{aligned} XCOM_{sagittal}(i) &= \alpha_i \times x_i & i=1\dots40 \\ YCOM_{frontal}(i) &= \beta_i \times Y_i \end{aligned} \quad \text{Equation 4.5}$$

The 2D position of the COM at each vertebral level ($XCOM_{sagittal}$ and $YCOM_{frontal}$) as a function of the optimization parameters was multiplied by the mass of the trunk slice (M_i) derived from literature (Pearsall, 1994; Pearsall, 1996). The mass of the head and neck was associated with the mass of the T1 trunk slice. The mass of the arms were distributed between the trunk slices at the T3, T4 and T5 vertebral levels by the method described by El-Rich (2005). The net position of the trunk center of mass as a function of the optimization parameters was defined from the barycenter of the trunk slices COM (equation 4.6):

$$COM_{net} = \sum_{i=1}^{40} M_i \times \begin{bmatrix} XCOM_{Sagittal} \\ YCOM_{Frontal} \end{bmatrix} \quad \text{Equation 4.6}$$

An optimization method (MATLAB optimization package, nonlinear constrained minimization, Mathworks, Natick, MA; R2008a) was used to minimize the absolute distance between the COM_{net} (equation 4.6) and the location of the COM from the regression equation ($COM_{regression}$) for each subject of the second experiment in the sagittal and frontal planes separately. Considering the COM position from literature, the optimization parameters (α and β)

were constrained between [-50, 50] mm from the center of the vertebral endplates (Pearsall, 1994; Pearsall, 1996). The objective function was defined in equation 4.7:

$$f = \min |COM_{\text{regression}} - COM_{\text{net}}| \quad \text{Equation 4.7}$$

Several optimization iterations were permitted to minimize the objective function to the level of 10e-3 mm. The origin of the coordinate system (heels midpoint) was transferred to midpoint between the femoral heads thus the COM position can be presented with respect to a more comprehensive anatomical landmark.

4.3.3 Sensitivity analysis: the impact of the COM position on the biomechanical loading of the sacrum

The effect of the variation in the position of the COM on the FEM analysis results in section 4.1 was tested. The stress distribution on the S1 endplate was calculated in the FE model of the 9 subjects who had participated in the second experiment by using the position of the upper body COM calculated by two different methods: first the optimized positions of the COM calculated in the section 4.2.2., and second the COM position from the literature (Pearsall, 1996; El-Rich, 2005). Mann Whitney U test (PASW statistics 18.0, SPSS Inc., Chicago, IL) was performed to evaluate the sensitivity of the patient specific FE model to the position of the upper body COM in calculation of the sacral loading in 9 subjects of the second study.

4.4 Results

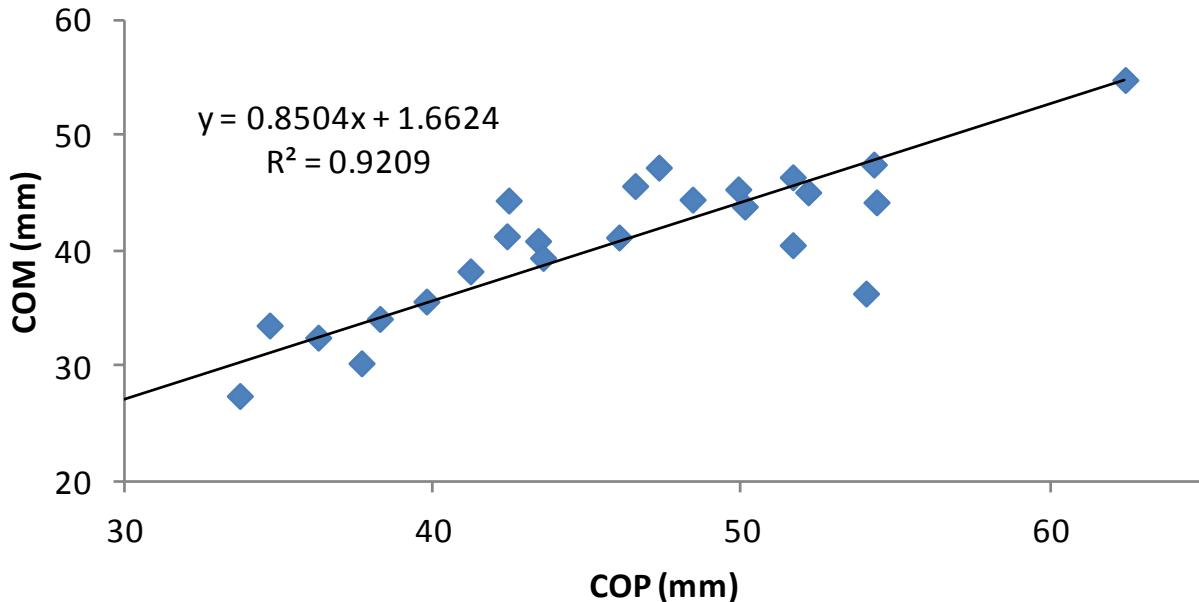
4.4.1 Results of the first experiment (regression analysis)

Linear regression analysis showed a significant correlation ($p<0.01$) between the position of the COM and the COP in antero-posterior (AP) and medio-lateral (ML) directions in the group of subjects (Equations 4.8 and 4.9 and figure 4.8). The linear relationship between the position of the COP and COM was defined as:

$$COM_{\text{AP}} = 0.85 COP_{\text{AP}} + 1.66, r^2 = 0.92, p < 0.01 \quad \text{Equation 4.8}$$

$$COM_{\text{ML}} = 0.34 COP_{\text{ML}} + 4.97, r^2 = 0.63, p < 0.01 \quad \text{Equation 4.9}$$

Antero-posterior



Medio-lateral

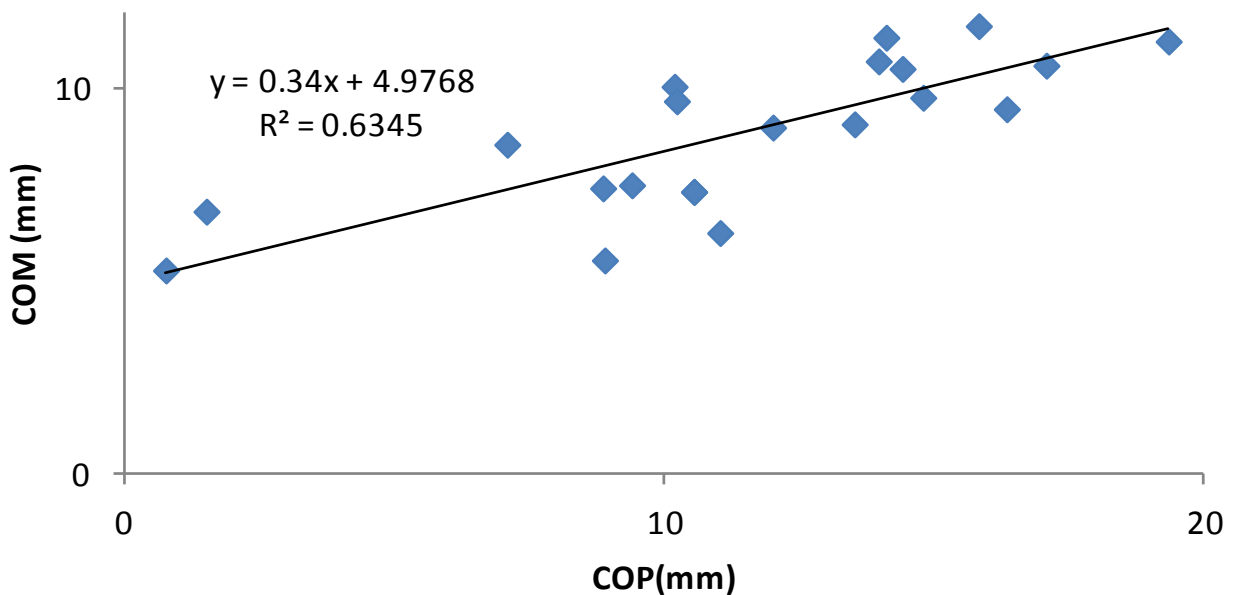


Figure 4.8: The correlation between the COM and the COP positions: a) in postero-anterior direction, b) in the medio-lateral direction.

4.4.2 Results of the second experiment (optimization process)

The optimization process minimized the distance between the $\text{COM}_{\text{regression}}$ and COM_{net} to the level of $10\text{e-}3$ mm. The results of the optimization process were shown for one subject (patient1) in figure 4.9. This figure represented the bi-planar radiographs (figure 4.9a), position of vertebrae endplate centers, position of the trunk slice's COM from literature, and the position of the COM at the level of each vertebra after optimization. Table 4.3 summarized the spinal parameters and the position of the spinal apex for this subject (patient1). The distances between the COM of the trunk slices and the center of the vertebrae were listed in table 4.4 for this subject.

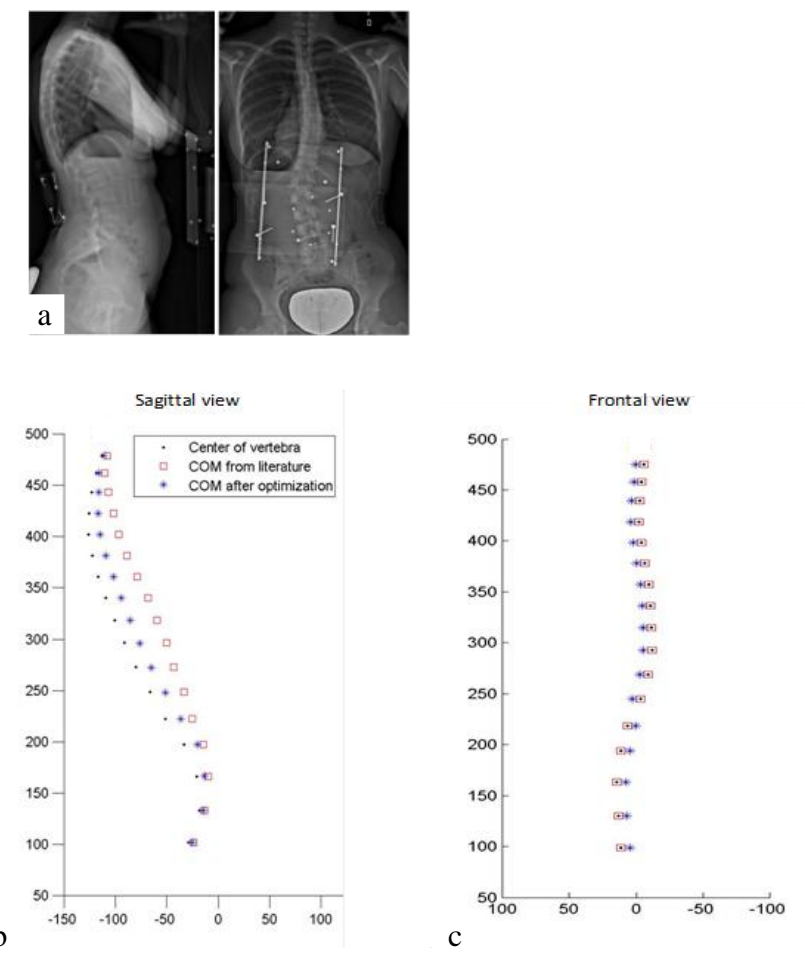


Figure 4.9: a) Presentation of the bi-planar radiographs and the calibration object b) The 3D position of the vertebrae and the center of mass of each vertebra slice after optimization in the sagittal plane and c) in the frontal plane. (0,0) is the position of the mid point of the femoral heads.

Table 4.3: The position of the spinal apices and spinal curvatures (angles) in frontal and sagittal planes in patient1.

	Thoracic Cobb	Lumbar Cobb	Kyphosis	Lordosis
Apex	T10	L3	T7	L4
Angle (degree)	20	32	40	47

Table 4.4: The distance between the center of each vertebra and the position of the center of mass at the level of each vertebra in sagittal and frontal planes. (+) direction is anterior (sagittal plane) and to the left (frontal plane) calculated for patient1.

	Sagittal plane (mm)	Frontal plane (mm)
T1	1.5	-6
T2	2.4	-5.3
T3	6.1	-5.3
T4	9.1	-5.2
T5	9.4	-5.1
T6	12.6	-4.8
T7	15.2	-4.3
T8	15.2	-4.1
T9	15.1	-3.7
T10	14.8	-3.5
T11	14.7	-3.8
T12	14.5	-4.3
L1	14.5	5.1
L2	14.3	5.8
L3	7.2	6.7
L4	4.6	6.5
L5	4.1	6.3

The average net position of the COM with respect to the midpoint of the femoral heads axis was calculated in the sagittal (11.2 mm, SD: 6.7) and frontal plane (-1.8 mm, SD: 5.1) in the cohort of subjects. The optimization process, on average, shifted the net position of the trunk COM projection on the transverse plane by 3.7 mm (SD: 2.8mm) in the medio-lateral direction and 7.8 mm (SD: 4.0mm) in the antero-posterior direction toward the midpoint of the femoral heads axis when compared to the COM position calculated by Pearsall's (1996) equations.

4.4.3 Sensitivity analysis: the impact of the COM position on the biomechanical loading of the sacrum

The compressive stress on the S1 endplate decreased slightly when the COM positions from literature (Liu, 1979; Pearsall, 1996) was replaced by the optimized position of the COM in the FE model (Figure 4.10). The maximum different between the stress magnitudes on the S1 endplate was 16% when two different positions of the COM were applied in the FEM. The Mann-Whitney U test (PASW statistics 18.0, SPSS Inc., Chicago, IL) showed no significant difference in the position of the COP_{SI} before and after optimization in the 9 studied subjects.

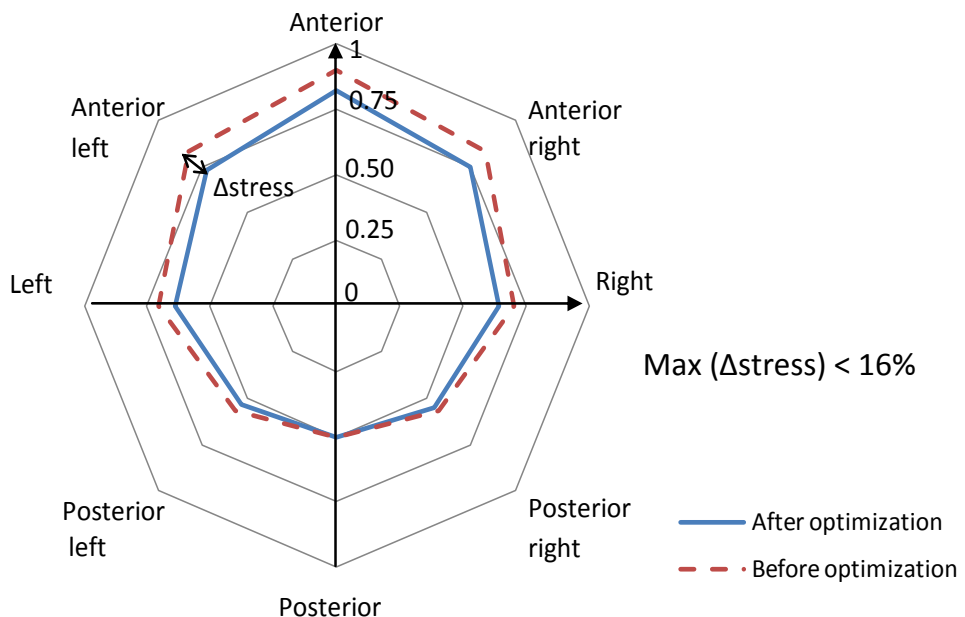


Figure 4.10: Stress distribution on the superior plate of sacrum before and after optimization of the position of the center of mass.

CHAPTER 5 STUDY OF THE IMPACT OF SPINAL INSTRUMENTATION ON THE SACRUM BIOMECHANICAL LOADING IN ADOLESCENT IDIOPATHIC SCOLIOSIS

In the current chapter the effect of the posterior spinal instrumentation and fusion (PSIF) surgery on the biomechanical loading of the sacrum was studied through a comprehensive FE model of the spine and pelvis. This study aimed to better understand the biomechanical relationship between the spine and pelvis after PSIF surgery in subjects with different curve types.

Spinal instrumentation aims to correct and stabilize the spine in severe cases of scoliosis until fusion occurs. Although the impact of the spinal fusion on the geometrical parameters of the spine and pelvis has been studied previously (Masso and Gorton, 2000) the effect of the spinal surgery on the vertebral loading, as was pointed out in Moore (2000), particularly in the distal unfused part is not well documented. Among different anatomical sections affected by scoliosis, the biomechanical loading of the sacrum is of special interest; since sacrum is the connective structure between the spine and pelvis, its mechanical loading plays an important role in conducting the force between the trunk and lower extremities and hence contributes to the standing postural equilibrium (Jiang, 2006).

5.1 Materials and methods

5.1.1 Cohort description

A total number of 9 AIS female subjects, age range [14, 17], average 15 years (SD: 2.4) who had undergone a posterior spinal instrumentation and fusion surgery (PSIF) with no postoperative instrumentation failure during an average follow-up of 16 months [12-18 months, SD: 3.1] were randomly selected from the database of our institution. Spinal and pelvic parameters of the studied samples are presented in table 5.1. The medical chart and pre- and post-operative postero-anterior and lateral radiographs of the patients were used. 5 patients had right thoracic deformity (MT) Cobb angle range [43°, 77°], 4 with a right thoracic (RT) [55°, 68°] and left lumbar (LL) [74°, 97°] deformities. The radiographic images of 12 asymptomatic female adolescent subjects with no history of spinal disease were added as the control group. The spinal

curvature was described by the thoracic and lumbar Cobb angles measured by the analytical method using the lines perpendicular to the projection of the spinal curve in the frontal and sagittal planes at its inflection points. In the sagittal plane kyphosis included T4 to T12 vertebrae and lordosis measured between L1 to S1. Sacro-pelvic parameters were characterized by pelvic incidence (PI), pelvic tilt (PT), and sacral slope (SS).

Table 5.1: Spinal and pelvic parameters of the studied samples

		Thoracic Cobb (°)	Lumbar Cobb (°)	Kyphosis (°)	Lordosis (°)	PI (°)	PT (°)	SS (°)
Pre-operative	MT	53±33	28±22	33±25	44±17	39±19	4±2	34±17
	RT/LL	40±25	55±27	32±12	43±13	52±13	11±8	31±5
Post-operative	MT	26±7	15±13	29±15	53±6	41±6	12±3	38±4
	RT/LL	23±18	24±20	26±13	50±13	55±7	18±9	36±9
Controls		-	-	47±10	50±7	44±7	9±7	35±4

5.1.2 Computation of the geometrical and biomechanical parameters of the spine and pelvis

An osseo-ligamentous FE model of the spine and pelvis (section 4.2.3) was personalized for all the 22 subjects. The position of the COP_{SI}, the high and low stress areas on the sacrum, and the position of the COM were determined by the method explained in the section 4.2.3.

Each patient was described by 7 geometrical parameters (thoracic and lumbar Cobb angles, kyphosis, lordosis, PI, PT, and SS) and two biomechanical parameters (the position of the COM and COP_{SI}). The positions of the COM and COP_{SI} were computed separately in the sagittal and frontal planes with respect to the central hip vertical axis (CHVA) and their relationships with the spinal and pelvic parameters were studied.

Radiographic images and sacral loading were shown for one typical subject from each group to show the global characteristics related to the MT and RT/LL subjects.

5.1.3 Statistical analysis

Non-parametric statistical analysis (Mann-Whitney U test, PASW statistics 18.0, SPSS Inc., Chicago, IL) was used to determine the differences between the spinal and pelvic

biomechanical and geometrical parameters between AIS and controls pre- and post-operatively. The Pearson correlation test (two tailed, PASW statistics 18.0, SPSS Inc., Chicago, IL) was used to determine the relationship between the biomechanical and geometrical spine and pelvic parameters in the studied group before and after operation.

5.2 Results

5.2.1 Case presentation

Figure 5.1 presented the bi-planar radiographs and the position of the high and low stress areas on the sacrum endplate in two scoliotic subjects. The sacral loading was asymmetric before operation while it is more equilibrated after operation in both subjects. Spinal and pelvic parameters of the two patients were presented in table 5.2.

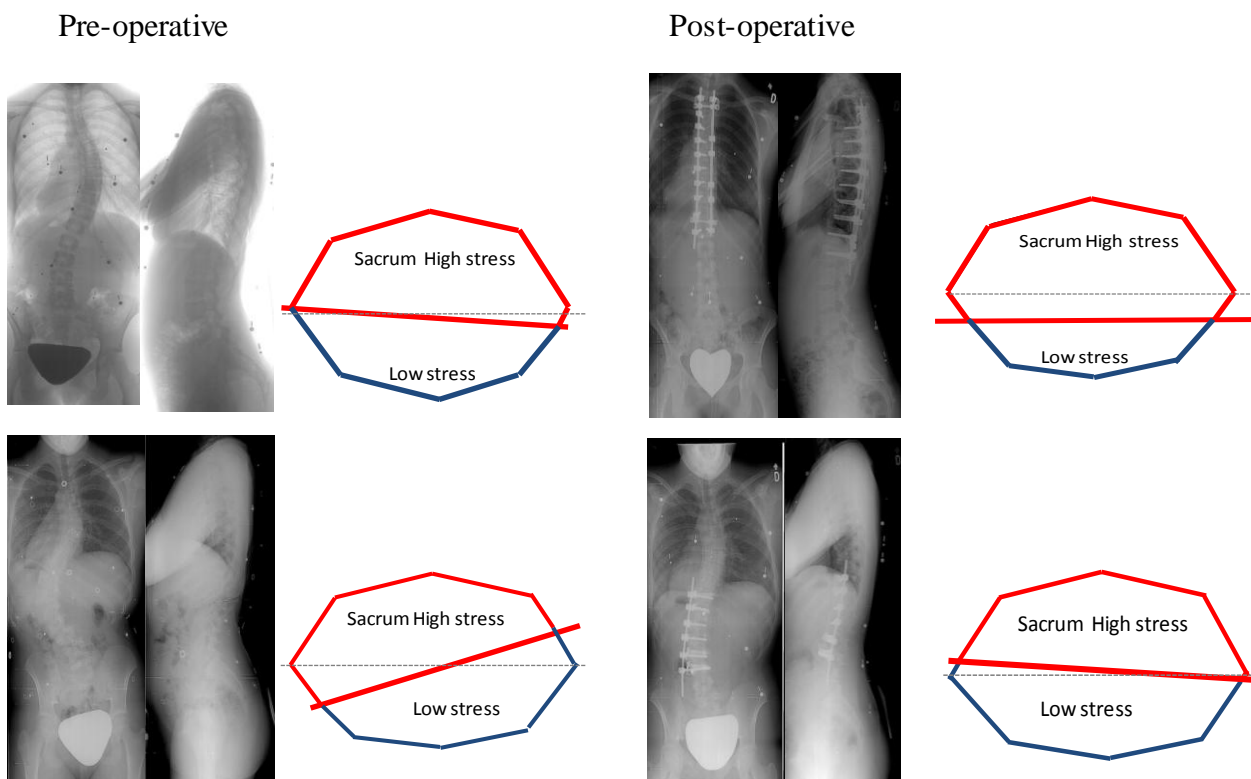


Figure 5.1: Biplanar radiographs and the location of the high and low stress areas on the sacrum endplate before and after surgery in a typical a) MT (Patient1) and b) RT/LL (Patient2) subject. The dash line separates the anterior and posterior parts of the sacrum.

Table 5.2: Pre- and post-operative spinal and pelvic parameters in a patient with a) thoracic deformity (patient1) and b) RT/LL curve (patient2).

		Thoracic Cobb(°)	Lumbar Cobb(°)	Kyphosis (°)	Lordosis (°)	PI (°)	PT (°)	SS (°)
a)Patient1 (MT)	Pre-operative	43	25	44	57	50	5	44
	Follow-up 16 months	24	8.5	32	55	40	11	27
b)Patient2 (RT/LL)	Pre-operative	55	81	50	64	50	10	41
	Follow-up 12 months	41	48	38	39	50	23	26

5.2.2 Comparison between the spinal and pelvic geometrical parameters pre- and post- operatively

Thoracic Cobb was decreased by 51% in MT subjects and 48% in RT/LL group. Lumbar Cobb angles were decreased by 52% in MT subject and 58% in RT/LL group after operation. Kyphosis was decreased by 8% and 14% in MT group and subjects with RT/LL curves respectively. Lordosis was increased by 20% in MT subjects and 12% in RT/LL group. Mann Whitney U test (PASW statistics 18.0, SPSS Inc., Chicago, IL) showed significant decrease in the frontal plane spinal curvature, while the spinal parameters in the sagittal plane did not change significantly ($p>0.05$).

PT was increased by 15% after operation while SS was decreased by 5%. However the Mann Whitney U test (PASW statistics 18.0, SPSS Inc., Chicago, IL) did not show any significant difference in the magnitude of the PI and the SS before and after operation ($p>0.05$).

5.2.3 Comparison between the spinal and pelvic biomechanical parameters pre- and post- operatively

The average positions of the COP_{SI} and COM were presented in table 5.3 for the studied groups. The medio-lateral parameters were presented in the frontal plane and the antero-posterior parameters are presented in the sagittal plane.

Table 5.3 : The average position of the pre- and post-operative biomechanical parameters (COM, COP_{S1}) in the studied groups.

		COP _{S1} (mm)		COM (mm)	
		With respect to the CHVA		With respect to the CHVA	
		Medio-lateral	Postero-anterior	Medio-lateral	Postero-anterior
Pre-operative	MT	-8±2	-6±1	-15±11	1±5
	RT/LL	8±4	-13±5	25±18	-5±8
Post-operative	MT	5±1	-13±2	6±9	-10±6
	RT/LL	4±1	-21±5	12±15	-16±10
Controls		3±4	-18±7	8±5	-23±12

The position of the COP_{S1} was significantly different pre- and post-operatively and between the cohort of the pre-operative subjects and control subjects ($p<0.05$) while no such difference was observed between the post-operative subjects and controls. The stress distribution on the sacrum was more symmetric after operation when comparing the right and the left parts of the upper sacral endplate.

The simulated distance between the COM and the COP_{S1} in average was decreased in both medio-lateral (88% MT, 65% RT/LL) and antero-posterior (55% MT, 57% RT/LL) directions after operation. Mann Whitney U test (PASW statistics 18.0, SPSS Inc., Chicago, IL) showed that the distance between the COM and COP_{S1} decreased significantly after operation ($p<0.05$).

A significant relationship was observed between the SS and the biomechanical parameters *i.e.* the position of the COP_{S1} and the COM; as the SS increased, the distance between the COM and COP_{S1} decreased significantly in the post-operative subjects ($r=0.6$, $p<0.05$, Pearson two tailed correlation test , PASW statistics 18.0, SPSS Inc., Chicago, IL).

CHAPTER 6 GENERAL DISCUSSION

The close relationship between the spinal deformities and various pelvic parameters in scoliotic subgroups was shown in this study. Static and biomechanical postural analyses were applied to study the spino-pelvic interaction in scoliosis. In the current literature, the geometrical spinal indices and the sacro-pelvic parameters mostly in the sagittal plane are descriptive of the spino-pelvic relative alignment; thus the biomechanics of the spino-pelvic interaction is not considered. The current study addressed shortcomings of the previous research in postural assessment of the scoliosis by including both biomechanical and geometrical parameters of the spine and pelvis. This study mainly contributed to the definition and analysis of the parameters which relate the pelvis to the spinal deformities in scoliotic subjects with different curve types and severity.

Differences in the spino-pelvic kinematic interaction were shown in scoliotic subgroups (section 3.2- article 1). This study aimed to determine to what extent the spinal deformities and spino-pelvic orientation impact the pelvic range of motion in different anatomical planes. It was observed that the initial alignment of the pelvis in the standing posture was a determinant factor in the spatial movement of the pelvis. Pelvic obliquity and pelvic rotation in the static standing position increased during the course of movement. The results subsequently showed the impact of the spinal deformities *i.e.* thoracic and lumbar curves on the pelvis motion. This study was the first to show that the pelvic range of motion in the anatomical planes and spino-pelvic interaction were specific to each scoliotic subgroup. The result showed the mechanism through which the spinal deformities modify the pelvic movement and its contribution to the total trunk ROM. While the pelvic obliquity or pelvic rotation is more prominent in subjects with severe scoliotic curves and is considered in the treatment of scoliosis (Dubousset, 1998), the current study showed that even small pelvic obliquity or rotation in subjects with moderate spinal curves impacted the pelvic range of motion and its interaction with the spine when executing different functional movements. This suggested the importance of considering the pelvic orientation, even if not significant, in the early stages of the postural evaluation of the AIS.

The skin markers during the kinematic experience were subject to move; however the study by Chokalingam (2002) confirmed the feasibility of the applying the motion capture data systems in the trunk movement analysis in controls and subjects with spinal deformities. For each

movement three trials were recorded and the average of the marker motion was calculated to reduce the effect of the marker placement and measurement errors on the results. More over although the pelvic orientations during the course of the movement were registered, this study focused on the spine and pelvis parameters at the maximum range of movement. Subsequently only the ROMs exceeding 10 degrees were considered in the analysis. Consideration of the pelvic markers errors due to the skin movement artifact does not adversely affect the results and general conclusions of the study. Statistically significant differences between the scoliotic subgroups in terms of the pelvic ROM in the three anatomical planes showed the relationship between the spinal deformities and pelvic motion in AIS subgroups. Another limitation of this study was the selected sample; the studied subjects mostly had moderate spinal deformities. The spino-pelvic kinematic interaction in subjects with moderate ($<40^\circ$) and severe curves ($>40^\circ$), such as pre-surgery subjects, can be compared to better identify the impact of the curve severity on the pelvic motion in isolated scoliotic subgroups. However the results of the current study showed the significant impact of the thoracic and lumbar deformities on the spine and pelvic ROM and suggested the importance of the pelvic orientation in postural assessment of the patient.

The proposed measurements in the standing postural analysis of the 3D spino-pelvic alignment (section3.3) provided a comprehensive method to characterize pelvic 3D orientation with respect to the spinal deformities. This approach distinguished itself from the previous studies where the pelvic asymmetry and orientation were measured in 2D in the local coordinate system of the pelvis in scoliosis and controls (Lucas, 2004; Gum, 2007; Stylianides, 2012). These researches mainly focused on comparing the iliac crest wing width, pubic bone, acetabulum, etc., on the right and left sides of the pelvis while the pelvic 3D orientation in the global coordinate system and with respect to the spine was not considered. The selection of the ASIS and PSIS as the most protruded pelvic anatomical landmarks, accessible by skin palpation, as was also suggested by Boulay (2006a), permitted to use same anatomical landmarks in the spino-pelvic kinematic and static analysis (chapter3- article1). Pelvic orientation correlated to both thoracic and lumbar deformities (Section 3.3). This finding allowed determining the spine and pelvis compensatory mechanisms which appear to have an important role in the postural balance of the scoliotic patient (Berthonnaud, 2009). Although clinicians have mostly focused on the sagittal spino-pelvic alignment in postural assessment of the patients the results of the current study additionally showed such a relationship exists between the spine and pelvis in the frontal and

transverse plane in scoliotic subgroups. While the sagittal spino-pelvic alignment is conventionally used to evaluate the postural equilibrium before and after a surgical instrumentation, the compensative spino-pelvic alignment in frontal and transverse planes suggested that the postural evolution in 3D merits attention and provides more information in AIS clinical assessment.

One important source of error in the 3D spino-pelvic alignment analysis (Section3.3) originated from the reconstruction technique. Although a maximum error of 5mm was reported in the position of the pelvic landmarks (Delorme, 2003) adding a normally distributed error to the 3D coordinates of the ASIS and PSIS in order to take into account the measurement errors embedded in the 3D reconstruction technique did not change the main conclusion of the study. The results of the validation analysis showed that the reconstruction technique may cause an error in determination of the pelvic orientation and could shift the position of the pelvic orientation from one quadrant to another (figure 3.7) in subjects with small pelvic frontal tilt or rotation ($<1.05^\circ$). This suggested the necessity of a more precise reconstruction technique and several measurements of the anatomical landmarks with different observers in cases with small pelvic tilt or rotation. However the main conclusion of the study which suggested the relationship between the curve types and pelvic orientation in a majority of the subjects remained valid. One may dispute the clinical significant of a 1.05° pelvic tilt, it was concluded that the proposed method as such is valid to determine the pelvic alignment with respect to the spine in cases with sever pelvic tilt or rotation. Despite these inevitable errors, the differences between the pelvic orientation in the frontal and transverse planes in subjects with different curve types was statistically significant.

Although sacro-pelvic parameters were used to define the spino-pelvic alignment in the sagittal plane, not much was known about the transferred loads between the spine and pelvis in subjects with different curve types. The impact of the spinal deformities and pelvic orientation on the biomechanical loading of the sacrum was studied in a detailed FE model of the spine and pelvis. The proposed method in this study (section 4.2- second article) permitted to investigate the role of the spinal deformities and pelvic orientation on the sacral loading in scoliotic subgroups. The results showed that the relative orientation of the spine and pelvis impacted the biomechanical loading of the sacrum. These results permitted, for the first time, to characterize the loads on the sacrum based on the spino-pelvic alignment incorporated in a FE model of the

scoliotic spine and pelvis. The proposed biomechanical parameter (COP_{S1}) in part represented the impact of the spinal geometrical deformity and the pelvic orientation on the sacral loading. The combination of the sacro-pelvic parameters and the position of the COP_{S1} can provide a comprehensive picture in scoliotic spino-pelvic postural analysis. However the position of the COP_{S1} cannot relate the spino-pelvic alignment to the position of the femoral heads directly. The relationship between the biomechanical loading of the sacrum and the position of the femoral heads did not study here and is to be undertaken in the future.

The FE model presented a few limitations. For instance, the muscle forces were not considered in the simulation. Also, the position of the COM was approximated from literature data. Such limitations impact the interpretation of the results in the patient- specific FE models. Due to the complexity of the personalized simulation of the muscle forces in scoliosis, this study focused on the effect of the gravitational force and the spino-pelvic alignment on the sacral loading without explicitly modeling the local muscle forces. However the study of geometrical spinal deformities on the sacral loading was not importantly affected by the presented limitations because the analyses were done in a relative fashion, comparing the general trend of the stress distribution on the sacrum in AIS subgroups. The reaction forces at the boundary condition levels, although not excessively important (< 35N), varied from patient to patient to assure the equilibrium of the spine under the gravitational force. In another study by Sevrain (2012), wherein the follower load was used as a representative of the muscle forces in a FE model of the spine and pelvis, the relationship between the sacral loading and PI was shown in spondylolisthesis. A more detailed model of the spine and pelvis which includes the major spinal muscles would permit to further study and compare the magnitude of the sacral loading between subjects in diverse musculoskeletal pathologies which is also valuable in the patient's treatment. For farther application of the FE model additional validation is required. While *in vivo* experimental validation of the FE model is difficult due to the invasive nature of the experiment, a physical model of the spine and pelvis with appropriate material properties which permits to directly measure the pressure distribution on the superior endplate of the sacrum can be used to assess sacral loading in different spino-pelvic configurations. Such model should include the muscular forces and a realistic model of the trunk mass distribution. As the further direction of this study such experimental model can be developed to validate the results of the FEM. Furthermore an analytical model which includes the ground reaction force in addition to the

trunk's weight can be developed to estimate the transferred load between the spine and pelvis. This model can be implied in validation of the FEM and subsequently provide additional information about the magnitude of the sacral loading in AIS subgroups pre- and post-operatively.

The proposed algorithm in this project (section 5.3) permitted to estimate the personalized position of the COM at the level of each vertebra in both sagittal and frontal planes in AIS subjects. The proposed method was cost and time efficient and permitted to consider the position of the COM as a biomechanical parameter to evaluate the spinal deformity in patient-specific FE models of the spine. Although it was known that the geometrical deformity of the spine and pelvis and the weight distribution of the trunk affect the spino-pelvic biomechanical interaction in AIS (Pearsall, 1996, Park, 2012), to date, no protocol had formulated the 3D personalized position of the center of mass with respect to the vertebral column in AIS.

To our knowledge no similar protocol was developed to determine the COM position in AIS subjects *in vivo* in a way that is applicable in numerical simulation of the spine. Zabjek (2008) used kinematic analysis and skin markers wherein the position of the COM in both frontal and sagittal planes with respect to the first sacral prominence was calculated in a group of scoliotic subjects. An average difference between the position of the COM and S1 prominence was measured at 65.4mm and -1.5 mm in the sagittal and frontal planes, respectively, in 22 female AIS (Zabjek, 2008). However differences in the applied methods, subjects' curve types, and anthropometrics parameters made the comparison between the results of the two studies limited.

The results were in line with the study by Pearsall (1996), where the position of the COM in the sagittal plane was anterior to the vertebrae center. Similar to our results, Pearsall (1996) suggested that the distance between the COM at the level of each vertebra and the center of the vertebrae is smaller at proximal thoracic and lower lumbar regions and is increased in the main thoracic and upper lumbar sections (figure 4.9). The distance between the vertebral slices COM and the center of vertebrae in the sagittal plane was smaller in our study when compared to the results in Pearsall (1996), which can be related to the differences in the studied samples (asymptomatic adult versus AIS), the body positioning (standing position in our study versus supine position in Pearsall (1996), and the experimental methods. Pearsall (1996) studied the

COM position using the gamma x-ray technique, while in the current study the COM was determined from the COP oscillation and an optimization process. The COP oscillation is the result of the central nervous system (CNS) effort to keep the COM within the base of support. In the ideal posture the COM should be close to the femoral heads (Pauwels, 1980). As it was explained by Pauwels (1980) in an economic posture the COM position was placed vertically above the center of the femoral heads, the upper body weight was equally distributed between the two femoral heads, and the muscle forces which provided the upright posture were minimized in sagittal and frontal planes. The CNS effort in providing such posture affected the COP oscillation and shifts it closer to the CHVA in the sagittal plane. This effect caused a posterior shift (closer to the vertebral center) in the position of the trunk slices' COM in the sagittal plane when the COP oscillation was applied in estimating the COM position. Such posterior shift in turn moved the net position of the COM closer to the CHVA and decreased the distance between the COM and the CHVA in the sagittal plane. As for the position of the COM in the frontal plane, the scoliotic deformities in the frontal plane prohibit us from comparing between the segmental COM position between AIS and non scoliotic subjects in the frontal plane.

Although two different cohorts of subjects were used in the first and second parts of the study (section 4.2 and 4.3) the severity and shape of the spinal deformities were similar in both groups. In the first experiment main thoracic and main thoracic with compensatory left lumbar subjects who had moderate curves were studied to relate the COM and COP positions in AIS. The COP-COM relationship was not significantly different between the two studied groups in the first part of the experiment. This observation allowed us to use the results of the first experiment in a new group of scoliotic subjects with similar moderate curves (main thoracic and thoracolumbar curves) in the second part of the experiment. Due to the limited number of subjects in the two studied scoliotic subgroups the formulation of the COM position with respect to the center of vertebrae was not possible. It is speculated that such formula should be specific to the scoliotic type and dependent to various parameters such as curve apex level and deformity severity in three dimensions. For better validation of the applied method a new experimental technique which uses the same group of subjects and same COP acquisition device in the first and second phases of the experiment with a higher number of subjects from each AIS subgroup can be inquired.

In addition to the 1cm shift in the position of the COM in the FE model, the optimized position of the COM at each vertebral level was used to better verify the sensitivity of the FE model to the position of the COM. The magnitude of the stress distribution decreased when the optimized COM position replaced the COM position from literature; however the general trend of the stress distribution remained unchanged (figure 4.10). Since the main goal of the FEM analysis (section 4.2- article2 and chapter 5) was to compare the general trend of the stress distribution on the sacrum and not the absolute compressive stress magnitude in subjects with different curve types it was concluded that the position of the COM of each trunk slice from literature (Liu, 1971; Pearsall, 1994; Pearsall, 1996) was a fair approximation of the position of the trunk COM in characterizing the biomechanical loading of the sacrum in AIS subgroups.

The comparison between the biomechanical loading of the sacrum before and after operation in the patient-specific FE models of the scoliotic spine permitted to assess the impact of the spinal surgery on the transferred loads between the spine and pelvis via the sacrum. It was shown that the post-operative spino-pelvic alignment helped to normalize the sacral loading. However pelvic 3D orientation and sacro-pelvic parameters did not vary in the same way for all the subjects post-operatively. This result was in line with the study by Skalli (2006), wherein pelvic retroversion or intversion was not the same for all the subjects after operation. It was also shown that the impact of the spinal operation is more prominent in the biomechanical parameters of the pelvis than the SS and PI angles. This result suggested that the position of the COP_{S1} can be used as a measure to evaluate the transferred load between the spine and pelvis after operation and hence alternatively assess the patient postural equilibrium. However this study was only conveyed for limited number of the subjects. A study that evaluates a higher number of subjects with different curve types and different fusion levels permits to better investigate the parameters involved in equilibrating the sacral loading post-operatively.

The biomechanical model of the spine and pelvis in the current study was able to illustrate how the sacral loading and the COM position relate to each other for maintaining a stable sagittal balance. In the post-operative subjects an anterior shift in the position of the COP_{S1} on the S1 endplate along with decreased distance between the COM and femoral heads in the sagittal plane was observed when compared to the pre-operative subjects. This finding shows the biomechanical significance of the COP_{S1} position and suggests that considering the

biomechanical parameters of the sacrum are beneficial in post-operative postural analysis of the patients.

CHAPTER 7 CONCLUSIONS AND RECOMMENDATIONS

The relationship between the spine and pelvic parameters was shown in scoliotic subgroups. The results of several experiments and research protocols investigated the close relationship between the spinal and pelvic deformities and its impact on the biomechanical loading of the sacrum. Identification of the different postural and biomechanical parameters permitted to study the 3D spino-pelvic alignment in scoliotic subgroups pre-and post-operatively. A total number of 60 subjects were recruited and over 250 medical charts of the patients from the Saint Justine university hospital database were used to examine different aspects of the spino-pelvic interaction in female adolescent idiopathic scoliosis.

This Ph.D. project placed more emphasis on the pelvis in the scoliotic postural analysis to highlight the link between the spine and pelvis. Several pelvic parameters were introduced which subsequently allowed to characterize the relationship between the spine and pelvis in the AIS with different curve types.

The principal objective of this project was fulfilled through analyzing spino-pelvic parameters in AIS subgroups using different biomechanical tools and simulation methods. This study not only analyzed the spino-pelvic 3D interaction in static, but also investigated the extended effect of the spino-pelvic alignment on the pelvic range of motion in the anatomical planes. The pelvic range of motion, spino-pelvic kinematic interaction, and their relative alignment were significantly different in scoliotic subgroups (hypotheses 1 and 2), which shows the significant relationship between the skeletal spinal deformities and the pelvic parameters in AIS subgroups.

For the first time, the biomechanical interaction between the spine and pelvis was studied in subjects with different curve types by assessing the sacral loading in AIS subgroups. Different sacral loading was shown in scoliotic subgroups (hypothesis 3). Biomechanical indices of the spine and pelvis varied significantly in AIS subgroups and controls and showed the specific relationship between the location and severity of the spinal deformities and the sacral loading in the studied groups. It was shown that the biomechanical analysis of the spino-pelvic interaction provides additional information about the postural alignment in AIS which are not accessible through the radiographic images. Finally as a clinical application of the developed methods, the biomechanical loading of the sacrum was studied pre- and post- operatively. The biomechanical

analysis of the sacrum showed the exclusive effect of the spinal instrumentation and pelvic realignment after spinal surgery on the transferred loads between the spine and pelvis (hypothesis 4). The positive effect of the scoliotic correction on equilibrating of the sacral loading was highlighted in patients post-operatively.

The association between the geometrical and biomechanical parameters was brought to attention which emphasized on the importance of the biomechanical indices in the postural analysis of the AIS subgroups. Due to the nature of the biomechanical parameters it is beneficial to apply these parameters to define the postural equilibrium in various spino-pelvic configurations. As the future direction of the project, the proposed postural and biomechanical parameters can be used to formulate the postural equilibrium in scoliotic subgroups. Combination of the biomechanical parameters such as the position of the COP_{S1} with respect to the CHVA and the relative COP_{S1} -COM position in the sagittal plane with the spino-pelvic geometrical indices in AIS subgroups can be used to better characterize the postural equilibrium and compensative mechanisms in scoliotic subjects from a biomechanical standpoint.

The proposed methods and different experimental techniques provided a collective knowledge about the spino-pelvic interaction in AIS subgroups. Different domains of biomechanical analysis from *in vivo* analysis to numerical simulation and mathematical modeling were used to study the postural parameters in AIS subgroups.

This Ph.D. project provided a deeper understanding of the postural analysis in scoliotic subgroups and rationalized the compensatory mechanisms in the spino-pelvic alignment by introducing biomechanical parameters in AIS. Application of the biomechanical indices as a complementary tool to the geometrical analysis of the postural parameters in this project provided a better sense of the postural analysis in scoliotic subgroups.

REFERENCES

Adams, M.A., Freeman, B.J.C., Morrison, H.P., Nelson, I. W. & Dolan, P. (2000). Mechanical initiation of intervertebral disc degeneration. *Spine*, 25(13), 1625-1636.

Al-Eisa, E., Egan, D., Deluzio, K., & Wassersug, R. (2006). Effects of pelvic skeletal asymmetry on trunk movement: Three-dimensional analysis in healthy individuals versus patients with mechanical low back pain. *Spine*, 31(3), E71-E79.

Allard, P., Chavet, P., Barbier, F., Gatto, L., Labelle, H., & Sadeghi, H. (2004). Effect of body morphology on standing balance in adolescent idiopathic scoliosis. *Am J Phys Med Rehabil*, 83(9), 689-697.

AMTI: Advanced Mechanical Technology Inc., Newton, MA, 1983

Aubin, C. -É., Dansereau, J., de Guise, J. A., & Labelle, H. (1996). A study of biomechanical coupling between spine and rib cage in the treatment by orthosis of scoliosis. *Ann Chir*, 50, 641-650.

Beaulieu, M., Toulotte, C., Gatto, L., Rivard, C.-H., Teasdale, N., Simoneau, M., et al. (2009). Postural imbalance in non-treated adolescent idiopathic scoliosis at different periods of progression. *Eur Spine J*, 18(1), 38-44.

Bergmark, A. (1989). Stability of the lumbar spine. A study in mechanical engineering. *Acta ortho scan suppl*, 230, 1-54.

Berthonnaud, E., Dimnet, J., & Hilmi, R. (2009). Classification of pelvis and spinal postural patterns in upright position. Specific cases of scoliotic patients. *Comput Med Imaging Graph*, 33(8), 634-643.

Berthonnaud, E., Dimnet, J., Roussouly, P., & Labelle, H. (2005). Analysis of the sagittal balance of the spine and pelvis using shape and orientation parameters. *J spinal disor tech*, 18(1), 40-47.

Boulay, C., Tardieu, C., Hecquet, J., Benaim, C., Mouilleseaux, B., Marty, C., et al. (2006). Sagittal alignment of spine and pelvis regulated by pelvic incidence: standard values and prediction of lordosis. *Eur Spine J*, 15(4), 415-422.

Boulay, C., Tardieu, C., Benaim, C., Hecquet, J., Marty, C., Prat-Pradal, D., et al. (2006). Three-dimensional study of pelvic asymmetry on anatomical specimens and its clinical perspectives. *J Anat*, 208, 21-33.

Breniere, Y. (1996). Why we walk the way we do? *J Motor Behav*, 28, 291-298.

Bridwell, K. H. (1999). Surgical treatment of AIS. *Spine*, 24, 2607-2616.

Burwell, R. G., Cole, A. A., Cook, T. A., Grivas, T. B., Kiel, A. W., Moulton, A., et al. (1992). Pathogenesis of idiopathic scoliosis: the Nottingham concept. *ACTA Orthopaedica Belgica (Bruxelles)*, 58(Supplement I), 33-58.

Chen, P. Q., Wang, J. L., Tsuang, Y. H., Liao, T. L., Huang, P. I., & Hang, Y. S. (1998). The postural stability control and gait pattern of idiopathic scoliosis adolescents. *Clin Biomech*, 13(Suppl 1), S52-S58.

Cheriet, F., Remaki, L., Bellefleur, C., Koller, A., Labelle, H., & Dansereau, J. (2002). A new X-ray calibration/reconstruction system for 3D clinical assessment of spinal deformities. *Stud Health Technol Inform*, 91, 257-261.

Chockalingam, N., Dangerfield, P.H., Giakas, G., & Cochrane, T. (2002). Study of marker placements in the back for opto-electronic motion analysis. *Stud Health Technol Inform*, 88:105-109.

Cholewicki, J., Panjabi, M., & Khachatrian, A. (1997). Stabilizing function of trunk flexor-extensor muscles around a neutral spine posture. *Spine*, 22 (19), 2207-2212.

Clin, J., Aubin, C.-É., & Labelle, H. (2007). Virtual prototyping of a brace design for the correction of scoliotic deformities. *Med Biol Eng Comput*, 45(5), 467-473.

Clin, J., Aubin, C. -É., Parent, S., & Labelle, H. (2010). A biomechanical study of the Charleston brace for the treatment of scoliosis. *Spine*, 35(19), E940-E947.

Clin, J., Aubin, C. -É., Lalonde, N., Parent, S., & Labelle, H. (2011). A new method to include the gravitational forces in a finite element model of the scoliotic spine. *Med Biol Eng Comput*, 49(8), 967-977.

Dalleau, G., Damavandi, M., Leroyer, P., Verkindt, C., Rivard, C. -H., & Allard, P. (2011). Horizontal body and trunk center of mass offset and standing balance in scoliotic girls. *Eur Spine J*, 20(1), 123-128.

Damavandi, M., Farahpour, N., & Allard, P. (2009). Determination of body segment masses and centers of mass using a force plate method in individuals of different morphology. *Med Eng Phys*, 31(9), 1187-1194.

Delorme, S., Labelle, H., Aubin, C. -É., de Guise, J. A., Rivard, C. -H., Poitras, B., et al. (1999). Intraoperative comparison of two instrumentation techniques for the correction of adolescent idiopathic scoliosis. Rod rotation and translation. *Spine*, 24(19), 2011-2017.

Delorme, S., Petit , Y., de Guise, J. A., Aubin, C. -É., & Dansereau, J. (2003). Assessment of the 3D reconstruction and high-resolution geometric modeling of the human skeletal trunk from 2D radiographic images. *IEEE Trans Biomedical Eng* 50(8), 989-998.

Driscoll, C.R., Aubin, C. -É., Labelle, H., & Dansereau, J. (2010). Optimized use of multi-functional positioning frame features for scoliosis surgeries. *Stud Health Technol Inform*, 158, 83-88.

Driscoll, C. R., Aubin, C. -É., Canet, F., Labelle, H., & Dansereau, J. (2011). Impact of prone surgical positioning on the scoliotic spine. *J Spinal Disord Tech*, 25(3):173-81.

Driscoll, M., Aubin, C. -É., Moreau, A., & Parent, S. (2010). Finite element comparison of different growth sparing instrumentation systems for the early treatment of idiopathic scoliosis. *Stud Health Technol Inform*, 158, 89-94.

Dubousset, J. (1994). *Three dimentional analysis of the scoliotic deformity*. New York: Raven Press.

Dubousset, J. (1996). *Pelvic obliquity correction*. NY: Lippincott-Raven.

Dubousset, J. (1998). *Application à la chirurgie de la colonne vertébrale chez l'enfant et l'adolescent Pied, équilibre et rachis*. Paris: Frison -Roche.

Duke, K., Aubin, C.-É., Dansereau, J., & Labelle, H. (2005). Biomechanical simulations of scoliotic spine correction due to prone position and anaesthesia prior to surgical instrumentation. *Clin Biomech*, 20(9), 923-931.

Durkina, J. L., Dowlingb, J. J., & Andrews, D. M. (2002). The measurement of body segment inertial parameters using dual energy X-ray absorptiometry. *J biomech*, 35(12), 1575-1580.

Duval-Beaupère, G., Hecquet, J., Dubousset, J., Graf, H., Roche, R., Tabuteau, C., et al. (1987). Center of the mass supported by each vertebrae on a 3D image of the spine, *EEEE ninth Annual Conference of the engineering in medicine and biology society*.

Duval-Beaupère, G. & Legaye, J. (2004). Composante sagittale de la statique rachidienne. *Rev Rhum*, 71, 105-119.

Duval-Beaupère, G., Schmidt, C., & Cosson, P. (1992). A barycentric study of the sagittal shape of spine and pelvis. The condition required for an economic standing position. *Ann Biomed Eng*, 20, 451-462.

El-Rich, M., & Shirazi-Adl, A. (2005). Effect of load position on muscle forces, internal loads and stability of the human spine in upright postures. *Comput Methods Biomed Eng, 8*(6), 359-368.

El Fegoun, A. B., Schwab, F., Gamez, L., Champain, N., Skalli, W., & Farcy, J.-P. (2005). Center of gravity and radiographic posture analysis: A preliminary review of adult volunteers and adult patients affected by scoliosis. *Spine, 10*(13), 1535-1540.

Ellis, H. (2006). *The abdomen and pelvis* (11 ed.). Massachusetts: Blackwell publishing.

Feipel, V., Aubin, C. -É., Ciolofan, O. C., Beauséjour, M., Labelle, H., & Mathieu, P. A. (2002). Electromyogram and kinematic analysis of lateral bending in idiopathic scoliosis patients. *Med Biol Eng Comput, 40*(5), 497-505.

Fernand, R. & Fox, D. E. (1985). Evaluation of lumbar lordosis: A prospective and retrospective study. *Spine, 10*(9), 799-803.

Gardner-Morse, M., Stokes, I. A., & Laible, J. P. (1995). Role of muscles in lumbar spine stability in maximum extension efforts. *J Orthop Res (New York, NY), 13*(5), 802-808.

Gharbi, H. (2008). Étude biomécanique de la spondylolyse et du spondylolisthésis chez l'enfant: étude de cas. Master's thesis. École polytechnique de Montréal. Institut de génie biomédical.

Granata, K. P., & Sanford, A. H. (2000). Lumbar -pelvic coordination is influenced by lifting task parameters. *Spine, 25*(11), 1413-1418.

Granata, W. (2001). Trunk posture and spinal stability. *Clin Biomech, 16*(8), 650-659

Gray, H. (1918). *Osteology. 6c2: The pelvis* (20 ed.). New York: Bartleby.com.

Grivas, T. B., Burwell, G. R., Vasiliadis, E. S., & Webb, J. K. (2006). A segmental radiological study of the spine and ribcage in children with progressive infantile idiopathic scoliosis. *scoliosis*, 1-17.

Guigui, P., Levassor, N., Richards, B. S., Wodecki, P., & Cardinne, L. (2003). Valeur physiologique des paramètres pelviens et rachidiens de l'équilibre sagittal du rachis. *Rev chir orthop*, 89, 496-506.

Gum, J. L., Asher, M. A., Burton, D. C., Lai, S.-M., & Lambart, L. (2007). Transverse plane pelvic rotation in adolescent idiopathic scoliosis: Primary or compensatory? *Eur Spine J*, 16, 1579-1586.

Harrington, P. R. (1962). Treatment of scoliosis: correction and internal fixation by spine instrumentation. *J Bone Joint Surg Am*, 84A(2), 316.

Harrison, D. E., Cailliet, R., Harrison, D. D., Janik, T. J., Troyanovich, S. J., & Coleman, R. R. (1999). Lumbar coupling during lateral translations of the thoracic cage relative to a fixed pelvis. *Clinic Biomech (Bristol, Avon)*, 14(10), 704-709.

Huang, H. K., & Suarez, F. R. (1983). Evaluation of cross-sectional geometry and mass density distributions of humans and laboratory animals using computerized tomography. *J Biomech*, 16(10), 821-832.

Hullin, M. G., McMaster, M.J., Draper, E.R., & Duff, E.S. (1991). The effect of Luque segmental sublaminar instrumentation on the rib hump in idiopathic scoliosis. *Spine*, 16(4), 402-428.

Jackson, R., Kanemura, T., Kawakami, N., & Hales, C. (2000). Lumbopelvic lordosis and pelvic balance on repeated standing lateral radiographs of adult volunteers and untreated patients with constant low back pain. *Spine*, 25(5), 575-586.

Jackson, R. P., Peterson, M. D., McManus, A. C., & Hales, C. (1998). Compensatory spino-pelvic balance over the hip axis and better reliability in measuring lordosis to the pelvic radius on standing lateral radiographs of adult volunteers and patients. *Spine*, 23(16), 1750-1767.

Jiang, Y., Nagasaki, S., You, M., & Zhou, J. (2006). Dynamic studies on human body sway by using a simple model with special concerns on the pelvis and muscle roles. *Asian J Control*, 8(3), 297-306.

Kadoury, S., Cheriet, F., Dansereau, J., & Labelle, H. (2007-a). Three-dimensional reconstruction of the scoliotic spine and pelvis from uncalibrated biplanar x-ray images. *J Spinal Disord Tech*, 20, 160-167.

Kadoury, S., Cheriet, F., Laporte, C., & Labelle, H. (2007-b). A versatile 3D reconstruction system of the spine and pelvis for clinical assessment of spinal deformities. *Med Biol Eng Comput*, 45(6), 591-602.

Kim, Y. J., Lenke, L. G., Cho, S. K., Bridwell, K. H., Sides, B., & Blanke, K. (2004). Comparative analysis of pedicle screw versus hook instrumentation in posterior spinal fusion of adolescent idiopathic scoliosis. *Spine*, 29(18), 2040-2048.

King, H. A., Moe, J. H., & Bradford, D. S. (1983). The selection of fusion levels in thoracic idiopathic scoliosis. *J Bone Joint Surg*, 65, 1302-1313.

Labelle, H., Roussouly, P., Berthonnaud, E., Dimnet, J., & O'Brien, M. (2005). The importance of spino-pelvic balance in L5-S1 developmental spondylolisthesis. *Spine*, 30(65), S27-S34.

Labelle, H., Aubin, C.-É., Jackson, R., Lenke, L., Newton, P. & Parent, S. (2011). Seeing the spine in 3D: how will it change what we do? *J Pediatr Orthop*, 31(1 Suppl), S37-S45.

Lafage, V., Dubousset, J., Lavaste, F., & Skalli, W. (2004). 3D finite element simulation of Cotrel-Dubousset correction. *Comput Aided Surg, 9* (1-2), 17-25.

Lafage, V., Schwab, F., Skalli, W., Hawkinson, N., Gagey, P. M., Ondra, S., et al. (2008). Standing balance and sagittal plane spinal deformity: analysis of spino-pelvic and gravity line parameters. *Spine, 33*, 1572-1578.

Lam, G.C., Hill, D.L., Le, L.H., Raso, J.V., & Lou, E.H. (2008). Vertebral rotation measurement: a summary and comparison of common radiographic and CT methods. *Scoliosis, 3*, 16-26.

Lamarre, M.-E., Parent, S., Labelle, H., Aubin, C.-É., Joncas, J., Cabral, A., et al. (2009). Assessment of spinal flexibility in adolescent idiopathic scoliosis: Suspension versus side-bending radiography. *Spine, 34*(6), 591-597.

Lavignolle, B., Vital, J. M., Senegas, J., Destandau, J., Toson, B., Bouyx, P., et al. (1983). An approach to the functional anatomy of the sacroiliac joints in vivo. *Surg Radiol Anat, 5*(3), 169-176.

Lee, R. Y. W., & Wong, T. K. T. (2002). Relationship between the movements of the lumbar spine and hip. *Hum Movement sci, 21*, 481-494.

Legaye, J., Duval-Beaupère, G., Hecquet, J., & Marty, C. (1998). Pelvic incidence: a fundamental pelvic parameter for three-dimensional regulation of spinal sagittal curves. *Eur Spine J, 7*(2), 99-103.

Lenke, L. G., Betz, R. R., Harms, J., Bridwell, K. H., Clements, D. H., Lowe, T. G., et al. (2001). Adolescent idiopathic scoliosis: A new classification to determine extent of spinal arthrodesis. *J Bone Joint Surg [Am], 83*, 1169-1181.

Li, S., Kukulka, C. G., Rogers, M. W., Brunt, D., & Bishop, M. (2004). Sural nerve evoked responses in human hip and ankle muscles while standing. *Neuroscience letters, 364*, 59-62.

Liu, Y. K., Laborde, J. M., & Van Buskirk, W. C. (1971). Inertial properties of a segmented cadaver trunk: their implications in acceleration injuries. *Aerosp Med*, 42, 650-657.

Lonstein, J. E., & Carlson, J. M. (1984). The prediction of curve progression in untreated idiopathic scoliosis during growth. *J Bone and Joint Surg Am*, 66, 1061 - 1071.

Lucas, B., Asher, M., McIff, T., Lark, R., & Burton, D. (2004). Estimation of transverse plane pelvic rotation using a posterior-anterior radiograph. *Spine*, 30(1), E20-E27.

Mac-Thiong, J.-M., Roussouly, P., Berthonnaud, E., & Guigui, P. (2011). Sagittal parameters of global spinal balance: normative values from a prospective cohort of seven hundred nine caucasian asymptomatic adults. *Spine*, 35(22), E1193-E1198.

Mac-Thiong, J.-M., Labelle, H., Berthonnaud, E., Betz, R. R., & Roussouly, P. (2007). Sagittal spino-pelvic balance in normal children and adolescents. *Eur Spine J*, 16(2), 227-234.

Mac-Thiong, J. -M., Labelle, H., Charlebois, M., Huot, M. P., & de Guise, J. A. (2003). Sagittal plane analysis of the spine and pelvis in adolescent idiopathic scoliosis according to the coronal curve type. *Spine*, 28(13), 1404-1409.

Mahaudens, P., Detrembleur, C., Mousny, M., & Banse, X. (2009). Gait in adolescent idiopathic scoliosis: energy cost analysis. *Eur Spine J*, 18(8), 1160-1168.

Mahaudens, P., Thonnard, J. L., & Detrembleur, C. (2005). Influence of structural pelvic disorders during standing and walking in adolescents with idiopathic scoliosis. *Spine J*, 5(4), 427-433.

Majdouline, Y., Aubin, C.-É., Sangole, A.P., & Labelle, H. (2009). Computer simulation for the optimization of instrumentation strategies in adolescent idiopathic scoliosis. *Med Biol Eng Comput*, 47(11), 1143-1154.

Marks, M. C., Stanford, C. F., Mahar, A. T., & Newton, P. (2003). Standing lateral radiographic positioning does not represent customary standing balance. *Spine, 28*(11), 1176-1182.

Marras, W. S., Parnianpour, M., Ferguson, S. A., Kim, J. Y., Crowell, R. R., Bose, S., et al. (1995). The classification of anatomic and symptom based low back disorders using motion measure models. *Spine, 20*, 2531-2546.

Masso, P. D., & Gorton, G. E. (2000). Quantifying changes in standing body segment alignment following spinal instrumentation and fusion in idiopathic scoliosis using an optoelectronic measurement system. *Spine, 25*(4), 457-462.

McMaster, M. J. (1991). Luque rod instrumentation in the treatment of adolescent idiopathic scoliosis. A comparative study with Harrington instrumentation. *J Bone and Joint Surg Brt, 73*(6), 982-989.

Milosavljevic, S., Pal, P., Bain, D., & Johnson, G. (2008). Kinematic and temporal interaction of the lumbar spine and hip during trunk extension in healthy male subjects. *Eur Spine J, 17*, 122-128.

Moen, K. Y., & Nachemson, A. L. (1999). Treatment of scoliosis: an historical perspective. *Spine, 24*, 2570-2575.

Nault, M. L., Allard, P., Hinse, S., Blanc, R. L., Caron, O., Labelle, H., et al. (2002). Relations between standing stability and body posture parameters in adolescent idiopathic scoliosis. *Spine, 27*(17), 1911-1917.

Nelson, J. M., Walmsley, R. P., & Stevenson, J. M. (1995). Relative lumbar and pelvic motion during loaded spinal flexion/extension. *Spine, 20*(2), 199-204.

Netter, F. H. (2010). *Pelvis and perineum* (5 ed.). Philadelphia: Saunders Elsevier.

Panjabi, M. M. (2003). Clinical spinal instability and low back pain. *J Electromyogr Kines*, 13(4), 371-379

Panjabi, M. M., Henderson, G., James, Y., & Timm, J. P. (2007). StabilimaxNZ) versus simulated fusion: evaluation of adjacent-level effects. *Eur Spine J*, 16(2), 2159-2165.

Panjabi, M. M., Lydon, C., Vasavada, A., Grob, D., Crisco, J. J. R., & Dvorak, J. (1994). On the understanding of clinical instability. *Spine*, 19(23), 2642-2650.

Park, W.M., Wang, S., Kim, Y.H., Wood, K.B., Sim, J.A., & Li, G., (2012). Effect of the intra-abdominal pressure and the center of segmental body mass on the lumbar spine mechanics – A computational parametric study. *J Biomech Eng*, 134 [Epub ahead of print].

Parkkola, R. & Kormano, M. 1992. Lumbar disc and back muscle degeneration on MRI: correlation to age and body mass. *J Spinal Disord Tech*, 5(1), 86-92.

Pataky, T. C., Zatsiorsky, V. M., & Challis, J. H. (2003). A simple method to determine body segment masses in vivo: reliability, accuracy and sensitivity analysis. *Clin Biomech*, 18, 364–368.

Patwardhan, A. G., Havey, R. M., Meade, K. P., Lee, B., & Dunlap, B. (1999). A follower load increases the load-carrying capacity of the lumbar spine in compression. *Spine*, 24(10), 1003-1009.

Pauwels, F. (1980). *Biomechanics of the locomotor apparatus*. New York: Springer Verlag.

Pearsall, D. J., Reid, J.G., & Ross, R. (1994). Inertial properties of the human trunk of males determined from magnetic resonance imaging. *Ann Biomed Eng*, 22, 692-706.

Pearsall, D.J., Reid, J.G., & Livingston, L.A . (1996). Segmental inertial parameters of the human trunk as determined from computed tomography. *Ann Biomed Eng*, 24, 198-210.

Perie, D., Aubin, C.-É, Lacroix, M., Lafon, Y., & Labelle, H. (2004). Biomechanical modelling of orthotic treatment of the scoliotic spine including a detailed representation of the brace-torso interface. *Med Biol Eng Comput*, 42, 339-344

Petit, Y., Aubin, C.-É, & Labelle, H. (2004) Patient-specific mechanical properties of a flexible multi-body model of the scoliotic spine. *Med Biol Eng Comput*, 42(1), 55-60.

Ponder, R. C., Dickson, J.H., Harrington, P.R., & Erwin, W.D. (1975). Results of Harrington instrumentation and fusion in the adult idiopathic scoliosis patient. *J Bone Joint Surg Am*, 57(6), 797-801.

Qiu, X.S., Zhang, J.J., Yang, S.W., Lv, F., Wang, Z.W., Chiew, J.,et al. (2012). Anatomical study of the pelvis in patients with adolescent idiopathic scoliosis. *J Anat*, 220(2), 173-178.

Richards, B. S., Scaduto, A., Vanderhave, K., & Browne, R. (2005). Assesment of trunk balance in thoracic scoliosis. *Spine*, 30(14), 1621-1626.

Rohlmann, A., Neller, S., Claes, L., Bergmann, G., & Wilke, H.-J. (2001). Influence of a follower load on intradiscal pressure and intersegmental rotation of the lumbar spine. *Spine*, 26(24), E557-E561.

Roussouly, P., Gollogly, S., Berthonnaud, E., & Dimnet, J. (2005). Classification of the normal variation in the sagittal alignment of the human lumbar spine and pelvis in the standing position. *Spine*, 30(3), 346-353.

Roussouly, P., & Pinheiro-Franco, J. L. (2011). Biomechanical analysis of the spino-pelvic organization and adaptation in pathology. *Eur Spine J*, 20 (Suppl 5), S609-S618.

Saji, M., Upadhyay, S., Leong, J. (1995). Increased femoral neck-shaft angles in adolescents idiopathic scoliosis. *Eur Spine J*, 7, 99-103.

Sangole, A. P., Aubin, C.-É., Labelle, H., Stokes, I. A. F., Lenke, L. G., Jackson, R., et al. (2009). Three-dimensional classification of thoracic scoliotic curves. *Spine*, 34(1), 91-99.

Sangole, A. P., Aubin, C.-É., Labelle, H., Lenke, L. G., Jackson, R. P., Newton, P. O., et al. (2010). The central hip vertical axis: a reference axis for the Scoliosis Research Society three-dimensional classification of idiopathic scoliosis. *Spine*, 35(12), E530-E534.

Schwab, F., Lafage, V., Boyce, R., Skalli, W., & Farcy, J. (2006). Gravity line analysis in adult volunteers: age-related correlation with spinal parameters, pelvic parameters, and foot position. *Spine*, 31, E959-E967.

Sevrain, A., Aubin, C.-É., Gharbi, H., Wang, X., & Labelle, H. (2012). Biomechanical evaluation of predictive parameters of progression in adolescent isthmic spondylolisthesis: a computer modeling and simulation study. *Scoliosis*, 7(1), 2-11.

Shirazi-Adl, A., El-Rich, M., Pop. D.G., & Parnianpour, M. (2005). Spinal muscle forces, internal loads, and stability in standing under various postures and loads-application of kinematics-based algorithm. *Eur Spine J*, 14(4), 381-392.

Skalli, W., Zeller, R. D., Miladi, L., Bourcereau, G., Savidan, M., Lavaste, F., et al. (2006). Importance of pelvic compensation in posture and motion after posterior spinal fusion using CD instrumentation for idiopathic scoliosis. *Spine*, 31(12), E359-366.

Snijders, C. J., Ribbers, M.T., de Bakker, H.V., Stoeckart, R., & Stam, H. J. (1998). EMG recordings of abdominal and back muscles in various standing postures: validation of a biomechanical model on sacroiliac joint stability. *J Electromyogr Kines*, 8, 205-214.

Stagnara, P. (1985). *Les déformations du rachis*. Paris: Masson Ed.

Steffen, J.-S., Obeid, I., Aurouer, N., Hauger, O., Vital, J.-M., Dubousset, J., et al. (2010). 3D postural balance with regards to gravity line: an evaluation in the transversal plane on 93 patients and 23 asymptomatic. *Eur Spine J*, 19, 760-767.

Stokes, I. A. F., Bigalow, L. C., & Moreland, M. S. (1986). Measurement of axial rotation of vertebrae in scoliosis. *Spine, 11*(3), 213-218.

Stokes, I. A. F., Laible, J. P. (1990). Three-dimensional osseo-ligamentous model of the thorax representing initiation of scoliosis by asymmetric growth. *J Biomech, 23*(6), 589–595.

Stokes I. A. F. (1994). Three-dimensional terminology of spinal deformity. A report presented to the Scoliosis Research Society by the Scoliosis Research Society Working Group on 3-D terminology of spinal deformity. *Spine (Phila Pa 1976), 19*(2), 236-248.

Stokes, I. A. F., & Aronsson, D. D. (2001). Disc and vertebral wedging in patients with progressive scoliosis. *J Spinal Disord, 14*, 317 - 322.

Stokes, I. A., Laible, J. P., Gardner-Morse, M. G., Costi, J. J., Iatridis, J. C. (2011). Refinement of elastic, poroelastic, and osmotic tissue properties of intervertebral disks to analyze behavior in compression. *Ann Biomed Eng, 39*(1), 122-31.

Stylianides, G., Beaulieu, M., Dalleau, G., Rivard, C.-H., & Allard, P. (2012). Iliac crest orientation and geometry in able-bodied and non-treated adolescent idiopathic scoliosis girls with moderate and severe spinal deformity. *Eur Spine J, 21*(4), 725-732.

Takemura, Y., Yamamoto, H., & Tani, T. (1999). Biomechanical study of the development of scoliosis, using a thoracolumbar spine model. *J Orthop Sci, 4*(6), 439-445.

Tanguay, F., Mac-Thiong, J. M., de Guise, J. A., & Labelle, H. (2007). Relation between the sagittal pelvic and lumbar spine geometries following surgical correction of adolescent idiopathic scoliosis. *Eur Spine J, 16*(4), 531-536.

Umehara, S., Zindrick, M. R., Patwardhan, A. G., Havey, R. M., Vrbos, L. A., Knight, G. W., et al. (2000). The biomechanical effect of postoperative hypolordosis in instrumented lumbar fusion on instrumented and adjacent spinal segments. *Spine, 25*(13), 1617-1624.

Upasani, V. V., Tis, J., Bastrom, T., Pawelek, J., Marks, M., Lonner, B., et al. (2007). Analysis of sagittal alignment in thoracic and thoracolumbar curves in adolescent idiopathic scoliosis. *Spine, 32*(12), 1355-1359.

Van Deursen, D. L., Lengsfeld, M., Snijders, C. J., Evers, J. J., & Goossens, R. H. (2000). Mechanical effects of continuous passive motion on the lumbar spine in seating. *J Biomech, 33*(6), 695-699.

Vaz, G., Roussouly, P., Berthonnaud, E., & Dimnet, J. (2002). Sagittal morphology and equilibrium of pelvis and spine. *Eur Spine J, 11*(1), 80-87.

Vialle, R., Levassor, N., Rillardon, L., Templier, A., Skalli, W., & Guigui, P. (2005). Radiographic analysis of the sagittal alignment and balance of the spine in asymptomatic subjects. *J Bone Joint Surg, Incorporated, 87*(2), 260-267.

Villemure, I., Aubin, C. -É., & Dansereau, J. (2002). Simulation of progressive deformities in adolescent idiopathic scoliosis using a biomechanical model integrating vertebral growth modulation. *J Biomech Eng, 124*, 784-790.

Voutsinas, S. A. & Macewen, G. D. (1986). Sagittal profiles of the spine. *Clin Orthop, 210*, 235-242.

Vrtovec, T., Ourselin, S., Gomes, L., Likar, B., & Pernus, F. (2006). Generation of curved planar reformations from magnetic resonance images of the spine. *Med Image Comput Comput Assist Interv, 9*(Pt 2), 135-143.

Wang, X., Aubin, C.-É, Crandall, D., Parent, S., & Labelle, H. (2012). Biomechanical analysis of 4 types of pedicle screws for sciotic spine instrumentation. *Spine, 37*(14), E823-835.

Wang, X., Aubin, C.-E., Crandall, D., & Labelle, H. (2011). Biomechanical modeling and analysis of a direct incremental segmental translation system for the instrumentation of sciotic deformities. *Clinical Biomechanics, 26*(6), 548-555.

Weiss, H. R. & Goodall, D. (2008). Rate of complications in scoliosis surgery - a systematic review of the Pub Med literature. *Scoliosis*, 3, 9-27.

Winter, D. (2009). *Biomechanics and motor control of human movement* (4 ed.). New Jersey: John Wiley & Sons, Inc.

White, A. A., & Panjabi, M. M. (1990). *Clinical biomechanics of the spine*. (2 ed.). Philadelphia: J.B. Lippincott.

Wilder, D. G., Pope, M. H., & Frymoyer, J. W. (1980). The functional topography of the sacroiliac joint. *Spine*, 5, 575-579.

Zabjek, K. F., Leroux, M. A., Coillard, C., Rivard, C.-H., & Prince, F. (2005). Evaluation of segmental postural characteristics during quiet standing in control and Idiopathic Scoliosis patients. *Clin Biomech*, 20(5), 483-490.

Zabjek, K. F., Coillard, C., Rivard, C.-H., & Prince, F. (2008). Estimation of the centre of mass for the study of postural control in Idiopathic Scoliosis patients: a comparison of two techniques. *Eur Spine J*, 17, 355–360.

Zatsiorsky, V. M., & Duarte, M. (2000). Rambling and trembling in quiet standing. *Motor Control*, 4(2), 185-200.

Zatsiorsky, V. M., & King, D. L. (1998). An algorithm for determining gravity line location from posturographic recording. *J Biomech*, 31, 161-164.

Zatsiorsky, V. M., & Seluyanov, V. N. (1983). *The mass and inertial characteristics of the main segments of the human body* (Vol. 1152–1159). Champagne, IL: Human Kinetics Publishers.